Versatile Synthesis of Cationic N-Heterocyclic Carbene-Gold(I) Complexes Containing a Second Ancillary Ligand. Design of Heterobimetallic Ruthenium-Gold Anticancer Agents.

Jacob Fernández-Gallardo,[a] Benelita T. Elie,[a,b] Mercedes Sanaú[c] and María Contel*[a,b,d]

Electronic Supplementary Information

Table of Contents

1. Experimental section

1.1. General information and instrumentation for the characterization and stability studies of the new compounds

NMR spectra were recorded in a Bruker AV400 (^{1}H-NMR at 400 MHz, ^{13}C{^{1}H} NMR at 100.6 MHz and ^{31}P{^{1}H} NMR at 161.9 MHz. Chemical shifts (δ) are given in ppm using $CDCl_3$ as solvent, unless otherwise stated. ^{1}H and ^{13}C NMR resonances were measured relative to solvent peaks considering tetramethylsilane = 0 ppm, and ^{31}P{^{1}H} NMR was externally referenced to H_3PO_4 (85%). Coupling constants *J* are given in hertz. IR spectra (4000-500 cm^{-1}) were recorded on a Nicolet 6700 Fourier transform infrared spectrophotometer on solid state (ATR accessory). Elemental analyses were performed on a Perkin-Elmer 2400 CHNS/O series II analyzer by Atlantic Microlab Inc. (US). Mass spectra electrospray ionization high resolution (MS ESI-HR) were performed on a Waters Q-Tof Ultima. The theoretical isotopic distributions have been calculated using enviPat Web 2.0.[1] Stability studies were performed in a Cary 100 Bio UV-visible spectrophotometer. The conductivity was measured in an OAKTON pH conductivity meter in acetonitrile solutions (10^{-3} M).

1.2. Synthesis

[AuCl(tht)],[2] [AuCl(NHC)] (NHC = IPr (**1**),[3] IMes (**10**),[3] ICy (**11**),[4] Goofy (**12**)[4]), [Ru(*p*-cymene)Cl(*μ*-Cl)]$_2$,[5] [Ru(*p*-cymene)Cl$_2$(η^1-dppm)][6] were prepared as previously reported. H[AuCl$_4$], $AgClO_4$, $AgOSO_2CF_3$ and $RuCl_3 \cdot nH_2O$ were purchased from STREM Chemicals. Tetrahydrothiophene, imidazolium salts, triphenylphosphine, triethylphosphine, triphenylphosphite, bipyridine, diphenylphosphinemethylene (dppm) were purchased from Sigma-Aldrich, triphenylphosphine (Acros Organics) and triphenylarsine (Alfa Aesar) were purchased from Fisher Scientific. All purchased reactants were used without further purification. Reaction solvents were purchased anhydrous from Fisher Scientific (BDH, ACS Grade) and used without further purification. Deuterated solvents were purchased from Cambridge Isotope Laboratories, Inc. and were kept over molecular sieves (3 Å, beads, 4-8 mesh). Celite (Celite 545, Diatomaceous Earth) was purchased from VWR International and used as received. Reactions involving silver salts were performed in the dark.

Synthesis of the intermediate [Au(IPr)OClO$_3$]: [Au(IPr)Cl] (**1**) (0.2 mmol) was dissolved in dichloromethane (5 mL) and added over a solution of the corresponding silver salt (0.2 mmol), $AgClO_4$ in diethyl ether (5 mL) at 0 ºC. The reaction mixture was stirred for 15 minutes at room temperature to afford a white precipitate (AgCl). The resulting solution was filtered through celite and the filtrate was collected at 0 ºC as a clear colorless solution. Evaporation of the solvent to dryness afforded a colorless oily material. IR (cm^{-1}) 1092 vb, vs; 623 m (OClO$_3$).[7]

[Au(IPr)L]A (2a, 2b, 3-6). [Au(IPr)Cl] (**1**) (0.2 mmol) was dissolved in dichloromethane (5 mL) and added over a solution of the corresponding silver salt (0.2 mmol), $AgClO_4$ or $AgOSO_2CF_3$, in diethyl ether (5 mL) at 0 ºC. The reaction mixture was stirred for 15 minutes at room temperature to afford a white precipitate (AgCl). The resulting solution was filtered through celite and the filtrate was collected at 0 ºC as a clear colorless solution. Then, a solution of the corresponding ligand L (0.2 mmol), L = PPh_3 (**2a** and **2b**), PEt_3 (**3**), $P(OPh)_3$ (**4**), $AsPh_3$ (**5**) or bipyridine (**6**) in 5 mL of dichloromethane was slowly poured over the aforementioned solution and the final reaction mixture stirred for 15 minutes at room temperature. The solvent volume was then reduced under vacuum up to ~3 mL and diethyl ether (15 mL) was added to precipitate the final product, which was washed with diethyl ether (3x10 mL). Complexes **2a**, **2b**, **3-6** were isolated as powdery white solids.

2a (L = PPh_3, A = ClO_4^-): 87% yield (0.164 g). Anal. Calc. for $C_{45}H_{51}AuClN_2O_4P$ (947.30): C, 57.06; H, 5.43; N, 2.96. Found: C, 56.78; H, 5.42; N, 2.97. ^{31}P{^{1}H} NMR ($CDCl_3$): δ 39.9 (s, PPh_3). ^{1}H NMR ($CDCl_3$): δ 7.63 (m, 4H, C*H* aromatic), δ 7.53 (t, $^3J_{HH}$ = 7.1 Hz, 2H, C*H* imidazole), 7.37 (m, 9H, C*H* aromatic), 6.99 (m, 8H, C*H* aromatic), δ 2.57 (septet, $^3J_{HH}$ = 6.8 Hz, 2H, C*H*(CH$_3$)$_2$), δ 1.29 (d, $^3J_{HH}$ = 6.8 Hz, 6H, CH(C*H*$_3$)$_2$), δ 1.18 (d, $^3J_{HH}$ = 6.8 Hz, 12H, CH(C*H*$_3$)$_2$). ^{13}C{^{1}H} NMR ($CDCl_3$, plus HSQC): δ 188.81 (d, $^2J_{PC}$ = 126.1 Hz, *C* carbene), δ 145.88 (s, C*H* aromatic IPr), δ 133.64 (d, $^4J_{PC}$ = 13.8 Hz, *m*-PPh$_3$), δ 133.29 (s, C*H* aromatic), δ 132.36 (d, $^3J_{PC}$ = 2.5 Hz, *p*-PPh$_3$), δ 131.19 (s, C*H* aromatic), δ 129.52 (d, $^2J_{PC}$ = 11.7 Hz, *o*-PPh$_3$), δ 127.52

(d, $^1J_{PC}$ = 58.8 Hz, *ipso*-PPh$_3$), δ 125.34 (d, $^4J_{PC}$ = 3.4 Hz, C*H* imidazole), δ 124.43 (s, C*H* aromatic), δ 28.84 (s, C*H*(CH$_3$)$_2$), δ 24.77 (s, CH(C*H*$_3$)$_2$), δ 23.97 (s, CH(C*H*$_3$)$_2$). MS(ESI+) [m/z]: 847.36 (100%) [M]$^+$. IR (cm^{-1}): 1092 vs, 623 m (ClO$_4^-$). Conductivity: κ = 178 µS/cm, 2 ions (1$^+$/1$^-$).

2b (L = PPh$_3$, A = CF$_3$SO$_3^-$): 87% yield (0.173 g). Anal. Calc. for C$_{46}$H$_{51}$AuF$_3$N$_2$O$_3$PS (996.92): C, 55.42; H, 5.16; N, 2.81; S, 3.22. Found: C, 54.99; H, 5.09; N, 2.81; S, 3.24. ^{31}P{^{1}H} NMR (CDCl$_3$): δ 39.9 (s, PPh$_3$). ^{19}F{^{1}H} NMR (CDCl$_3$): δ -78.1 (s, C*F*$_3$SO$_3^-$). ^{1}H NMR (CDCl$_3$): δ 7.63 (m, 4H, C*H* aromatic), δ 7.52 (t, $^3J_{HH}$ = 7.1 Hz, 2H, C*H* imidazole), 7.36 (m, 9H, C*H* aromatic), 7.00 (m, 8H, C*H* aromatic), δ 2.57 (m, 2H, C*H*(CH$_3$)$_2$), δ 1.29 (d, $^3J_{HH}$ = 6.8 Hz, 6H, CH(C*H*$_3$)$_2$), δ 1.18 (d, $^3J_{HH}$ = 6.9 Hz, 12H, CH(C*H*$_3$)$_2$). ^{13}C{^{1}H} NMR (CDCl$_3$, plus HSQC): δ 188.73 (d, $^2J_{PC}$ = 126.2 Hz, *C* carbene), δ 145.90 (s, C*H* aromatic IPr), δ 133.64 (d, $^4J_{PC}$ = 13.8 Hz, *m*-PPh$_3$), δ 133.30 (s, C*H* aromatic), δ 132.33 (d, $^3J_{PC}$ = 2.5 Hz, *p*-PPh$_3$), δ 131.15 (s, C*H* aromatic), δ 129.50 (d, $^2J_{PC}$ = 11.7 Hz, *o*-PPh$_3$), δ 127.54 (d, $^1J_{PC}$ = 58.8 Hz, *ipso*-PPh$_3$), δ 125.42 (d, $^4J_{PC}$ = 3.3 Hz, C*H* imidazole), δ 124.41 (s, C*H* aromatic), δ 28.84 (s, C*H*(CH$_3$)$_2$), δ 24.76 (s, CH(C*H*$_3$)$_2$), δ 23.92 (s, CH(C*H*$_3$)$_2$). MS(ESI+) [m/z]: 847.40 (100%) [M]$^+$. IR (cm^{-1}): 1283 s (CF$_3$SO$_3^-$), 1262 vs (CF$_3$SO$_3^-$), 1146 s (CF$_3$SO$_3^-$), 1032 s (CF$_3$SO$_3^-$), 637 m (CF$_3$SO$_3^-$). Conductivity: κ = 210 µS/cm, 2 ions (1$^+$/1$^-$).

3 (L = PEt$_3$, A = ClO$_4^-$): 82% yield (0.131 g). Anal. Calc. for C$_{33}$H$_{51}$AuClN$_2$O$_4$P (803.17): C, 49.35; H, 6.40; N, 3.49. Found: C, 49.43; H, 6.41; N, 3.47. ^{31}P{^{1}H} NMR (CDCl$_3$): δ 39.6 (s, PEt$_3$). ^{1}H NMR (CDCl$_3$): δ 7.57 (t, $^3J_{HH}$ = 7.6 Hz, 2H, C*H* aromatic IPr), δ 7.47 (s, 2H, C*H* imidazole), δ 7.35 (d, $^3J_{HH}$ = 7.8 Hz, 4H, C*H* aromatic IPr), δ 2.53 (septet, $^3J_{HH}$ = 6.8 Hz, 2H, C*H*(CH$_3$)$_2$), δ 1.64 (m, 6H, P(C*H*$_2$CH$_3$)$_3$), δ 1.30 (d, $^3J_{HH}$ = 6.8 Hz, 6H, CH(C*H*$_3$)$_2$), δ 1.28 (d, $^3J_{HH}$ = 6.9 Hz, 12H, CH(C*H*$_3$)$_2$), δ 0.79 (m, 6H, P(CH$_2$(C*H*$_3$)$_3$). ^{13}C{^{1}H} NMR (CDCl$_3$, plus HSQC): δ 192.41 (d, $^2J_{PC}$ = 192.43 Hz, *C* carbene), δ 145.67 (s, C*H* aromatic), δ 133.13 (s, C*H* aromatic), δ 131.21 (s, C*H* aromatic), δ 124.64 (d, $^4J_{PC}$ = 3.2 Hz, C*H* imidazole), δ 124.36 (s, C*H* aromatic), δ 28.84 (s, C*H*(CH$_3$)$_2$), δ 24.83 (s, CH(C*H*$_3$)$_2$), δ 23.95 (s, CH(C*H*$_3$)$_2$), δ 17.50 (d, $^1J_{PC}$ = 34.61 Hz, P(*C*H$_2$CH$_3$)$_3$), δ 8.86 (s, P(CH$_2$*C*H$_3$)$_3$). MS(ESI+) [m/z]: 703.37 (100%) [M]$^+$. IR (cm^{-1}): 1094 vs, 622 m (ClO$_4^-$). Conductivity: κ = 181 µS/cm, 2 ions (1$^+$/1$^-$).

4 (L = P(OPh)$_3$, A = ClO$_4^-$): 84% yield (0.167 g). Anal. Calc. for C$_{45}$H$_{51}$AuClN$_2$O$_7$P (995.30): C, 54.30; H, 5.17; N, 2.81. Found: C, 54.04; H, 5.24; N, 2.73. ^{31}P{^{1}H} NMR (CDCl$_3$): δ 128.0 (s, P(OPh)$_3$). ^{1}H NMR (CDCl$_3$): δ 7.63 (t, $^3J_{HH}$ = 7.8 Hz, 2H, C*H* aromatic IPr), δ 7.56 (s, 2H, C*H* imidazole), δ 7.81 (d, $^3J_{HH}$ = 7.8 Hz, 4H, C*H* aromatic IPr), δ 7.26 (m, 2H, C*H* P(OPh)$_3$), δ 6.78 (m, 2H, C*H* P(OPh)$_3$) δ 7.38 (m, 8H, C*H* aromatic), δ 2.38 (septet, $^3J_{HH}$ = 6.8 Hz, 2H, C*H*(CH$_3$)$_2$), δ 1.22 (d, $^3J_{HH}$ = 6.8 Hz, 6H, CH(C*H*$_3$)$_2$), δ 1.00 (d, $^3J_{HH}$ = 6.8 Hz, 12H, CH(C*H*$_3$)$_2$). ^{13}C{^{1}H} NMR (CDCl$_3$, plus HSQC): δ 185.17 (d, $^2J_{PC}$ = 192.43 Hz, *C* carbene), δ 148.65 (d, $^2J_{PC}$ = 5.6 Hz, *o*-P(OPh)$_3$), δ 145.60 (s, C*H* aromatic), δ 132.69 (s, C*H* aromatic), δ 131.28 (s, C*H* aromatic), δ 130.64 (s, C*H* aromatic), δ 126.74 (s, C*H* imidazole), δ 126.05 (d, $^4J_{PC}$ = 5.0 Hz, *p*-P(OPh)$_3$), δ 124.44 (s, C*H* aromatic), δ 120.04 (d, $^2J_{PC}$ = 5.6 Hz, *m*-P(OPh)$_3$), δ 28.70 (s, C*H*(CH$_3$)$_2$), δ 24.78 (s, CH(C*H*$_3$)$_2$), δ 23.82 (s, CH(C*H*$_3$)$_2$). MS(ESI+) [m/z]: 895.33 (100%) [M]$^+$. IR (cm^{-1}): 1091 vs, 622 (m) (ClO$_4^-$). Conductivity: κ = 176 µS/cm, 2 ions (1$^+$/1$^-$).

5 (L = AsPh$_3$, A = ClO$_4^-$): White solid, 81% yield (0.160 g). Anal. Calc. for C$_{45}$H$_{51}$AsAuClN$_2$O$_4$ · ½ CH$_2$Cl$_2$ (991.25): C, 52.87; H, 5.07; N, 2.71. Found: C, 52.87; H, 4.94; N, 2.78. ^{1}H NMR (CDCl$_3$): δ 7.67 (s, 2H, C*H* imidazole), δ 7.63 (t, $^3J_{HH}$ = 7.8 Hz, 2H, C*H* aromatic), δ 7.52 (t, $^3J_{HH}$ = 7.5 Hz, 2H, C*H* aromatic), δ 7.38 (m, 11H, C*H* aromatic), δ 7.63 (d, $^3J_{HH}$ = 7.0 Hz, 4H, C*H* aromatic), δ 2.60 (septet, $^3J_{HH}$ = 6.8 Hz, 2H, C*H*(CH$_3$)$_2$), δ 1.31 (d, $^3J_{HH}$ = 6.8 Hz, 6H, CH(C*H*$_3$)$_2$), δ 1.21 (d, $^3J_{HH}$ = 6.8 Hz, 12H, CH(C*H*$_3$)$_2$). ^{13}C{^{1}H} NMR (CDCl$_3$, plus HSQC): δ 184.96 (s, *C* carbene), δ 145.92 (s, C*H* aromatic), δ 133.29 (s, C*H* aromatic), δ 132.85 (s, C*H* aromatic), δ 131.78 (s, C*H* aromatic), δ 131.18 (s, C*H* aromatic), δ 130.13 (s, C*H* aromatic), δ 129.92 (s, C*H* aromatic), δ 125.44 (s, C*H* imidazole), δ 124.45 (s, C*H* aromatic), δ 28.85 (s, C*H*(CH$_3$)$_2$), δ 24.94 (s, CH(C*H*$_3$)$_2$), δ 23.91 (s, CH(C*H*$_3$)$_2$). MS(ESI+) [m/z]: 891.29 (100%) [M]$^+$. IR (cm^{-1}): 1092 vs, 622 m (ClO$_4^-$). Conductivity: κ = 194 µS/cm, 2 ions (1$^+$/1$^-$).

6 (L = bipy, A = ClO$_4^-$): White solid, 73% yield (0.122 g). Anal. Calc. for C$_{37}$H$_{44}$AuClN$_4$O$_4$ · ⅓ CH$_2$Cl$_2$ (841.20): C, 51.57; H, 5.18; N, 6.80. Found: C, 51.90; H, 5.46; N, 6.38. ^{1}H NMR (CDCl$_3$): δ 8.01 (m, 4H, C*H* aromatic), δ 7.71 (t, $^3J_{HH}$ = 7.8 Hz, 2H, C*H* aromatic), δ 7.42 (m, 10H, C*H* aromatic), δ 2.56 (m, 2H, C*H*(CH$_3$)$_2$), δ 1.28 (d, $^3J_{HH}$ = 6.8 Hz, 6H, CH(C*H*$_3$)$_2$), δ 1.21 (d, $^3J_{HH}$ = 6.9 Hz, 12H, CH(C*H*$_3$)$_2$). ^{13}C{^{1}H} NMR (CDCl$_3$, plus HSQC): δ 169.62 (s, *C* carbene), δ 153.85 (s, C*H* aromatic), δ 150.09 (s, C*H* aromatic), δ 145.92 (s, C*H* aromatic), δ 139.79 (s, C*H* aromatic), δ 134.26 (s, C*H* aromatic), δ 131.08 (s, C*H* aromatic), δ 125.54

(s, C*H* aromatic), δ 124.83 (s, C*H* aromatic), δ 124.594 (s, C*H* imidazole), δ 124.24 (s, C*H* aromatic), δ 28.89 (s, C*H*(CH_3)$_2$), δ 24.53 (s, CH(C*H*$_3$)$_2$), δ 23.90 (s, CH(C*H*$_3$)$_2$). MS(ESI+) [m/z]: 626.28 (16%) [Au(IPr)(CH_3CN)]$^+$, 613.26 (18%) [Au(IPr)(CH_2=CH_2)]$^+$, 157.08 (100%) [bipy-H]$^+$. IR (cm^{-1}): 1094 vs, 623 m (ClO_4^-). Conductivity: κ = 201 μS/cm, 2 ions (1$^+$/1$^-$).

[Ru(*p*-cymene)Cl$_2$(*μ*-dppm)Au(NHC)]ClO$_4$ (13-16). The corresponding gold NHC complex (**1**, **10-12**) (0.1 mmol) was dissolved in dichloromethane (5 mL) and added over a solution of $AgClO_4$ (0.1 mmol) in diethyl ether (5 mL) at 0 ºC. The mixture was stirred for 15 minutes at room temperature. The resulting solution was filtered through celite and collected at 0 ºC. Then, a red-brown solution of complex **9** (0.1 mmol) in 5 mL of dichloromethane was poured into the filtrate. The mixture was stirred for 15 minutes at room temperature. The solvent was partly removed to a volume of ~3 mL and the addition of 15 mL of diethyl ether yielded a precipitate. This precipitate was washed with extra diethyl ether (3x10 mL) to afford the heterobimetallic complexes (**13-16**) that were isolated as powdery solids.

13: Brown solid, 87% yield (0.119 g). Anal. Calc. for $C_{62}H_{72}AuCl_3N_2O_4P_2Ru$ (1375.60): C, 54.13; H, 5.28; N, 2.04. Found: C, 54.43; H, 5.18; N, 2.07. $^{31}P\{^1H\}$ NMR ($CDCl_3$): δ 26.7 (d, $^2J_{PP}$ = 25.9 Hz, Au-PPh$_2$), δ 20.0 (d, $^2J_{PP}$ = 25.9 Hz, Ru-PPh$_2$). ^1H NMR ($CDCl_3$): δ 7.63 (m, 6H, PPh$_2$), δ 7.39 (s, 2H, C*H* imidazole), δ 7.32 (d, $^3J_{HH}$ = 7.8 Hz, 4H, *m*-IMes), δ 7.27 (m, 4H, PPh$_2$), δ 7.12 (td, $^3J_{HH}$ = 7.9 Hz, $^4J_{HH}$ = 2.5 Hz, 4H, PPh$_2$), δ 6.98 (td, $^3J_{HH}$ = 7.9 Hz, $^4J_{HH}$ = 2.2 Hz, 4H, PPh$_2$), δ 6.81 (dd, $^3J_{HH}$ = 7.3 Hz, $^3J_{HH}$ = 13.0 Hz, 4H, PPh$_2$), δ 5.22 (d, $^3J_{HH}$ = 5.2 Hz, 2H, 3-C$_6$H$_4$), δ 5.01 (d, $^3J_{HH}$ = 6.2 Hz, 2H, 2-C$_6$H$_4$), δ 3.80 (t, 2H, $^2J_{PH}$ = 10.0 Hz, PC*H*$_2$P), δ 2.46 (2m, 1+4H, *p*-cymene-C*H*(CH_3)$_2$ + IMes-C*H*(CH_3)$_2$), δ 1.76 (m, 3H, CH$_3$-*p*-cymene), δ 1.19 (d, $^3J_{HH}$ = 6.8 Hz, 6H, CH(C*H*$_3$)$_2$), δ 1.02 (d, $^3J_{HH}$ = 6.9 Hz, 12H, CH(C*H*$_3$)$_2$), δ 0.77 (d, 6H, $^3J_{HH}$ = 6.9 Hz, CH(C*H*$_3$)$_2$). $^{13}C\{^1H\}$ NMR ($CDCl_3$, plus HSQC): δ 187.81 (d, $^2J_{PC}$ = 129.6 Hz, *C* carbene), δ 145.53 (s, C*H* aromatic IPr), δ 133.61 (s, C*H* aromatic IPr), δ 132.75 (d, $^2J_{PC}$ = 13.6 Hz, *o*-PPh$_2$), δ 132.71 (d, $^2J_{PC}$ = 9.1 Hz, *o*-PPh$_2$), δ 131.68 (d, $^4J_{PC}$ = 2.3 Hz, *p*-PPh$_2$), δ 131.42 (s, C*H* aromatic IPr), δ 131.32 (d, $^4J_{PC}$ = 2.2 Hz, *p*-PPh$_2$), 130.22 (dd, $^1J_{PC}$ = 44.1 Hz, $^3J_{PC}$ = 2.0 Hz, *ipso*-PPh$_2$), δ 129.06 (d, $^2J_{PC}$ = 11.5 Hz, *m*-PPh$_2$), δ 128.65 (d, $^2J_{PC}$ = 10.0 Hz, m-PPh$_2$), 128.18 (m, *ipso*-PPh$_2$), δ 124.53 (s, C*H* aromatic IPr), δ 125.48 (d, $^4J_{PC}$ = 3.2 Hz, C*H* imidazole), δ 109.14 (s, 4-C$_6$H$_4$), δ 94.23 (s, 1-C$_6$H$_4$), δ 90.58 (d, $^2J_{PC}$ = 4.3 Hz, 3-C$_6$H$_4$), δ 85.65 (d, $^2J_{PC}$ = 6.2 Hz, 2-C$_6$H$_4$), δ 30.09 (s, *p*-cymene-*C*H(CH_3)$_2$), δ 28.85 (s, IPr-*C*H(CH_3)$_2$), δ 24.50 (s, IPr-CH(*C*H$_3$)$_2$), δ 24.04 (s, *p*-cymene-CH(*C*H$_3$)$_2$), δ 21.16 (s, P*C*H$_2$P), δ 17.36 (s, *p*-cymene-*C*H$_3$). MS(ESI+) [m/z]: 1272.35 (88%) [M]$^+$, 969.42 (100%) [Au(IMes)$_2$(η^1-dppm)]$^+$ 655.10 (16%) [RuCl(*p*-cymene)(η^2-dppm)]$^+$. IR (cm^{-1}): 1089, 623 m vs (ClO_4^-). Conductivity: Λ = 174 μS/cm, 2 ions (1$^+$/1$^-$).

14: Orange-brown solid, 78% yield (0.101 g). Anal. Calc. for $C_{56}H_{60}AuCl_3N_2O_4P_2Ru$ · ½ CH_2Cl_2 (1291.44): C, 50.87; H, 4.61; N, 2.10. Found: C, 50.64; H, 4.66; N, 2.36. $^{31}P\{^1H\}$ NMR ($CDCl_3$): δ 25.3 (d, $^2J_{PP}$ = 25.0 Hz, Au-PPh$_2$), δ 21.1 (d, $^2J_{PP}$ = 24.9 Hz, Ru-PPh$_2$). ^1H NMR ($CDCl_3$): δ 7.69 (m, 4H, *o*-PPh$_2$), δ 7.35-7.21 (m, 6H), δ 7.17-7.08 (m, 12H), δ 6.91-6.86 (m, 4H), δ 5.31 (d, $^3J_{HH}$ = 5.3 Hz, 2H, 3-C$_6$H$_4$), δ 5.10 (d, $^3J_{HH}$ = 6.1 Hz, 2H, 2-C$_6$H$_4$), δ 3.87 (t, 2H, $^2J_{PH}$ = 9.4 Hz, PCH$_2$P), δ 2.51 (s, 6H, *p*-CH$_3$-IMes), δ 2.39 (m, 1H, C*H*(CH_3)$_2$), δ 2.02 (s, 12H, *o*-CH$_3$-IMes), δ 1.80 (m, 3H, CH$_3$), δ 0.75 (d, 6H, $^3J_{HH}$ = 6.9 Hz, CH(C*H*$_3$)$_2$). $^{13}C\{^1H\}$ NMR ($CDCl_3$, plus HSQC): δ 186.25 (d, $^2J_{PC}$ = 227.18 Hz, *C* carbene), δ 140.46 (s, C*H* aromatic IMes), δ 134.67 (s, C*H* aromatic IMes), δ 132.87 (d, $^2J_{PC}$ = 9.4 Hz, *o*-PPh$_2$), δ 132.59 (d, $^2J_{PC}$ = 13.9 Hz, *o*-PPh$_2$), δ 131.63 (d, $^4J_{PC}$ = 2.5 Hz, *p*-PPh$_2$), δ 131.36 (d, $^4J_{PC}$ = 2.4 Hz, *p*-PPh$_2$), δ 129.75 (s, C*H* aromatic IMes), 129.72 (dd, $^1J_{PC}$ = 44.6 Hz, $^3J_{PC}$ = 2.1 Hz, *ipso*-PPh$_2$), δ 128.99 (m, *m*-PPh$_2$), 128.48 (d, $^3J_{PC}$ = 1.9 Hz, *ipso*-PPh$_2$, second doublet overlaped with multiplet at 128.99), δ 124.26 (d, $^4J_{PC}$ = 3.0 Hz, C*H* imidazole), δ 123.04 (s, C*H* aromatic IMes), δ 108.69 (s, 4-C$_6$H$_4$), δ 94.27 (s, 1-C$_6$H$_4$), δ 90.74 (d, $^2J_{PC}$ = 4.3 Hz, 3-C$_6$H$_4$), δ 85.78 (d, $^2J_{PC}$ = 6.1 Hz, 2-C$_6$H$_4$), δ 30.11 (s, *p*-cymene-*C*H(CH_3)$_2$), δ 21.39 (s, IMes-*p*-*C*H$_3$), δ 21.08 (s, *p*-cymene-CH(*C*H$_3$)$_2$), δ 18.04 (s, IMes-*o*-*C*H$_3$), δ 19.39 (dd, $^1J_{PC}$ = 23.8 Hz, $^1J_{PC}$ = 19.2 Hz, P*C*H$_2$P),δ 17.29 (s, *p*-cymene-*C*H$_3$). MS(ESI+) [m/z]: 1191.23 (95%) [M]$^+$, 885.28 (49%) [Au(IMes)$_2$(η^1-dppm)]$^+$, 805.35 (100%) [Au(IMes)$_2$]$^+$, 655.10 (3%) [RuCl(*p*-cymene)(η^2-dppm)]$^+$. IR (cm^{-1}): 1095 vs, 622 m (ClO_4^-). Conductivity: Λ = 182 μS/cm, 2 ions (1$^+$/1$^-$).

15: Yellow-orange solid, 82% yield (0.100 g). Anal. Calc. for $C_{50}H_{60}AuCl_3N_2O_4P_2Ru$ (1219.37): C, 49.25; H, 4.96; N, 2.30. Found: C, 49.66; H, 4.98; N, 2.33. $^{31}P\{^1H\}$ NMR ($CDCl_3$): δ 28.7 (d, $^2J_{PP}$ = 20.2 Hz, Au-PPh$_2$), δ 21.5 (d, $^2J_{PP}$ = 20.3 Hz, Ru-PPh$_2$). ^1H NMR ($CDCl_3$): δ 8.00 (m, 4H), δ 7.44-7.22 (m, 18H), δ 5.39 (d, $^3J_{HH}$ = 5.2 Hz, 2H, 3-C$_6$H$_4$), δ 5.24 (d, $^3J_{HH}$ = 6.9 Hz, 2H, 2-C$_6$H$_4$), δ 4.18 (m, 4H, PCH$_2$P + 2 C*H*-ICy), δ 2.41 (m, 1H, C*H*(CH_3)$_2$), δ 2.21-1.23 (m, 23H, , *p*-cymene-C*H*(CH_3)$_2$ + C*H*$_2$ ICy), δ 0.87 (d, 6H, $^3J_{HH}$ = 6.9 Hz, CH(C*H*$_3$)$_2$). $^{13}C\{^1H\}$ NMR ($CDCl_3$, plus HSQC): δ 182.27 (d, $^2J_{PC}$ = 127.6 Hz, *C* carbene), δ 133.42 (d, $^2J_{PC}$ = 9.4 Hz, *o*-

PPh_2), δ 132.77 (d, $^2J_{PC}$ = 14.9 Hz, *o*-PPh_2), δ 131.72 (m, *p*-PPh_2), 130.96 (dd, $^1J_{PC}$ = 44.0 Hz, $^3J_{PC}$ = 3.0 Hz, *ipso*-PPh_2), 129.92 (d, $^3J_{PC}$ = 2.6 Hz, *ipso*-PPh_2, second doublet overlaped with doublet at 129.33), δ 129.33 (d, $^2J_{PC}$ = 11.6 Hz, *m*-PPh_2), δ 128.90 (d, $^2J_{PC}$ = 9.8 Hz, m-PPh_2), δ 118.73 (d, $^4J_{PC}$ = 3.6 Hz, C*H* imidazole), δ 109.08 (s, 4-C_6H_4), δ 95.99 (s, 1-C_6H_4), δ 90.36 (d, $^2J_{PC}$ = 4.4 Hz, 3-C_6H_4), δ 85.78 (d, $^2J_{PC}$ = 6.0 Hz, 2-C_6H_4), δ 61.27 (s, ICy-*C*H), δ 34.33 (s, ICy-*C*H_2), δ 30.24 (s, *p*-cymene-*C*H(CH_3)$_2$), δ 25.72 (s, ICy-*C*H_2), δ 25.59 (s, ICy-*C*H_2), δ 24.90 (s, *p*-cymene-CH(*C*H_3)$_2$), δ 21.39 (m, P*C*H_2P), δ 17.30 (s, *p*-cymene-*C*H_3). MS(ESI+) [m/z]: 1119.24 (100%) $[M]^+$, 813.28 (81%) $[Au(ICy)_2(\eta^1\text{-dppm})]^+$, 661.36 (3%) $[Au(ICy)_2]^+$. IR (cm^{-1}): 1089 vs, 622 m (ClO_4^-). Conductivity: K = 187 μS/cm, 2 ions ($1^+/1^-$).

16: Red-orange solid, 75% yield (0.085 g). Anal. Calc. for $C_{44}H_{52}AuCl_3N_2O_4P_2Ru$ (1139.24): C, 46.39; H, 4.60; N, 2.46. Found: C, 46.11; H, 4.58; N, 2.18. $^{31}P\{^1H\}$ NMR ($CDCl_3$): δ 28.1 (d, $^2J_{PP}$ = 20.7 Hz, Au-PPh_2), δ 21.4 (d, $^2J_{PP}$ = 20.8 Hz, Ru-PPh_2). ^1H NMR ($CDCl_3$): δ 8.01 (m, 4H, PPh_2), δ 7.40-7.22 (m, 16H, PPh_2), δ 5.38 (d, $^3J_{HH}$ = 5.3 Hz, 2H, 3-C_6H_4), δ 5.21 (d, $^3J_{HH}$ = 6.0 Hz, 2H, 2-C_6H_4), δ 4.50 (m, 2H, N-C*H*(CH_3)$_2$). δ 4.19 (t, 2H, $^2J_{PH}$ = 10.0 Hz, PCH_2P), δ 2.43 (m, 1H, C*H*(CH_3)$_2$), δ 1.82 (s, 3H, CH_3-*p*-cymene), δ 1.60 (d, $^3J_{HH}$ = 6.8 Hz, 6H, N-CH(C*H*$_3$)$_2$), δ 1.52 (d, $^3J_{HH}$ = 6.8 Hz, 6H, N-CH(C*H*$_3$)$_2$), δ 0.84 (d, 6H, $^3J_{HH}$ = 6.9 Hz, CH(C*H*$_3$)$_2$). $^{13}C\{^1H\}$ NMR ($CDCl_3$, plus HSQC): δ 182.16 (d, $^2J_{PC}$ = 127.7 Hz, *C* carbene), δ 118.44 (d, $^4J_{PC}$ = 3.5 Hz, C*H* imidazole), δ 133.32 (d, $^2J_{PC}$ = 9.3 Hz, *o*-PPh_2), δ 132.79 (d, $^2J_{PC}$ = 13.9 Hz, *o*-PPh_2), δ 131.75 (m, *p*-PPh_2), 130.71 (dd, $^1J_{PC}$ = 44.0 Hz, $^3J_{PC}$ = 2.4 Hz, *ipso*-PPh_2), 129.86 (d, $^3J_{PC}$ = 2.6 Hz, *ipso*-PPh_2, second doublet overlaped with doublet at 129.36), δ 129.36 (d, $^2J_{PC}$ = 11.5 Hz, *m*-PPh_2), δ 128.90 (d, $^2J_{PC}$ = 9.8 Hz, *m*-PPh_2), δ 118.44 (d, $^4J_{PC}$ = 3.5 Hz, C*H* imidazole), δ 108.98 (s, 4-C_6H_4), δ 95.16 (s, 1-C_6H_4), δ 90.52 (d, $^2J_{PC}$ = 4.5 Hz, 3-C_6H_4), δ 85.78 (d, $^2J_{PC}$ = 6.0 Hz, 2-C_6H_4), δ 53.81 (s, Goofy-*C*H), δ 30.20 (s, *p*-cymene-*C*H(CH_3)$_2$), δ 23.70 (s, *p*-cymene-CH(*C*H_3)$_2$), δ 21.28 (s, Goofy-*C*H_3), δ 21.04 (m, CH_2, overlaped with singlet at 21.28), δ 17.34 (s, *p*-cymene-*C*H_3). MS(ESI+) [m/z]: 1139.17 (15%) $[M]^+$, 733.22 (20%) $[Au(Goofy)(\eta^1\text{-dppm})]^+$, 501.23 (100%) $[Au(Goofy)_2]^+$, 655.10 (44%) $[RuCl(p\text{-cymene})(\eta^2\text{-dppm})]^+$. IR ($cm^{-1}$): 1092 vs, 622 m ($ClO_4^-$). Conductivity: K = 189 μS/cm, 2 ions ($1^+/1^-$).

2. NMR spectra of all compounds in $CDCl_3$

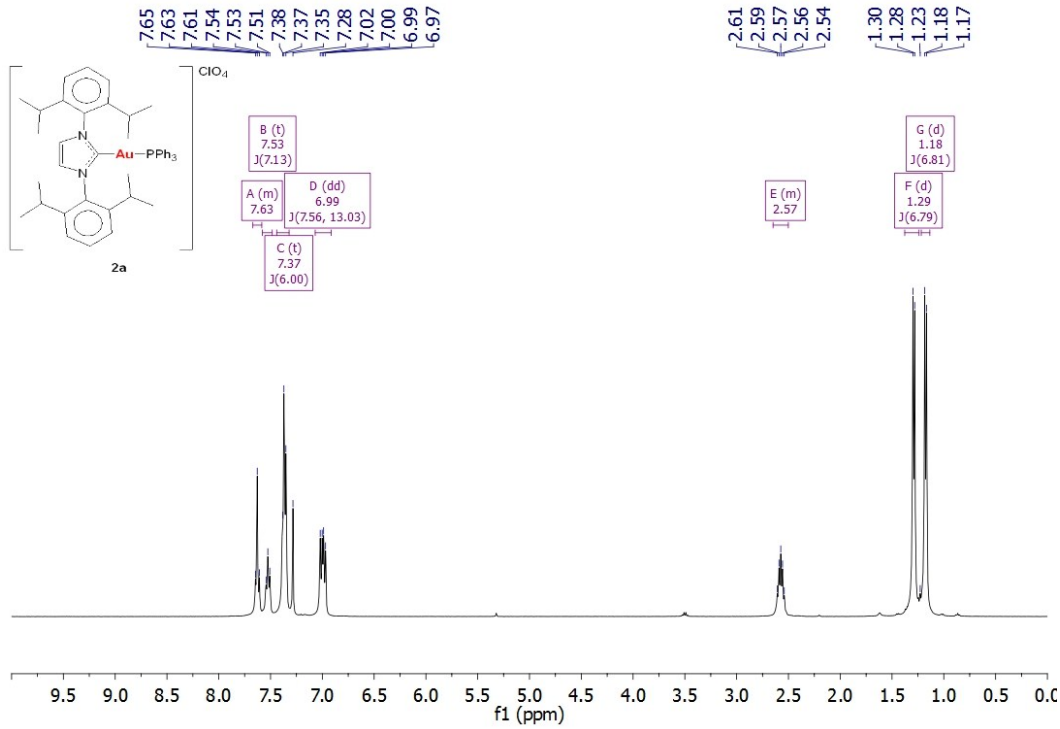

Figure S1. ^{1}H NMR spectrum of compound **2a** in $CDCl_3$.

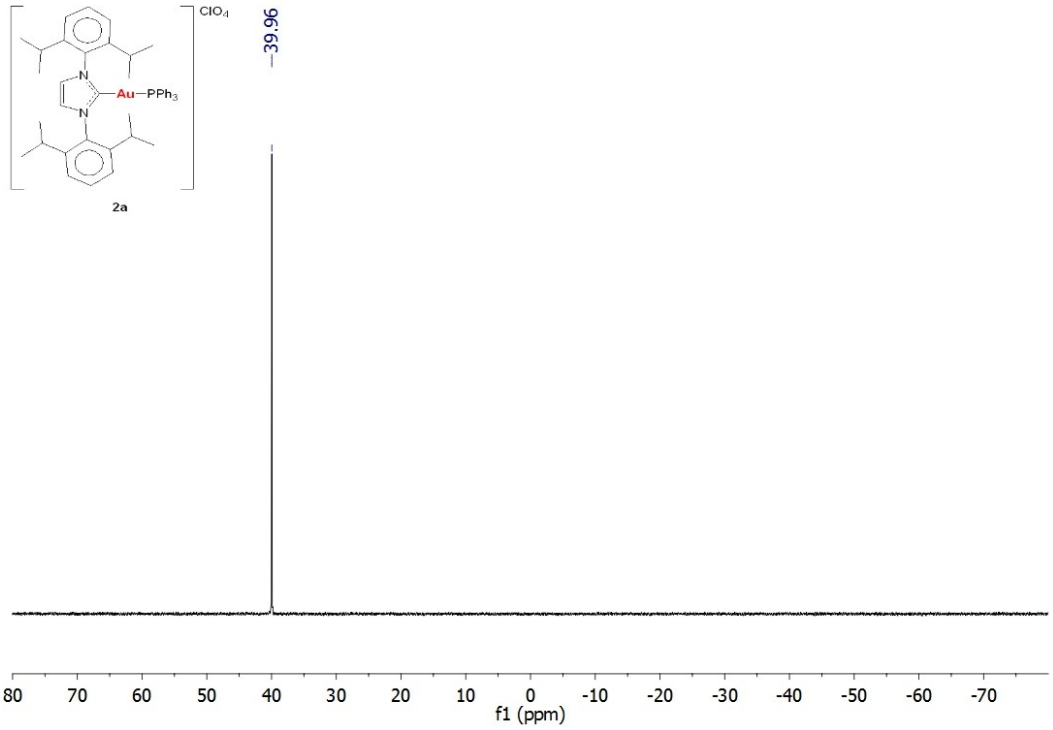

Figure S2. $^{31}P\{^{1}H\}$ NMR spectrum of compound **2a** in $CDCl_3$.

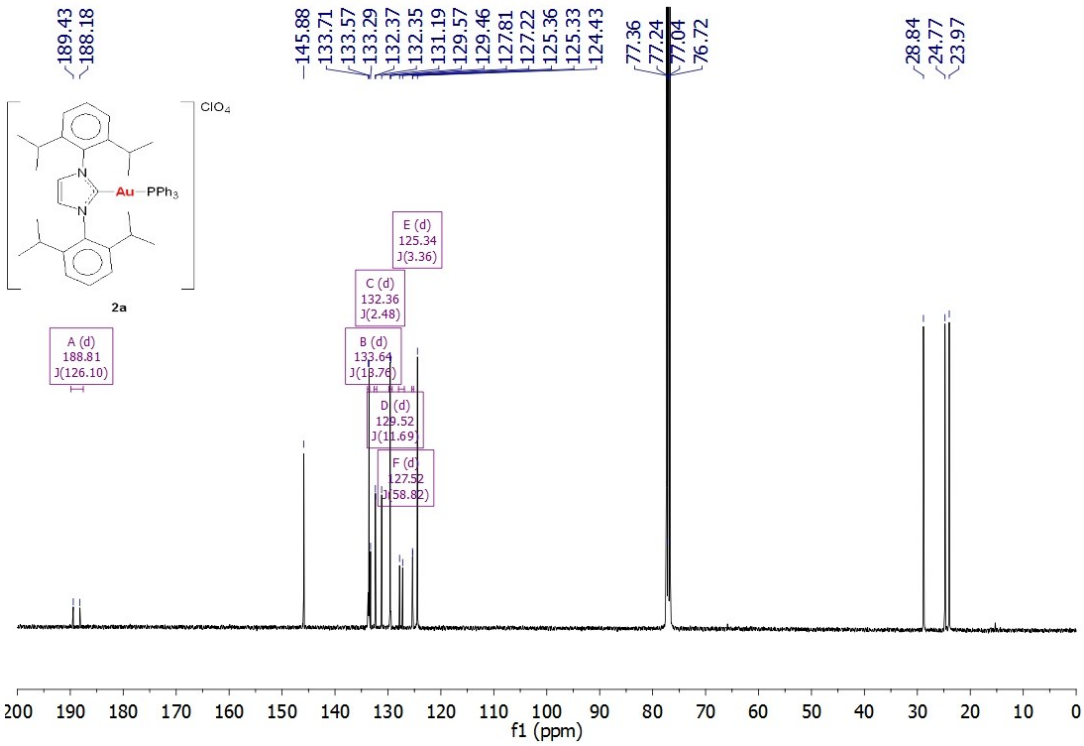

Figure S3. $^{13}C\{^{1}H\}$ NMR spectrum of compound **2a** in $CDCl_3$.

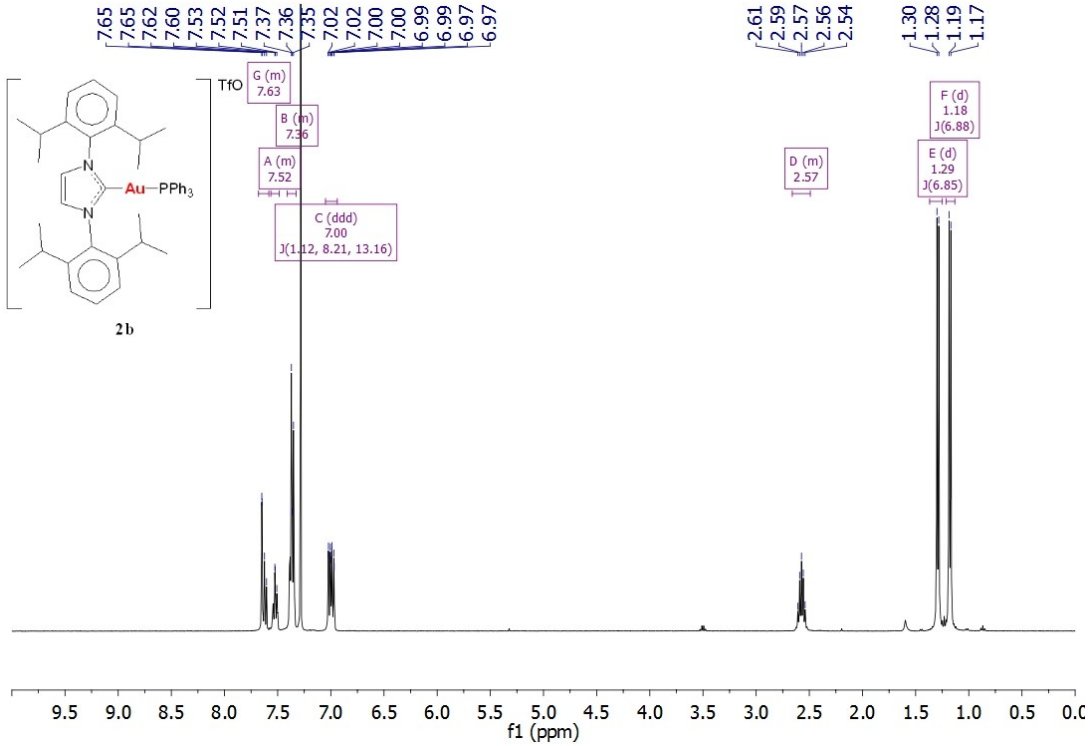

Figure S4. ^{1}H NMR spectrum of compound **2b** in $CDCl_3$.

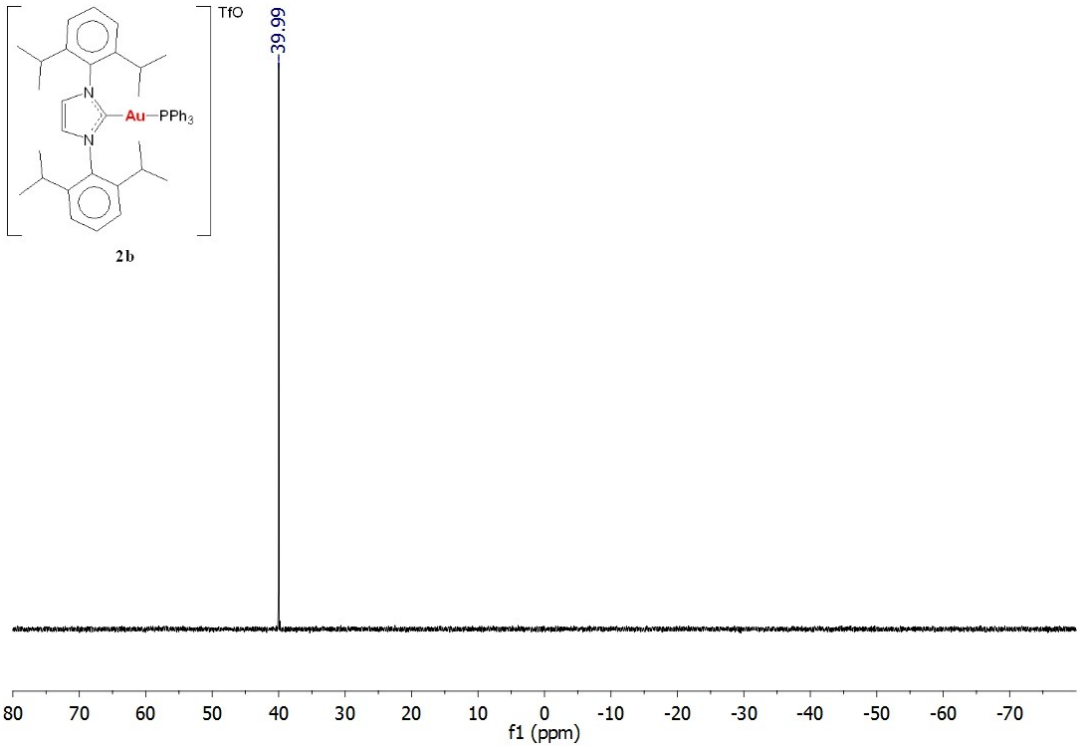

Figure S5. $^{31}P\{^{1}H\}$ NMR spectrum of compound **2b** in $CDCl_3$.

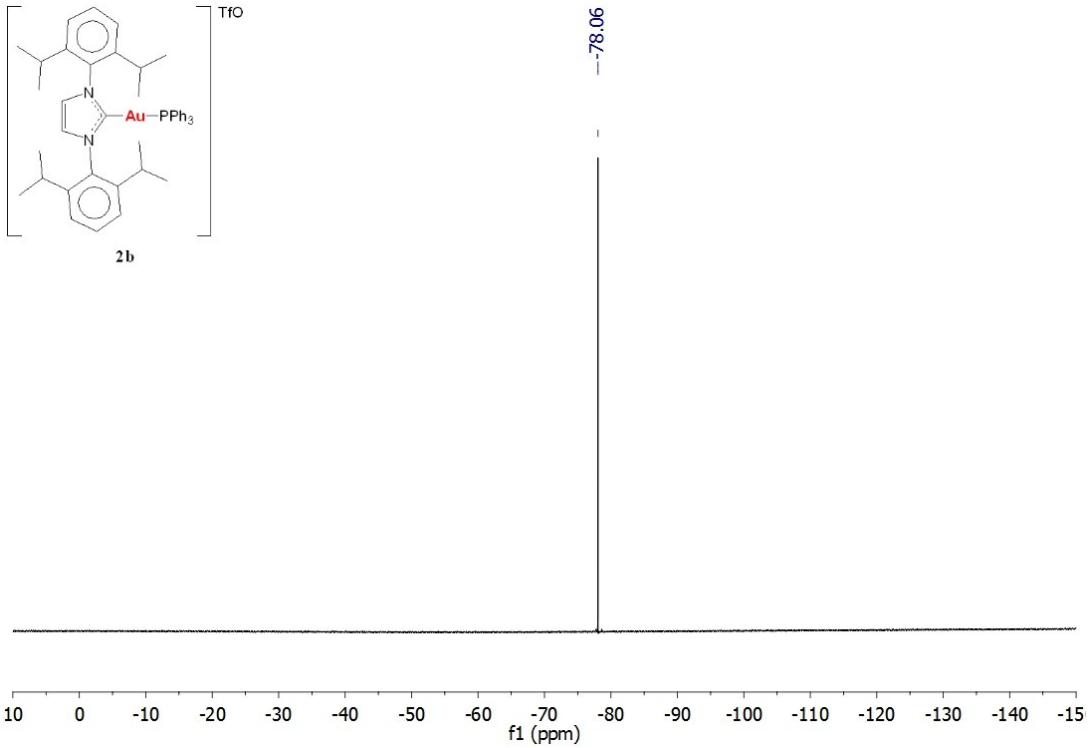

Figure S6. $^{19}F\{^{1}H\}$ NMR spectrum of compound **2b** in $CDCl_3$.

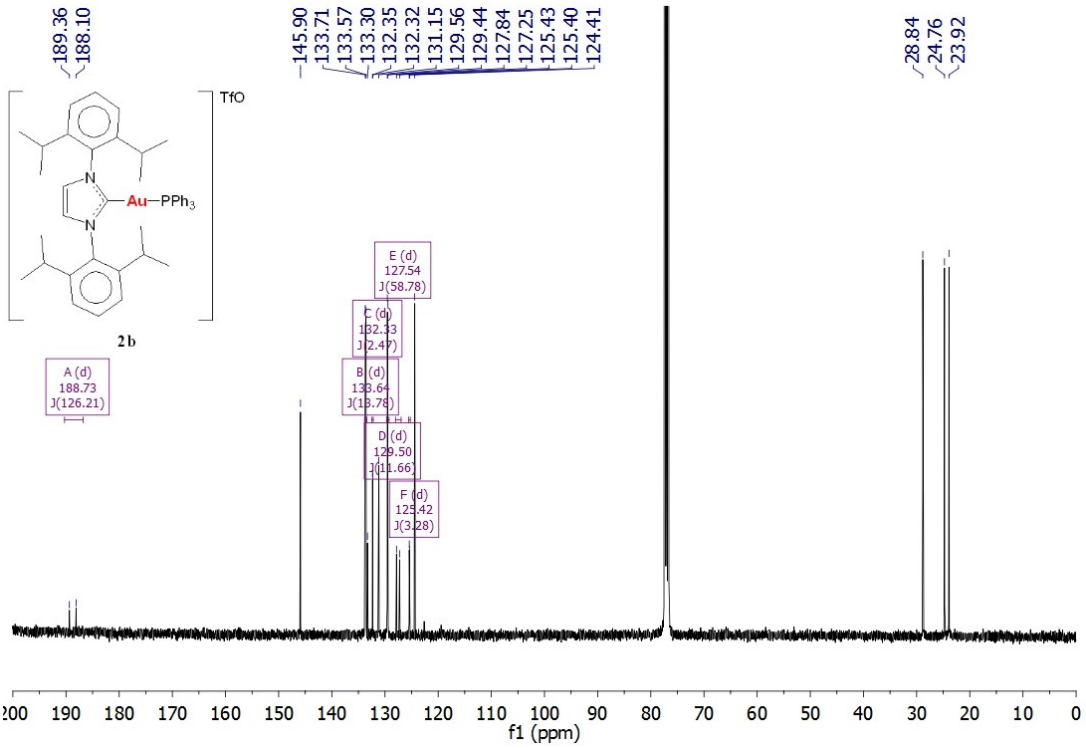

Figure S7. $^{13}C\{^{1}H\}$ NMR spectrum of compound **2b** in $CDCl_3$.

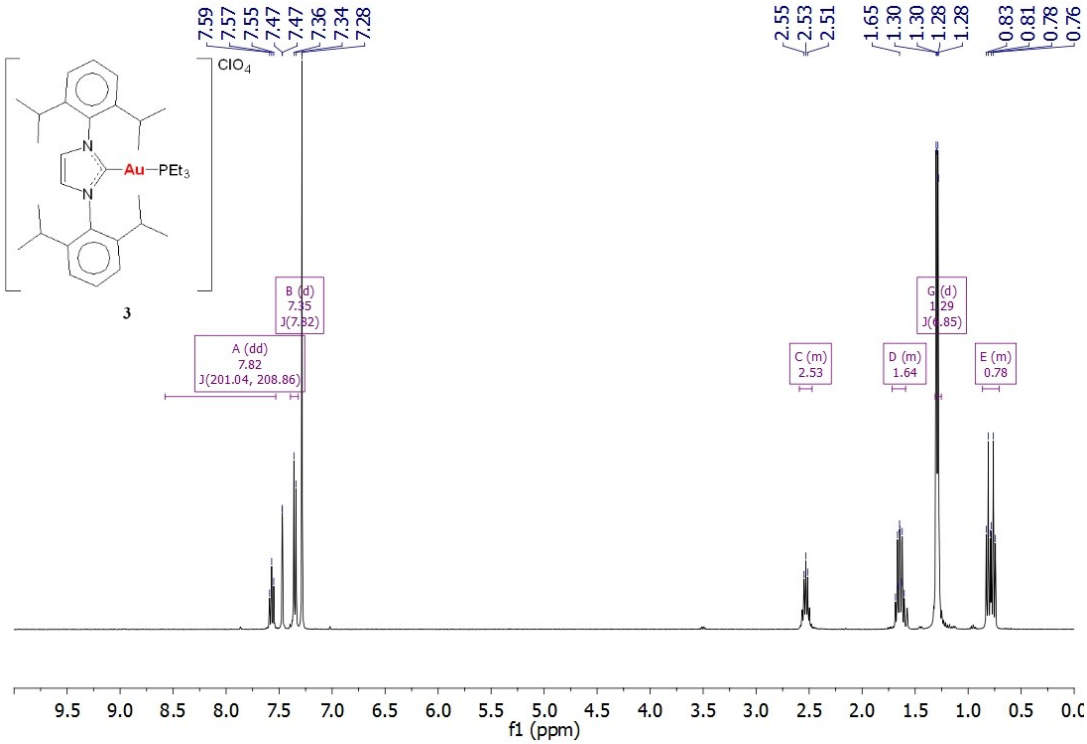

Figure S8. ^{1}H NMR spectrum of compound **3** in $CDCl_3$.

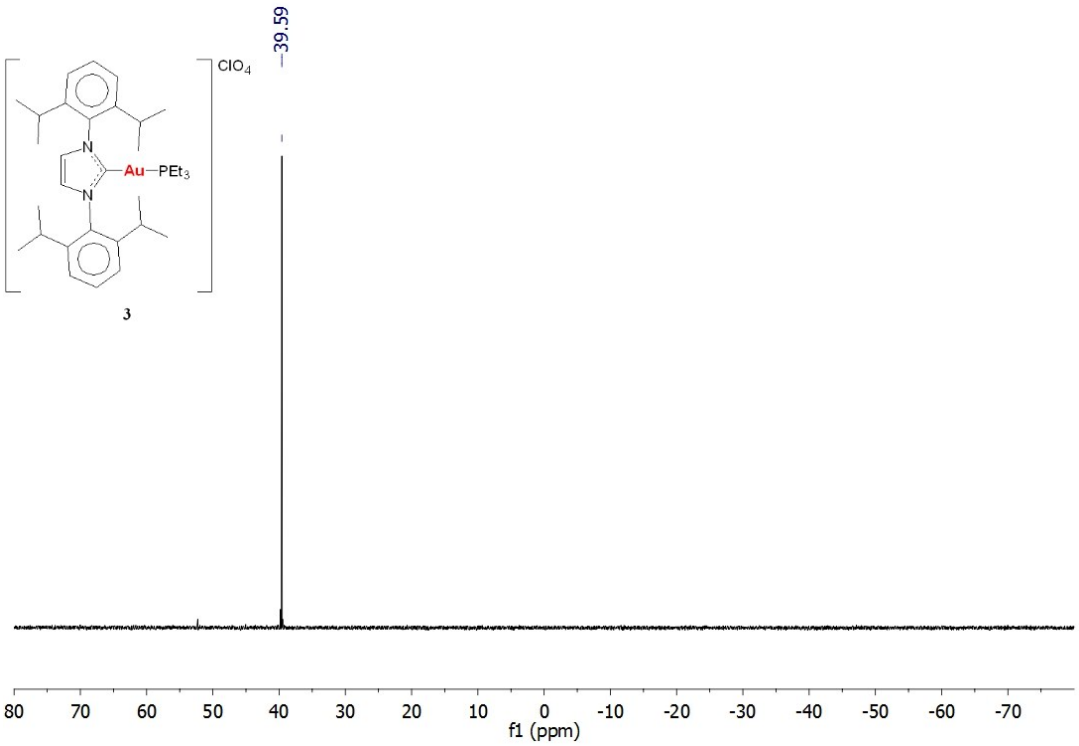

Figure S9. $^{31}P\{^{1}H\}$ NMR spectrum of compound **3** in $CDCl_3$.

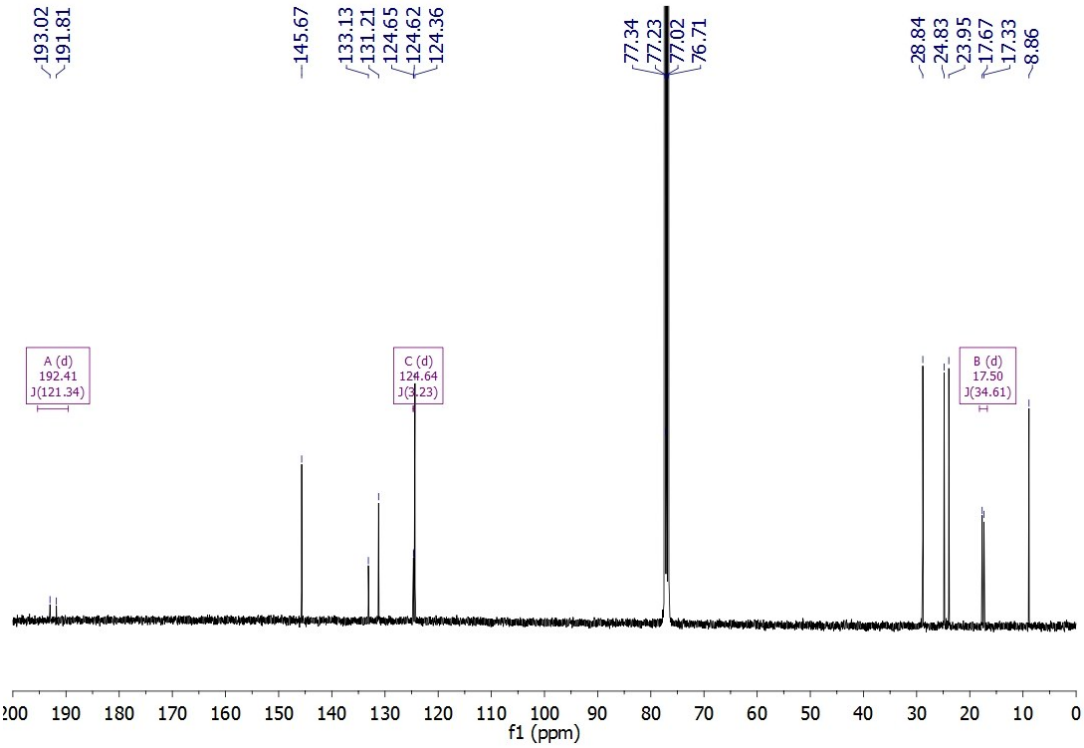

Figure S10. $^{13}C\{^{1}H\}$ NMR spectrum of compound **3** in $CDCl_3$.

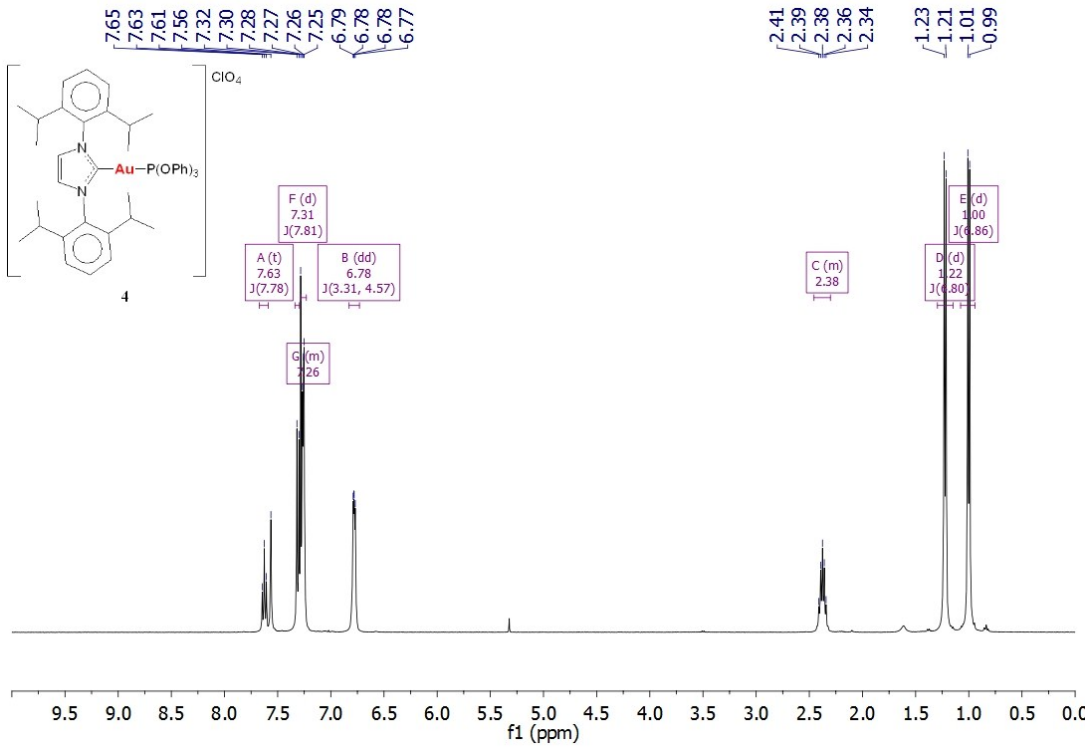

Figure S11. ^{1}H NMR spectrum of compound **4** in $CDCl_3$.

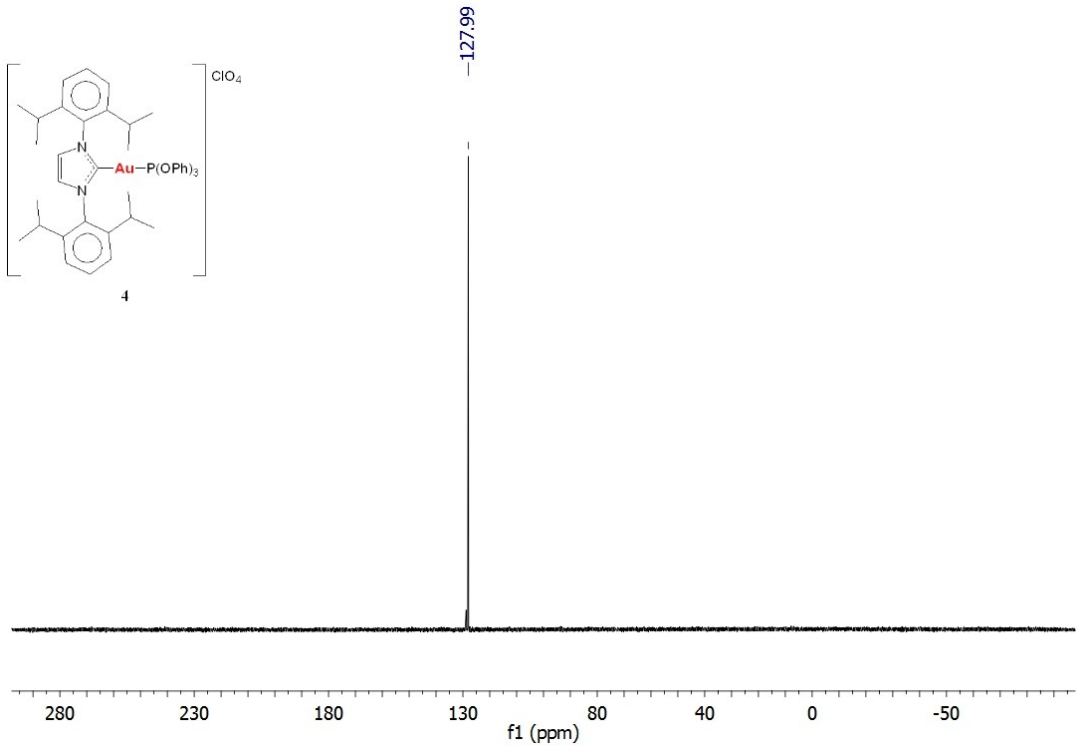

Figure S12. ^{31}P{^{1}H} NMR spectrum of compound **4** in $CDCl_3$.

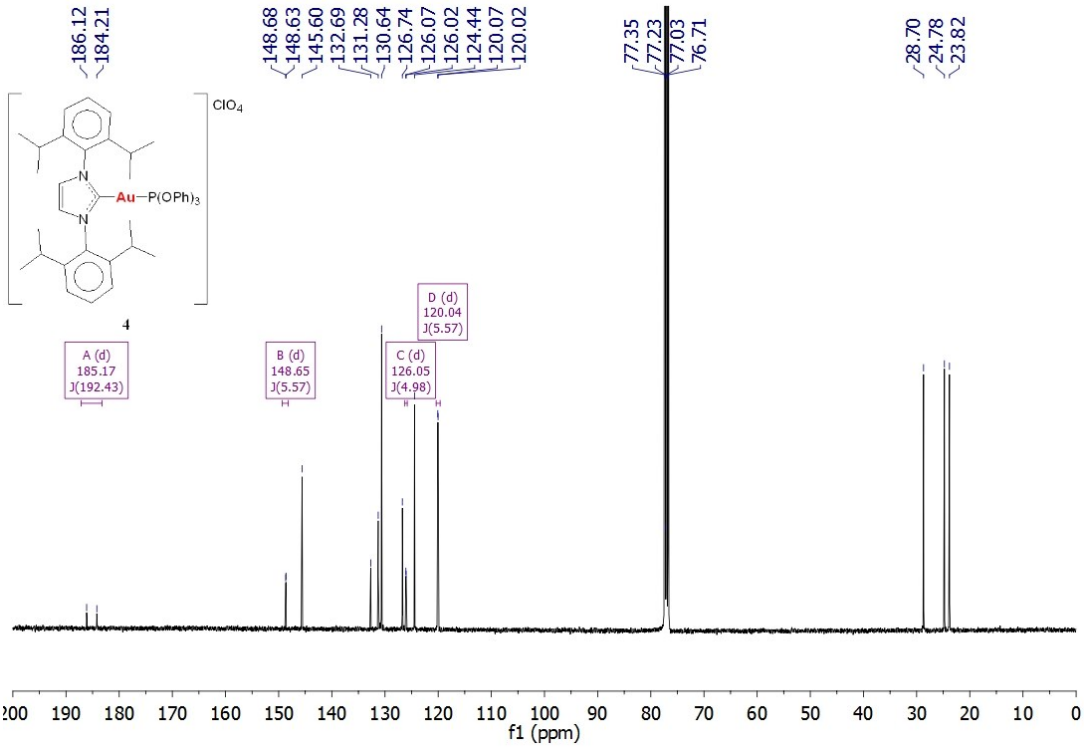

Figure S13. $^{13}C\{^{1}H\}$ NMR spectrum of compound **4** in $CDCl_3$.

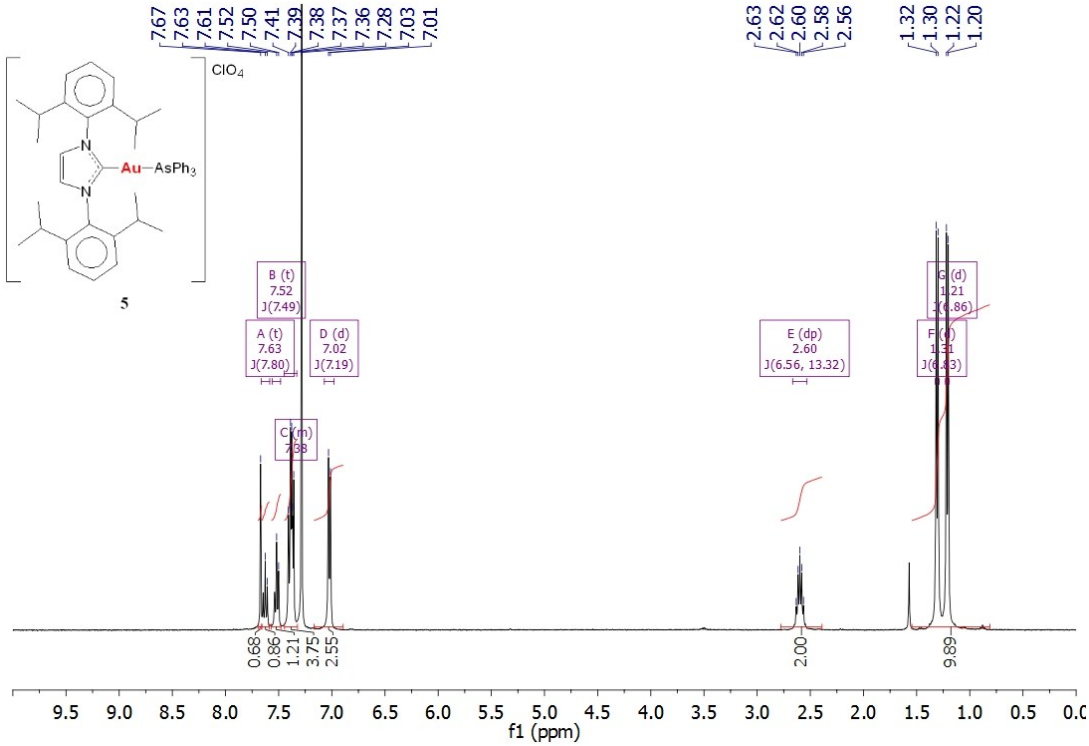

Figure S14. ^{1}H NMR spectrum of compound **5** in $CDCl_3$.

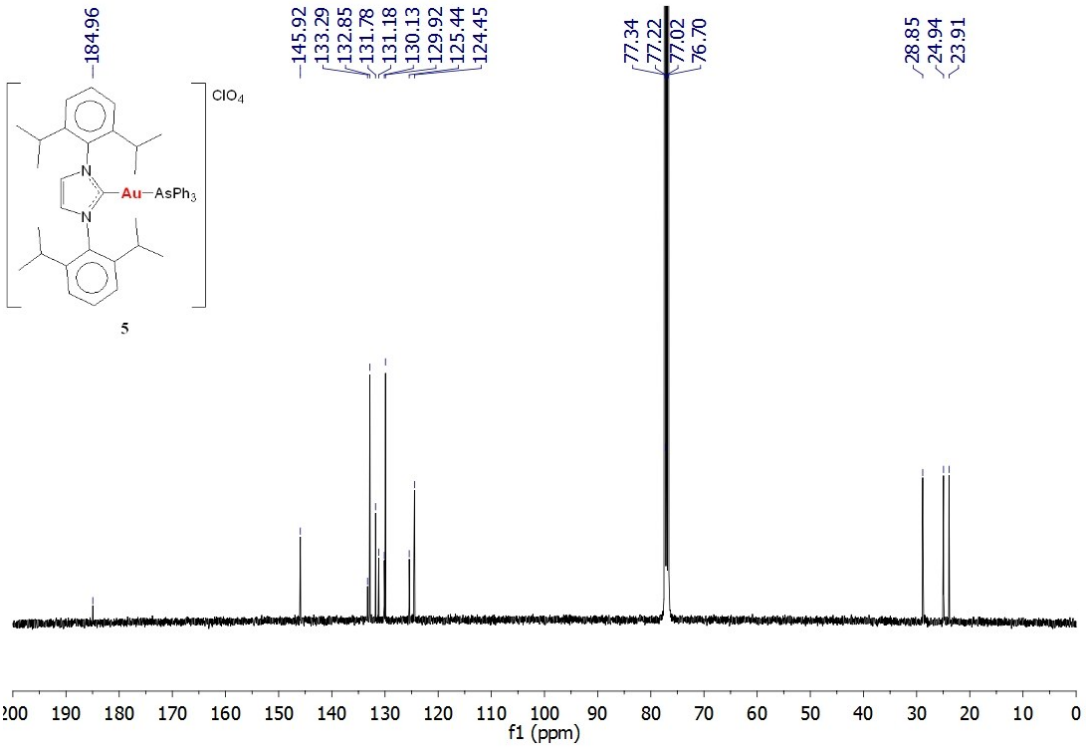

Figure S15. $^{13}C\{^{1}H\}$ NMR spectrum of compound **5** in $CDCl_3$.

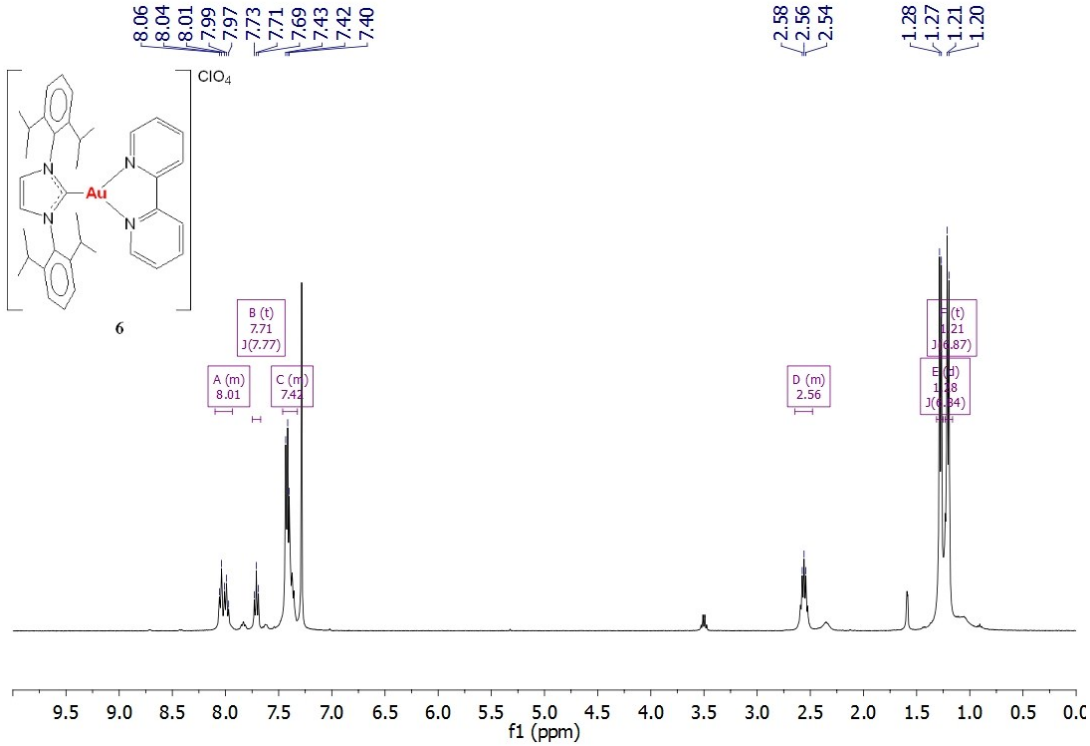

Figure S16. ^{1}H NMR spectrum of compound **6** in $CDCl_3$.

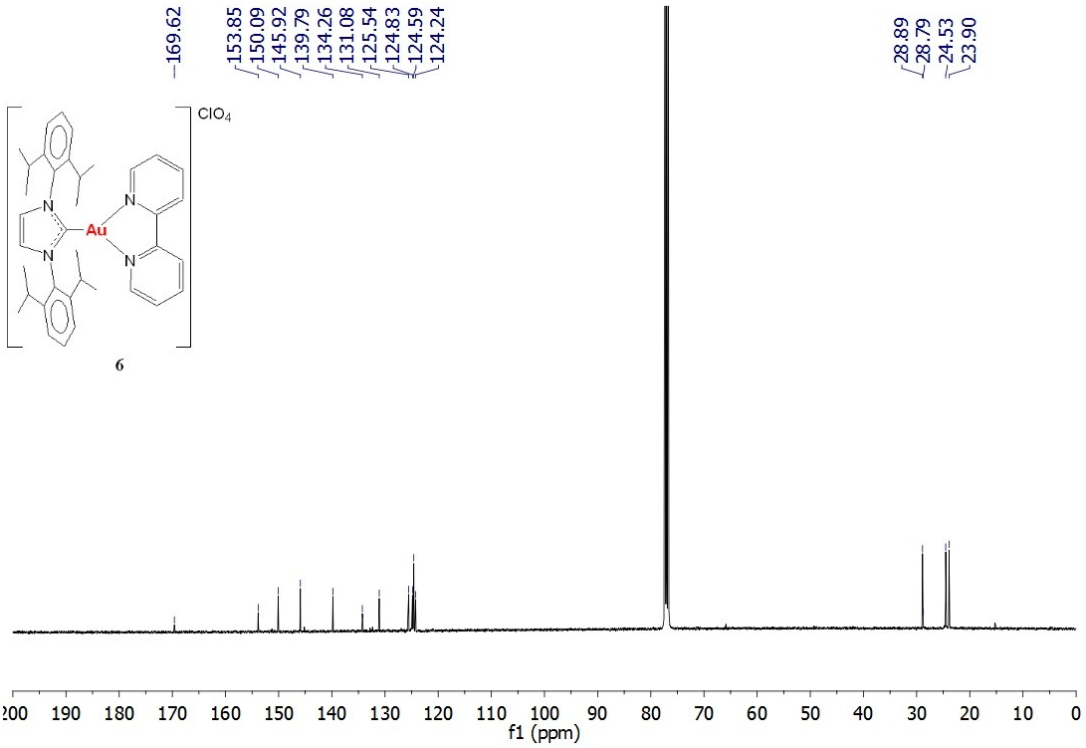

Figure S17. $^{13}C\{^{1}H\}$ NMR spectrum of compound **6** in $CDCl_3$.

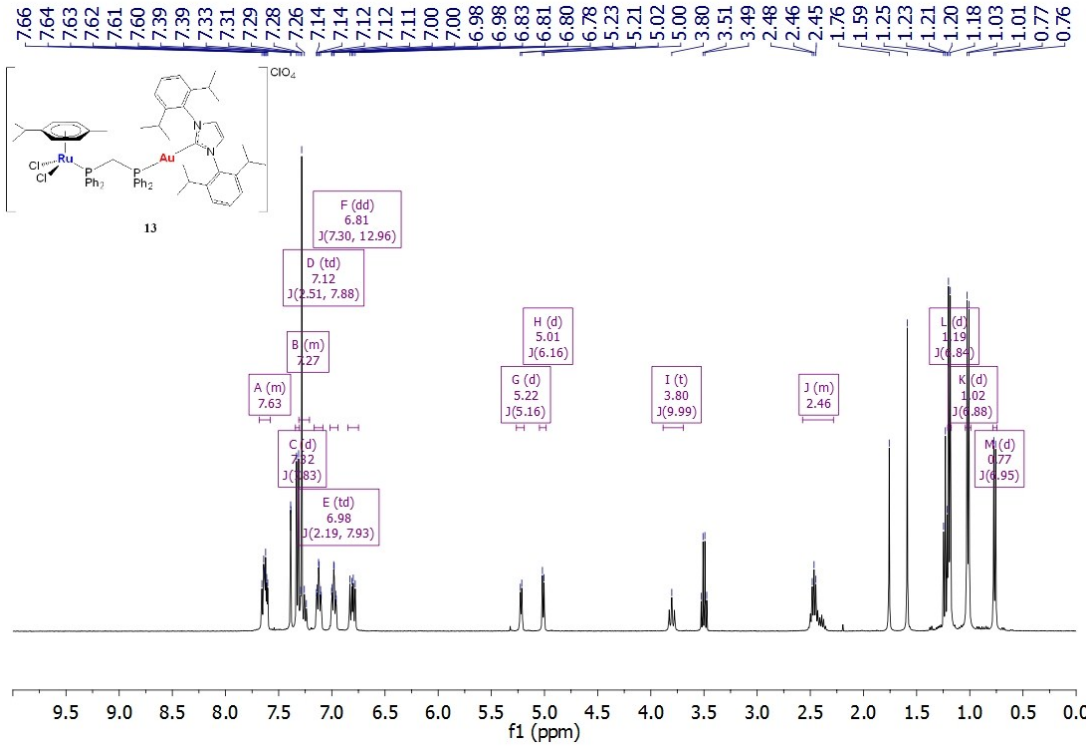

Figure S18. ^{1}H NMR spectrum of compound **13** in $CDCl_3$.

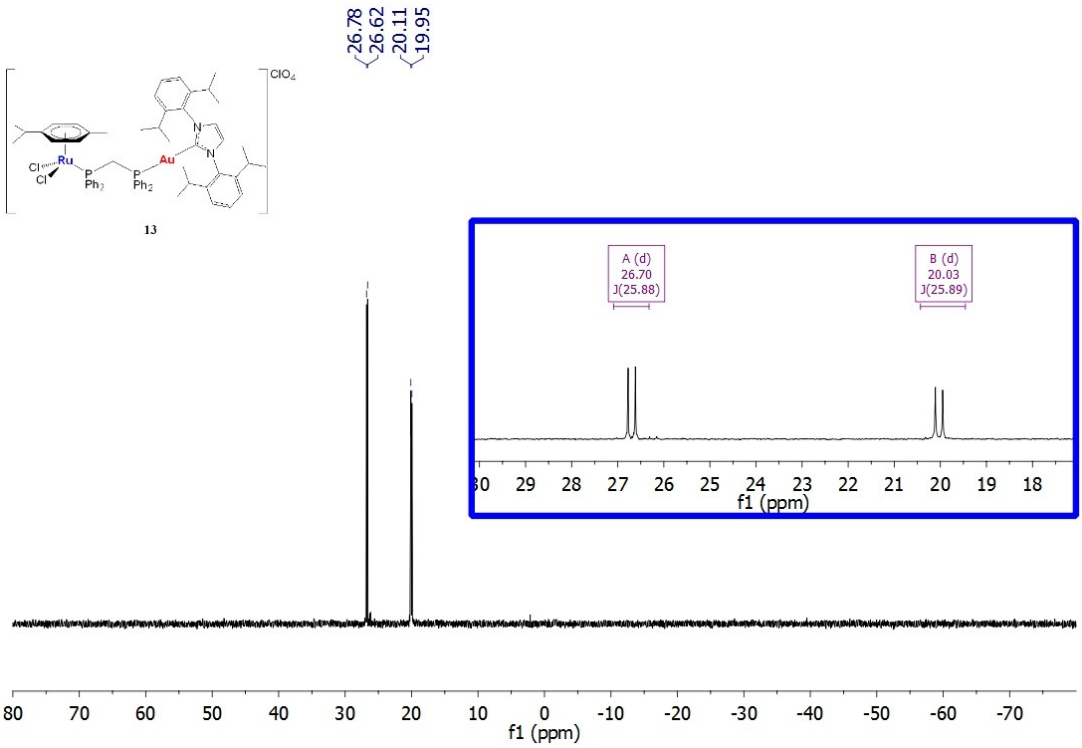

Figure S19. $^{31}P\{^{1}H\}$ NMR spectrum of compound **13** in $CDCl_3$.

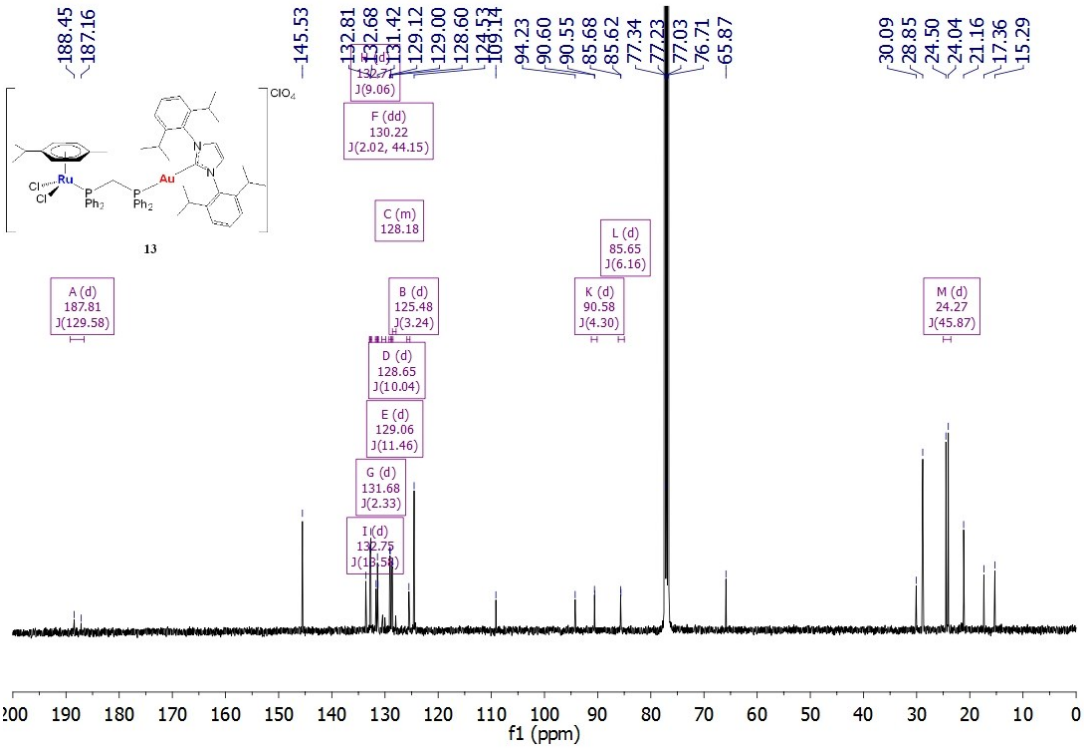

Figure S20. $^{13}C\{^{1}H\}$ NMR spectrum of compound **13** in $CDCl_3$.

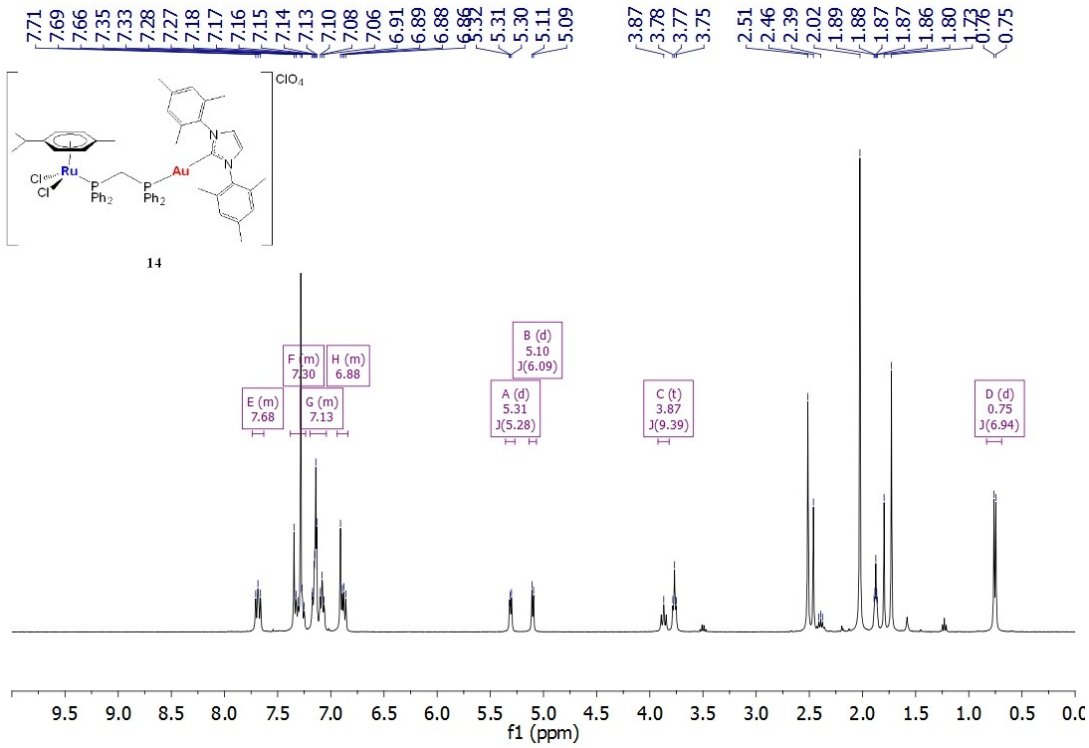

Figure S21. ^{1}H NMR spectrum of compound **14** in $CDCl_3$.

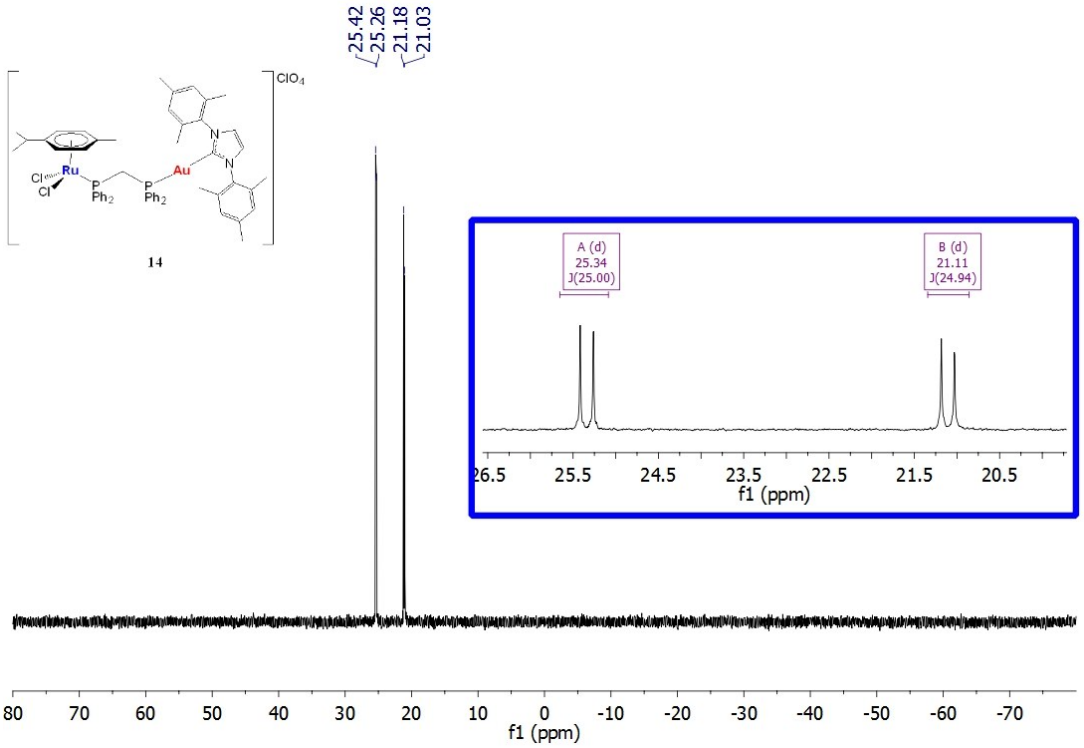

Figure S22. ^{31}P{^{1}H} NMR spectrum of compound **14** in $CDCl_3$.

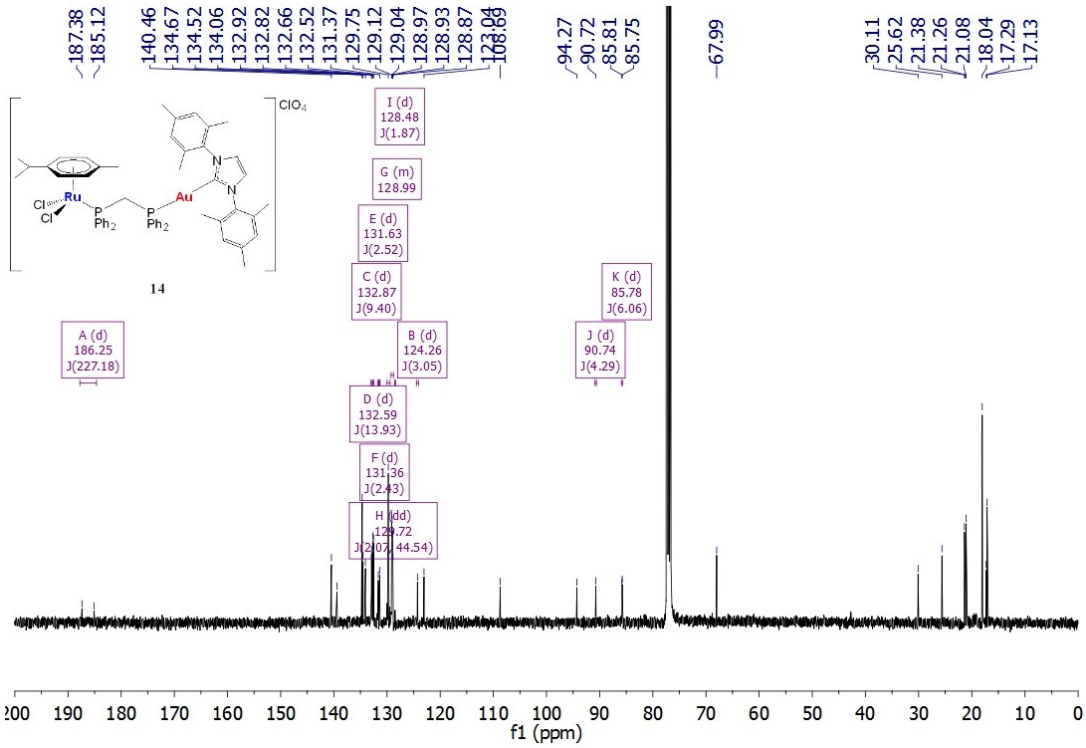

Figure S23. $^{13}C\{^{1}H\}$ NMR spectrum of compound **14** in $CDCl_3$.

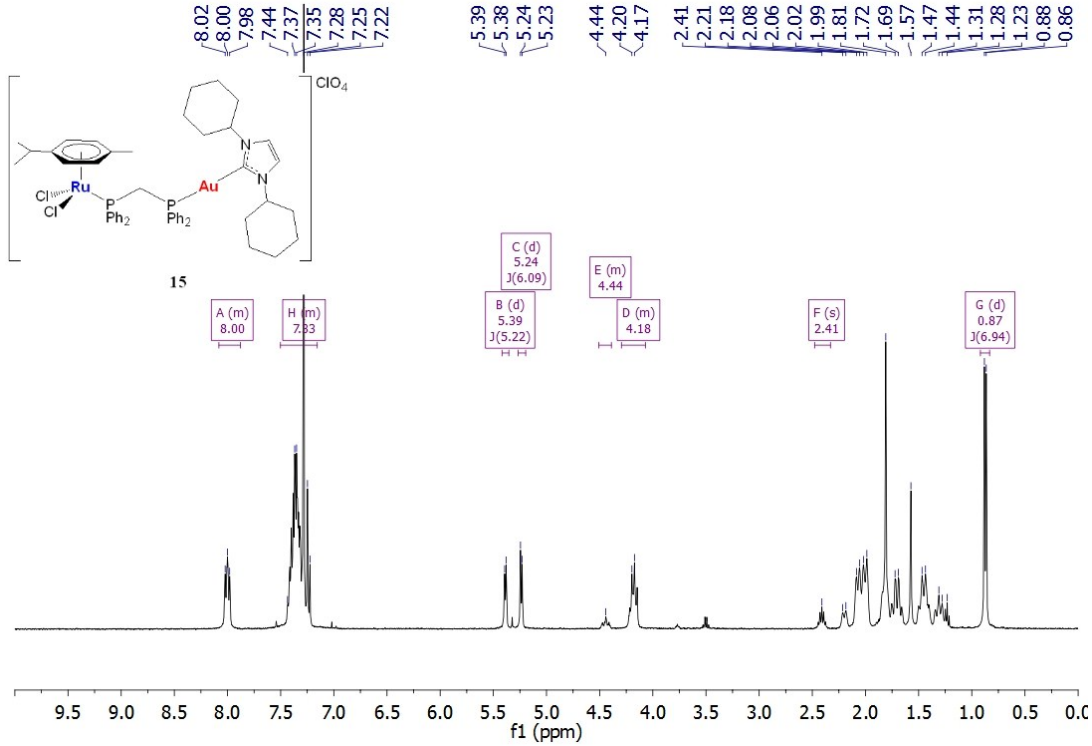

Figure S24. ^{1}H NMR spectrum of compound **15** in $CDCl_3$.

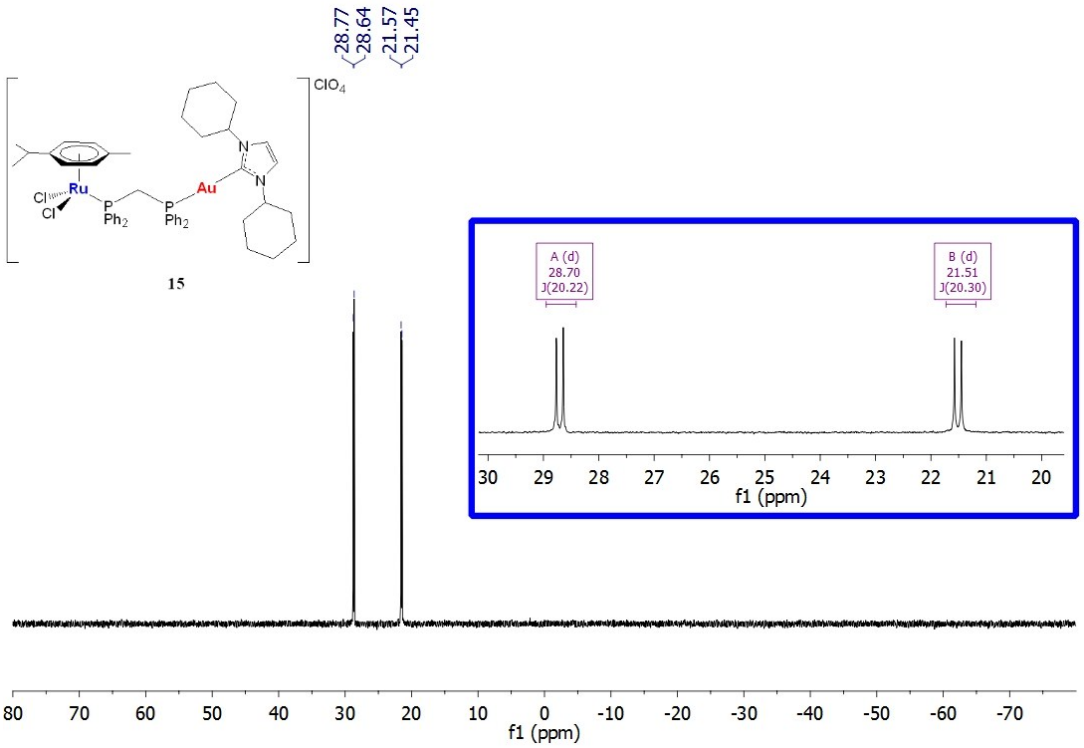

Figure S25. $^{31}P\{^{1}H\}$ NMR spectrum of compound **15** in $CDCl_3$.

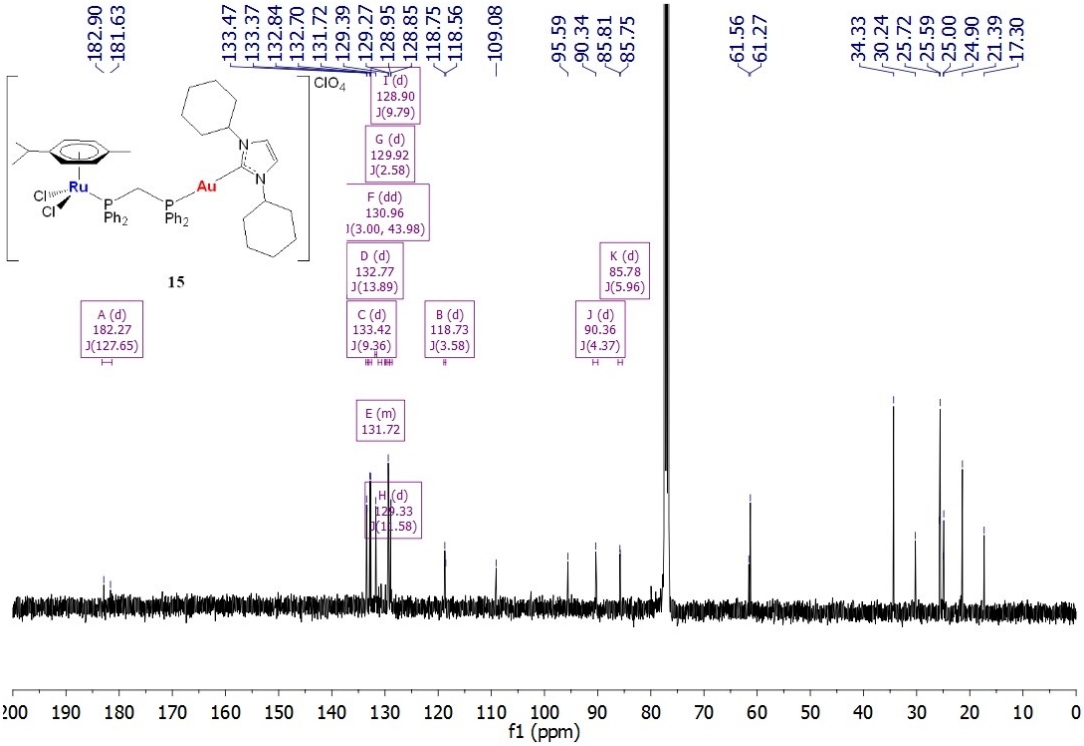

Figure S26. $^{13}C\{^{1}H\}$ NMR spectrum of compound **15** in $CDCl_3$.

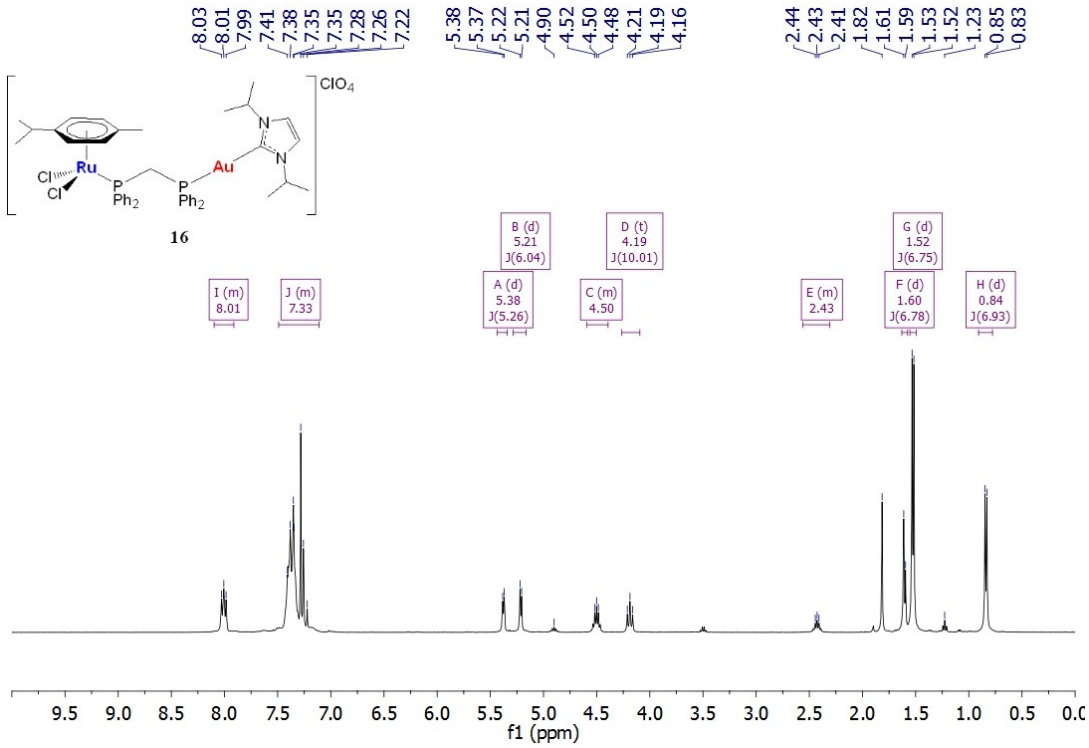

Figure S27. ^{1}H NMR spectrum of compound **16** in $CDCl_3$.

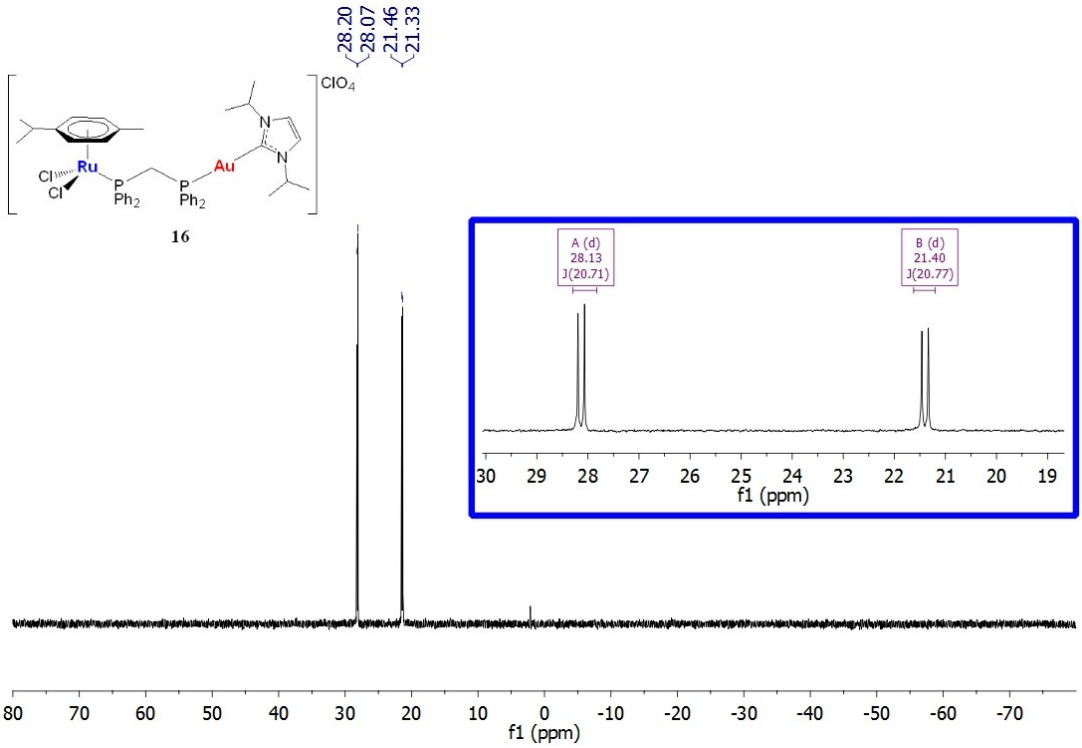

Figure S28. ^{31}P{^{1}H} NMR spectrum of compound **16** in $CDCl_3$.

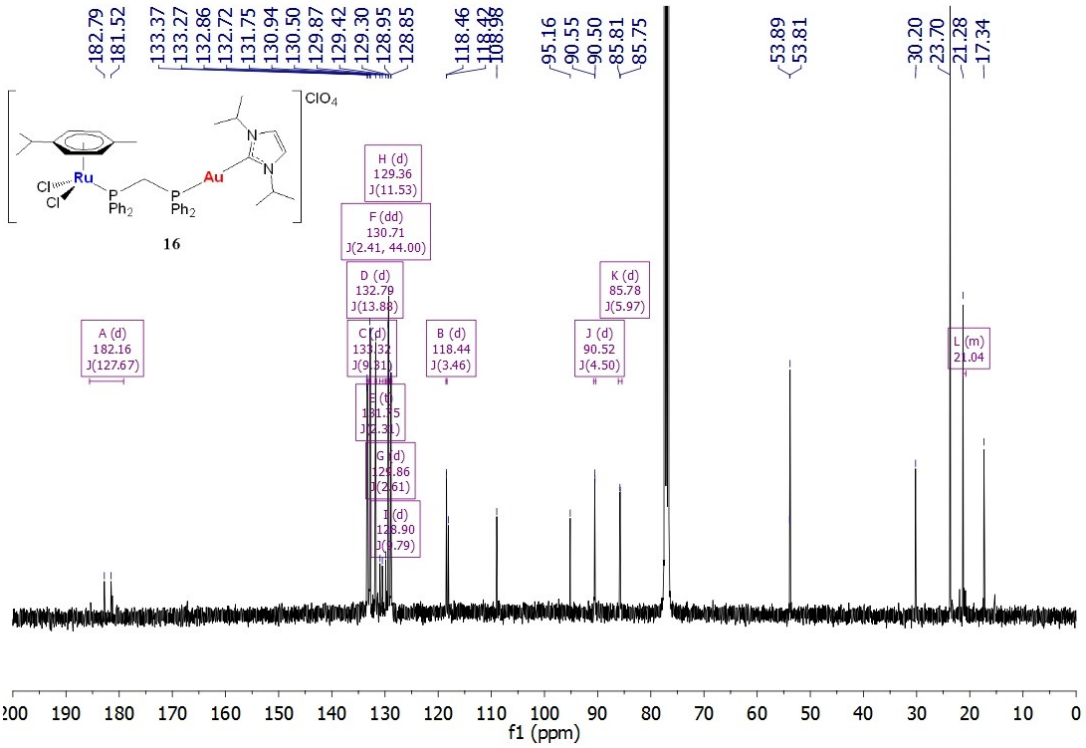

Figure S29. $^{13}C\{^{1}H\}$ NMR spectrum of compound **16** in $CDCl_3$.

3. Selected NMR spectra of decomposition of compounds **13-16** in DMSO-d_6

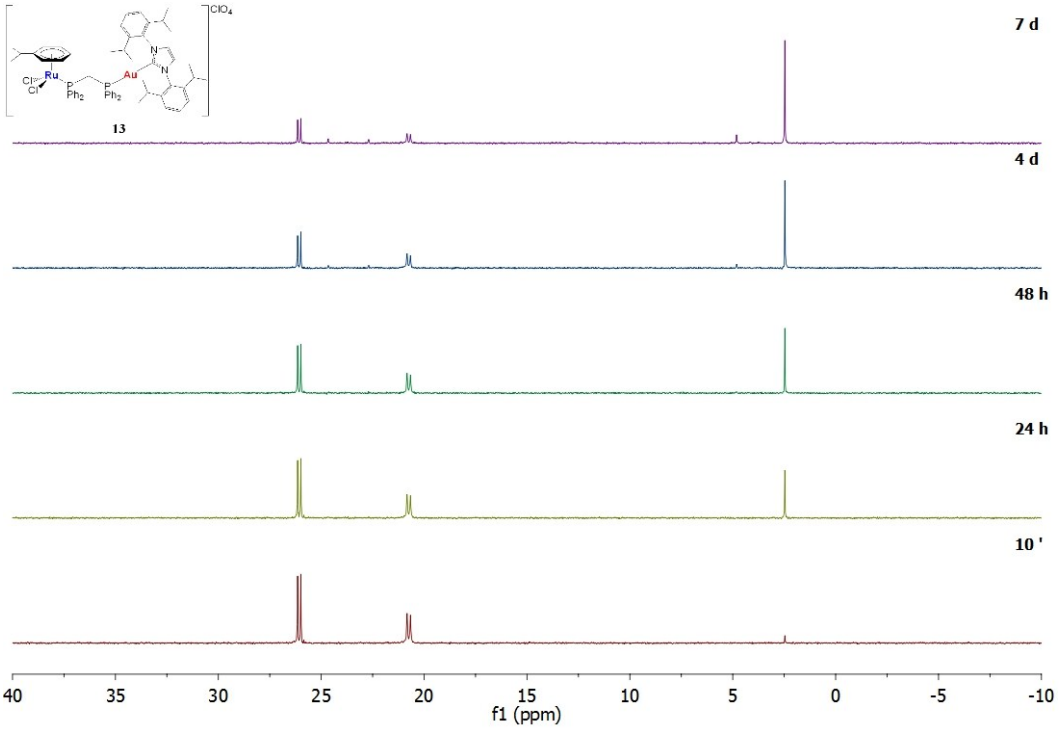

Figure S30. Time course $^{31}P\{^{1}H\}$ NMR spectrum in DMSO-d_6 of compound **13**. $t_{½}$ = 7d.

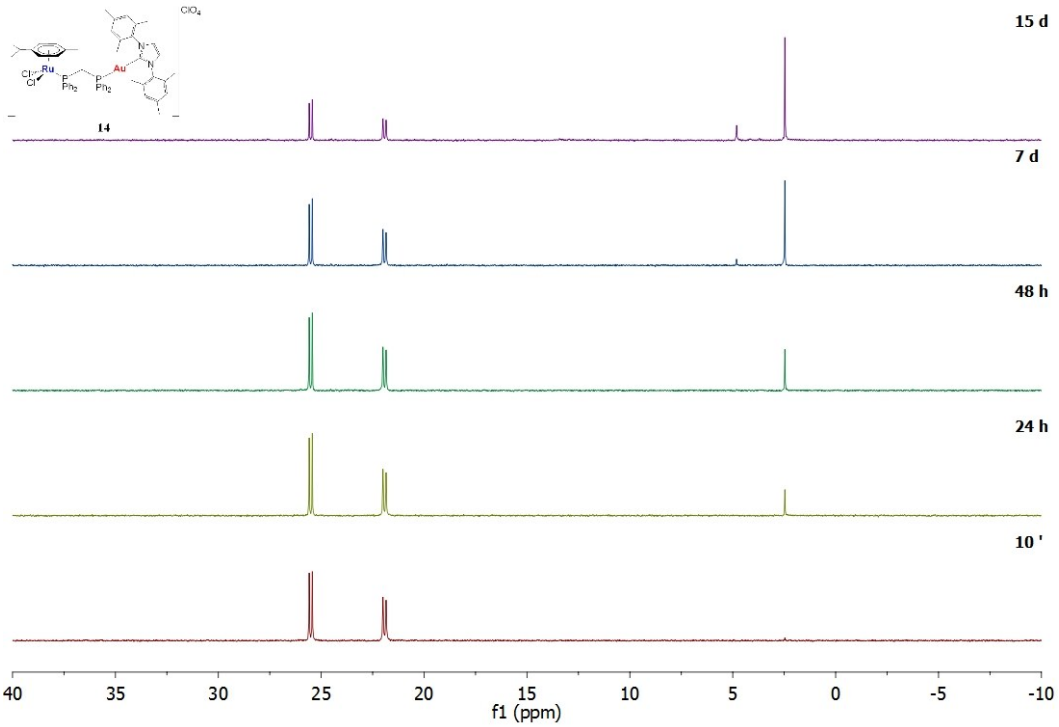

Figure S31. Time course $^{31}P\{^{1}H\}$ NMR spectrum in DMSO-d_6 of compound **14**. $t_{½}$ = 15d.

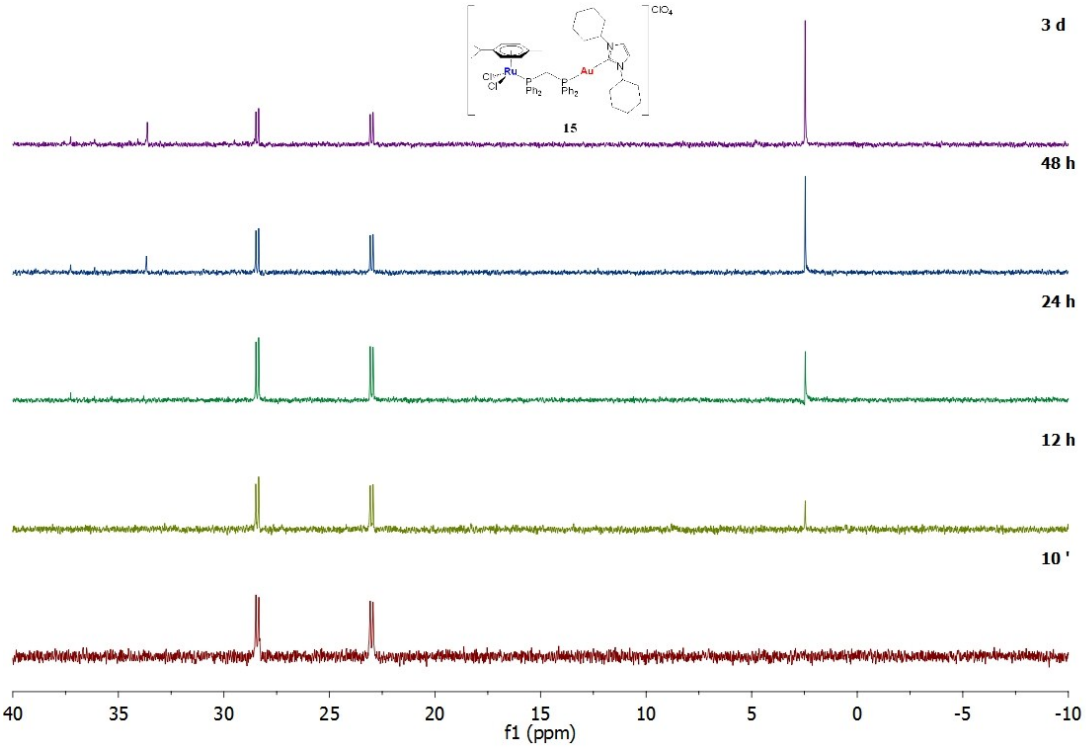

Figure S32. Time course $^{31}P\{^{1}H\}$ NMR spectrum in DMSO-d_6 of compound **15**. $t_{½}$ = 3d.

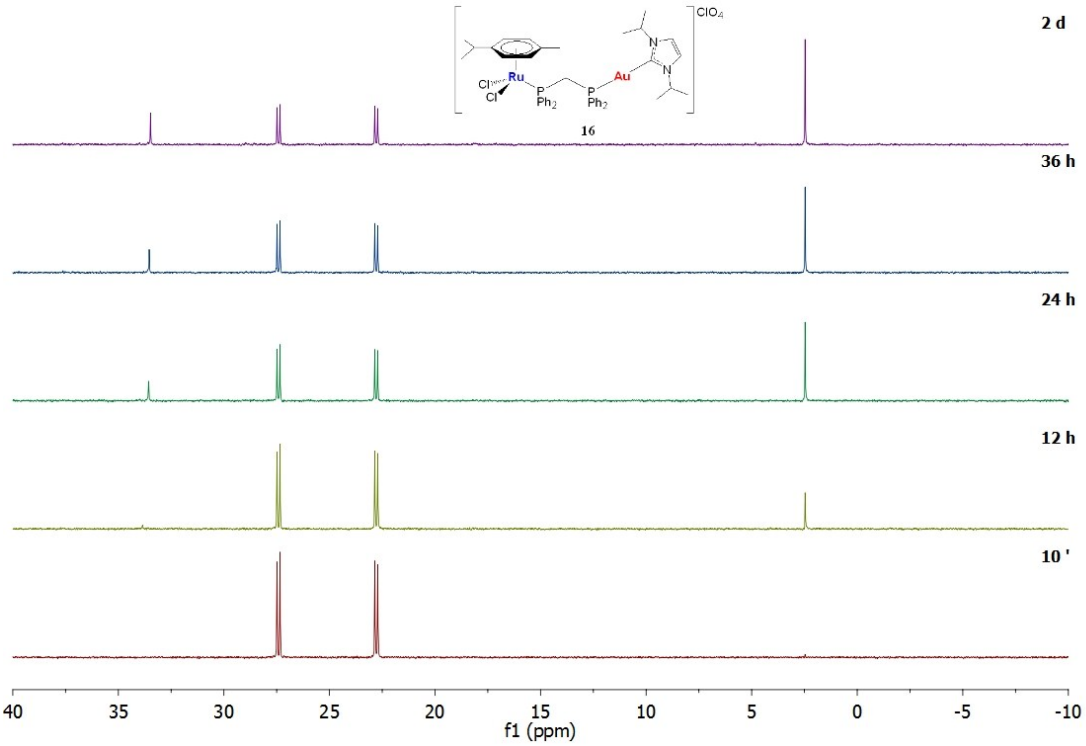

Figure S33. Time course $^{31}P\{^{1}H\}$ NMR spectrum in DMSO-d_6 of compound **16**. $t_{½}$ = 2d.

4. MS ESI+ spectra of all compounds and theoretical isotopic distributions of relevant peaks

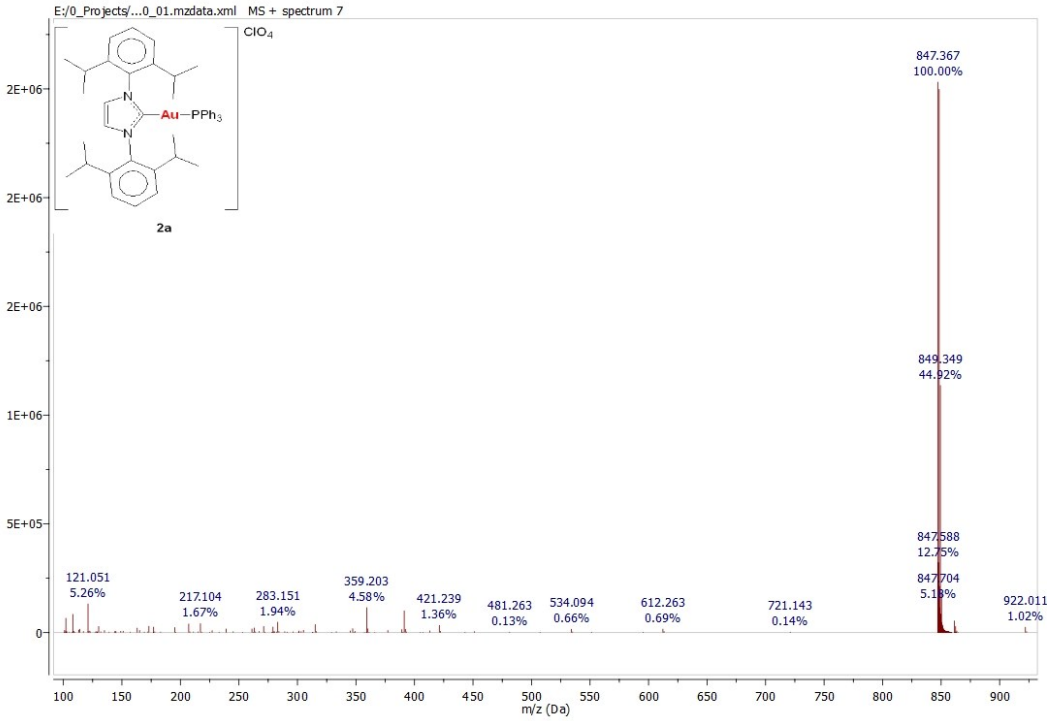

Figure S34. Overall MS ESI+ spectrum of compound **2a** in CH_3CN/H_2O (95:5) solution.

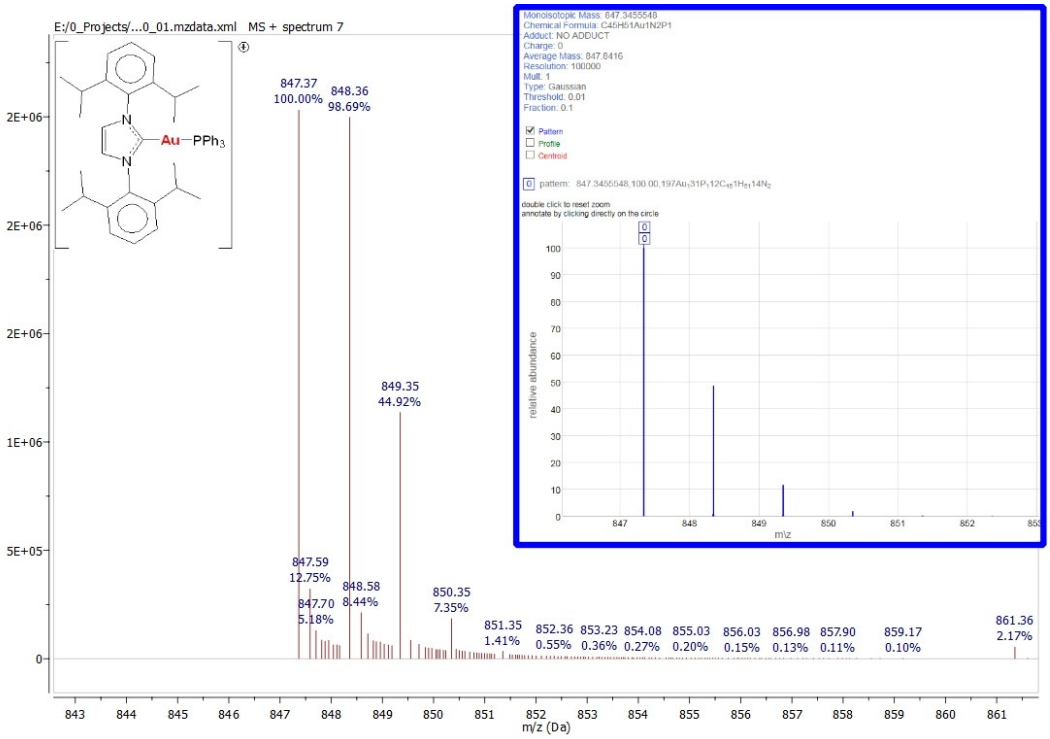

Figure S35. Magnification of peak at [m/z]: 847.36 $[Au(IPr)(PPh_3)]^+$ in MS ESI+ of compound **2a** in CH_3CN/H_2O (95:5) solution. Insert: theoretical isotopic distribution.

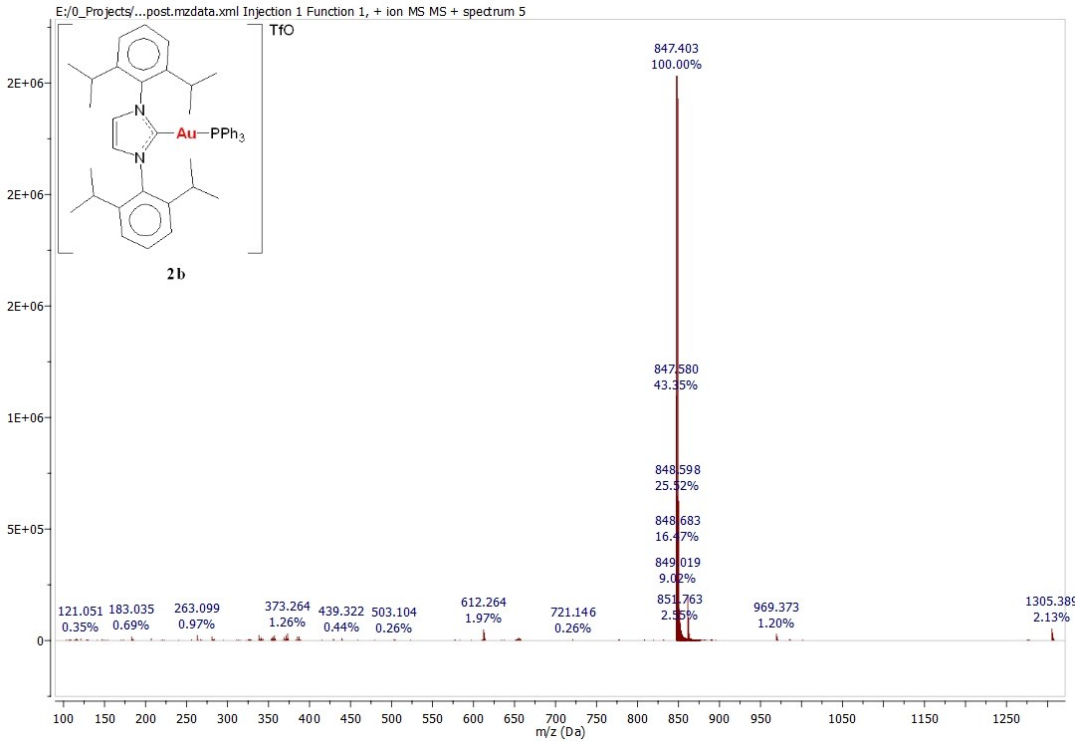

Figure S36. Overall MS ESI+ spectrum of compound **2b** in CH_3CN/H_2O (95:5) solution.

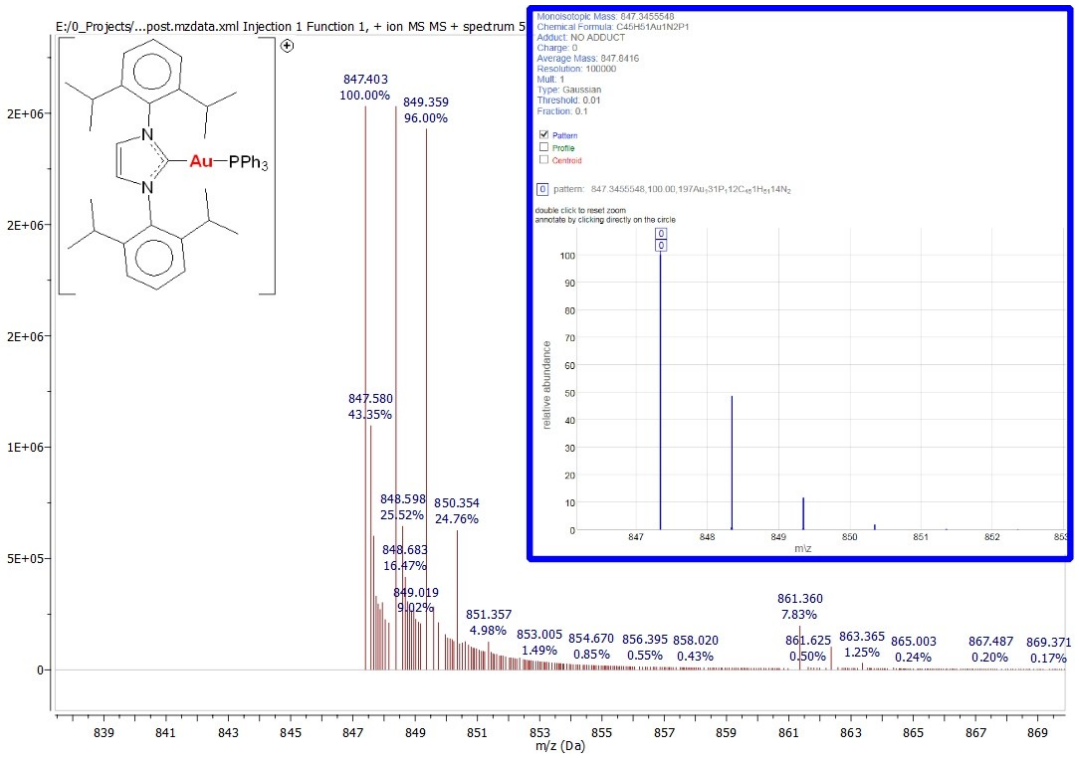

Figure S37. Magnification of peak at [m/z]: 847.36 $[Au(IPr)(PPh_3)]^+$ in MS ESI+ of compound **2b** in CH_3CN/H_2O (95:5) solution. Insert: theoretical isotopic distribution.

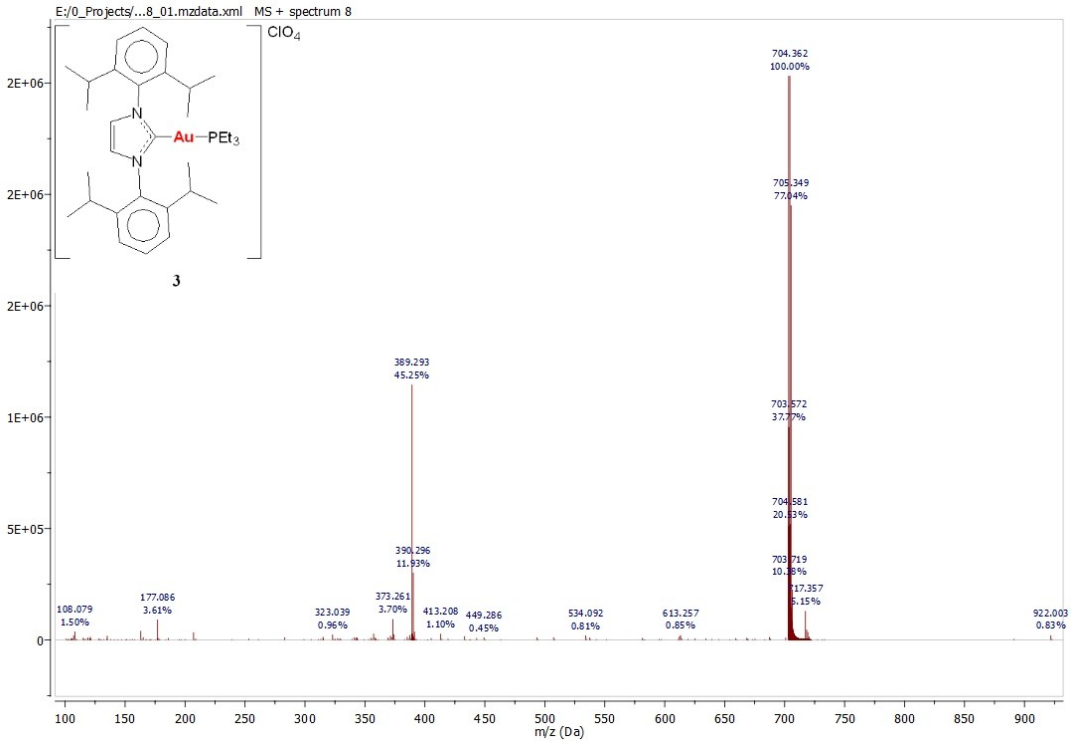

Figure S38. Overall MS ESI+ spectrum of compound **3** in CH_3CN/H_2O (95:5) solution.

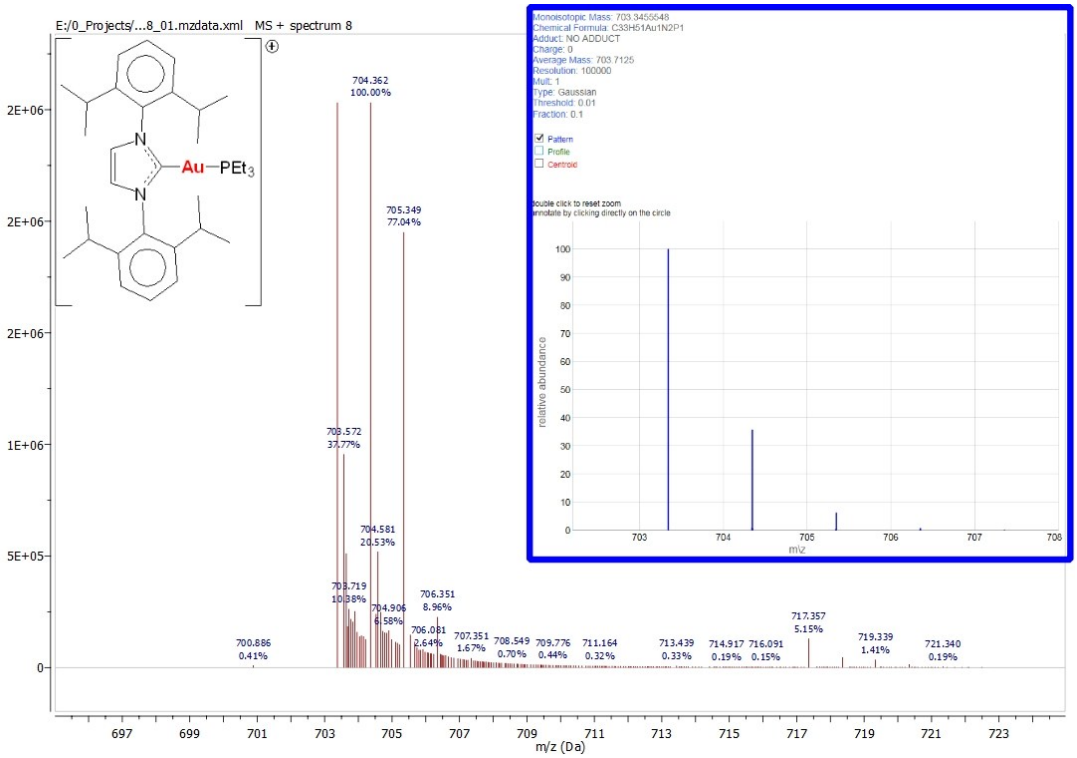

Figure S39. Magnification of peak at [m/z]: 703.36 $[Au(IPr)(PEt_3)]^+$ in MS ESI+ of compound **3** in CH_3CN/H_2O (95:5) solution. Insert: theoretical isotopic distribution.

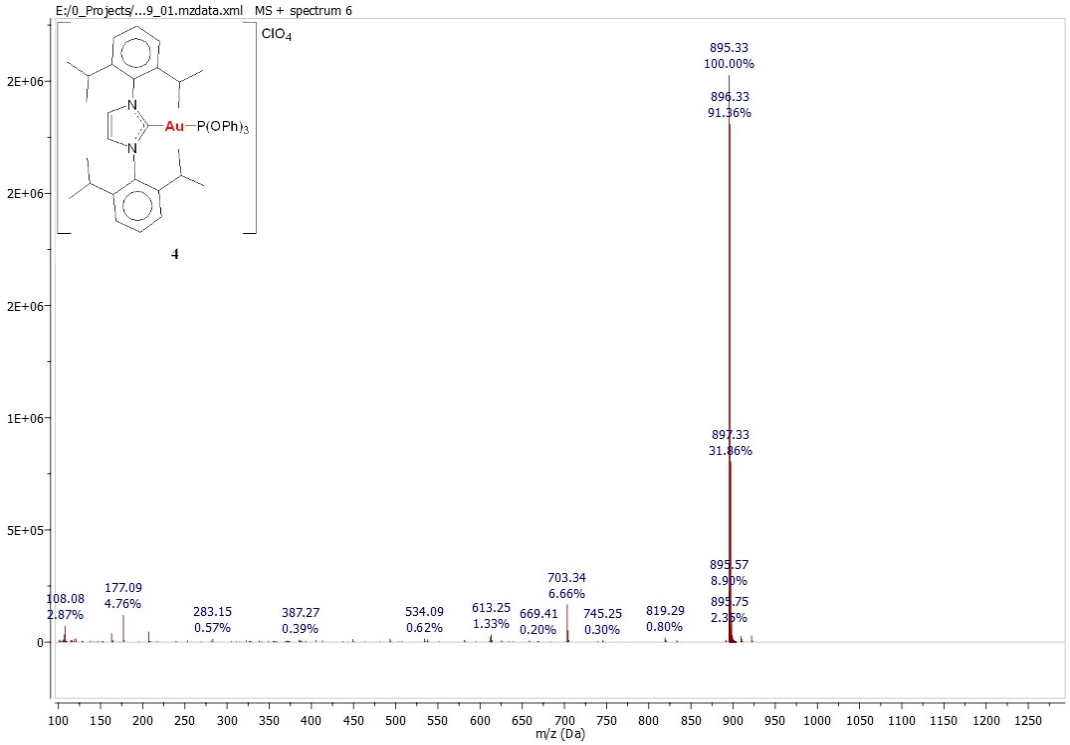

Figure S40. Overall MS ESI+ spectrum of compound **4** in CH_3CN/H_2O (95:5) solution.

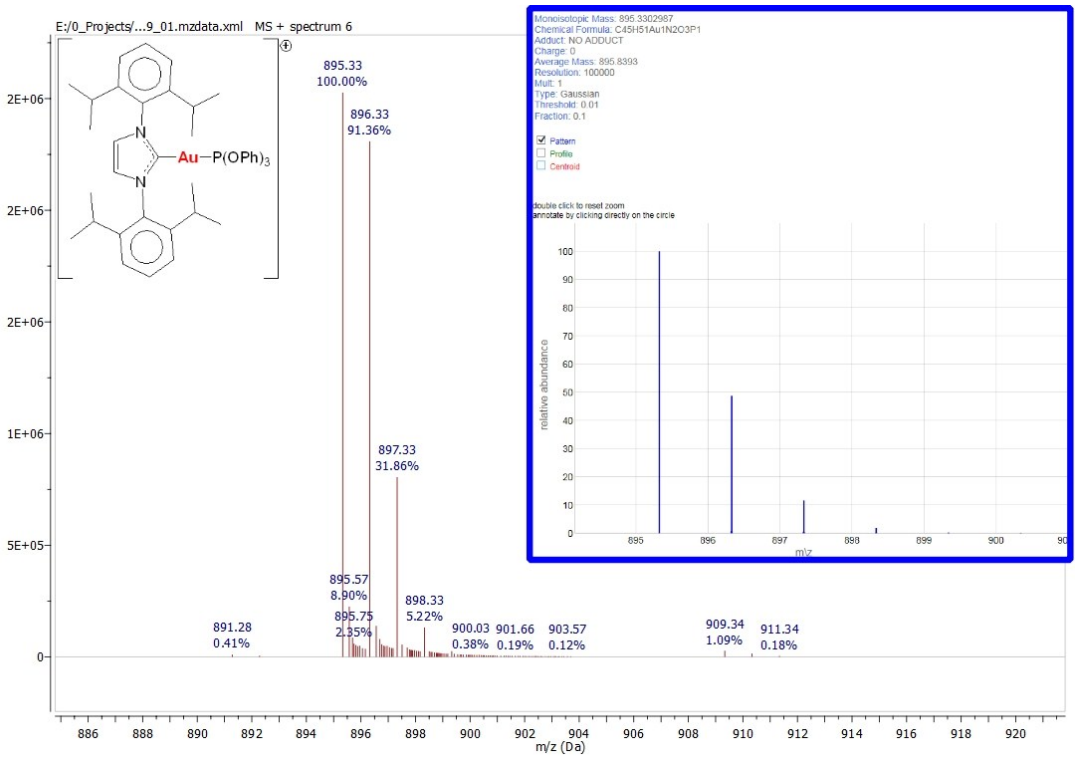

Figure S41. Magnification of peak at [m/z]: 895.33 $[Au(IPr)(P(OPh)_3)]^+$ in MS ESI+ of compound **4** in CH_3CN/H_2O (95:5) solution. Insert: theoretical isotopic distribution.

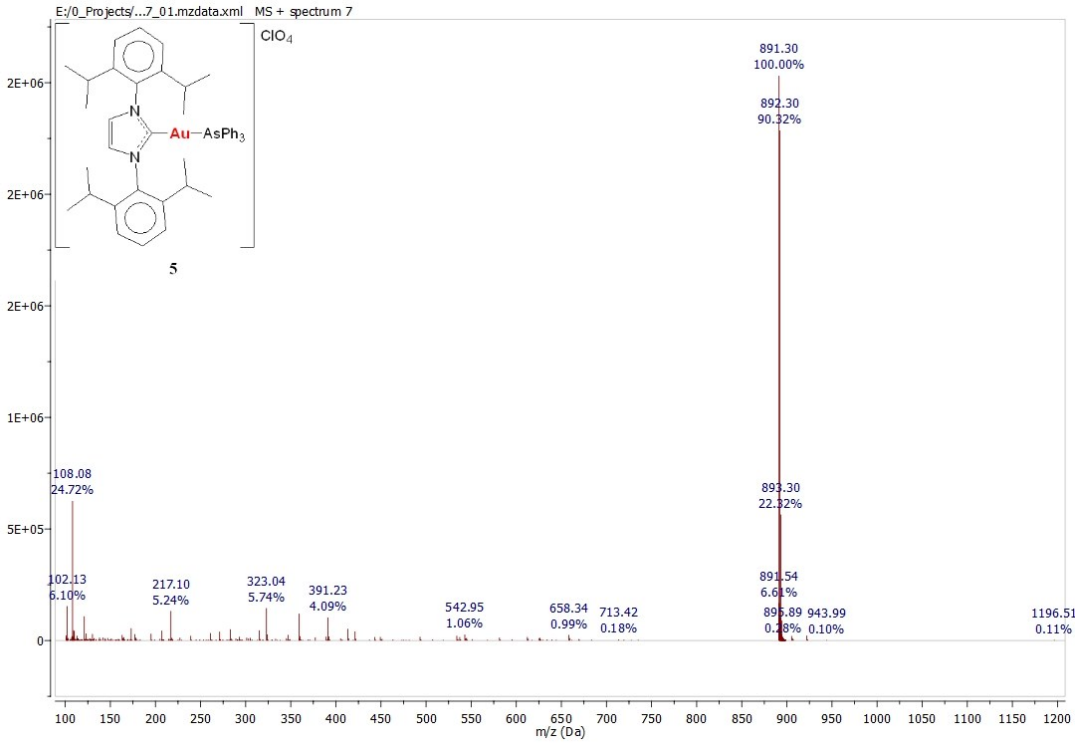

Figure S42. Overall MS ESI+ spectrum of compound **5** in CH_3CN/H_2O (95:5) solution.

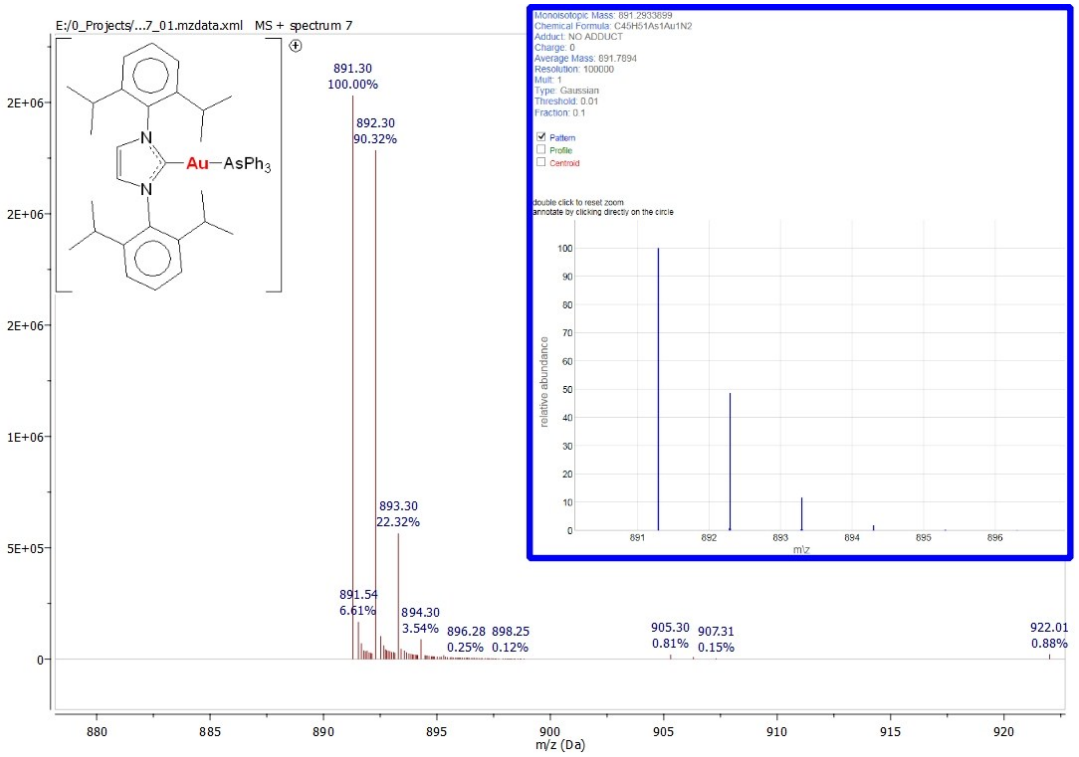

Figure S43. Magnification of peak at [m/z]: 891.30 $[Au(IPr)(AsPh_3)]^+$ in MS ESI+ of compound **5** in CH_3CN/H_2O (95:5) solution. Insert: theoretical isotopic distribution.

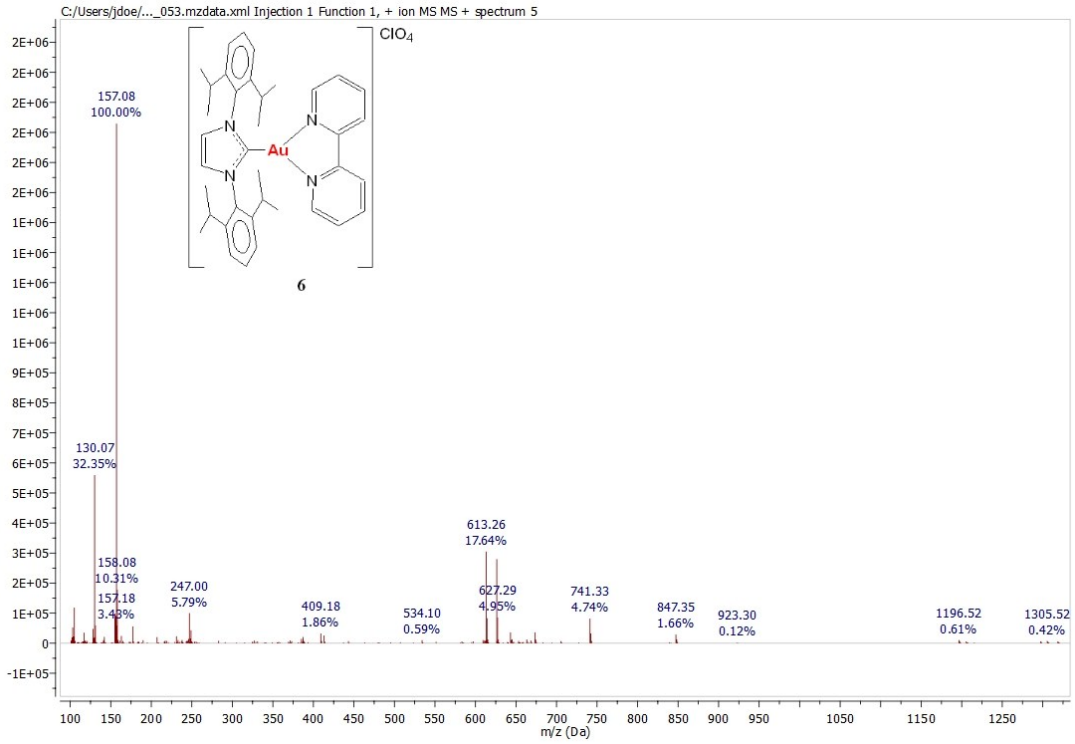

Figure S44. Overall MS ESI+ spectrum of compound **6** in CH_3CN/H_2O (95:5) solution.

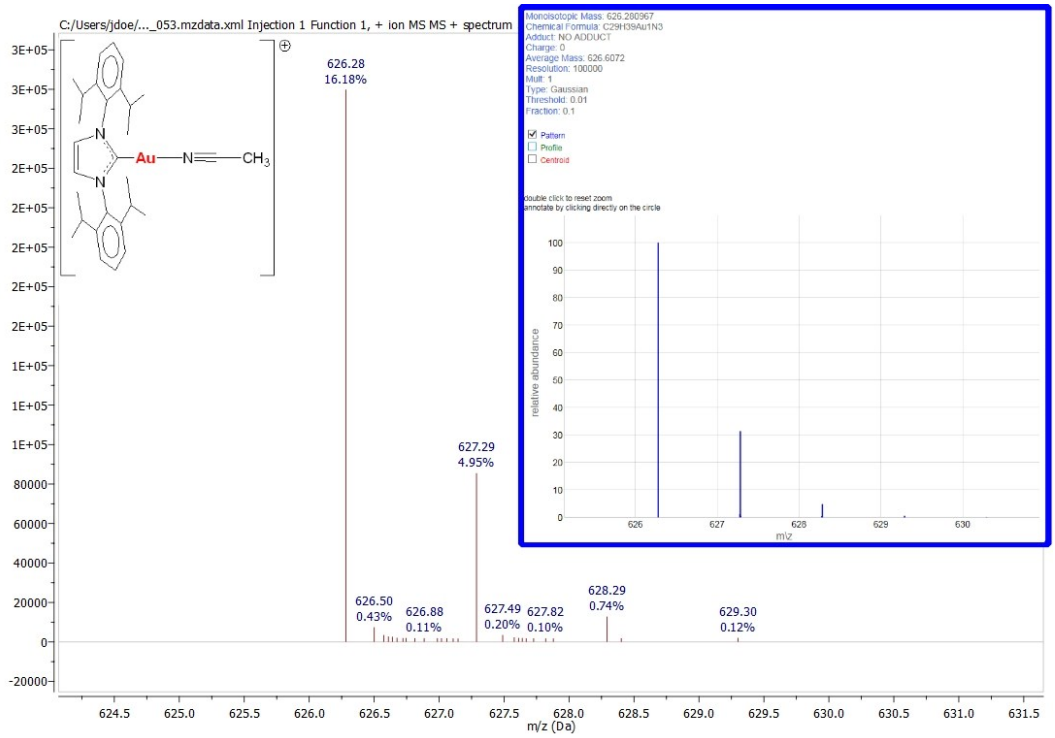

Figure S45. Magnification of peak at [m/z]: 626.28 $[Au(IPr)(CH_3CN)]^+$ in MS ESI+ of compound **6** in CH_3CN/H_2O (95:5) solution. Insert: theoretical isotopic distribution.

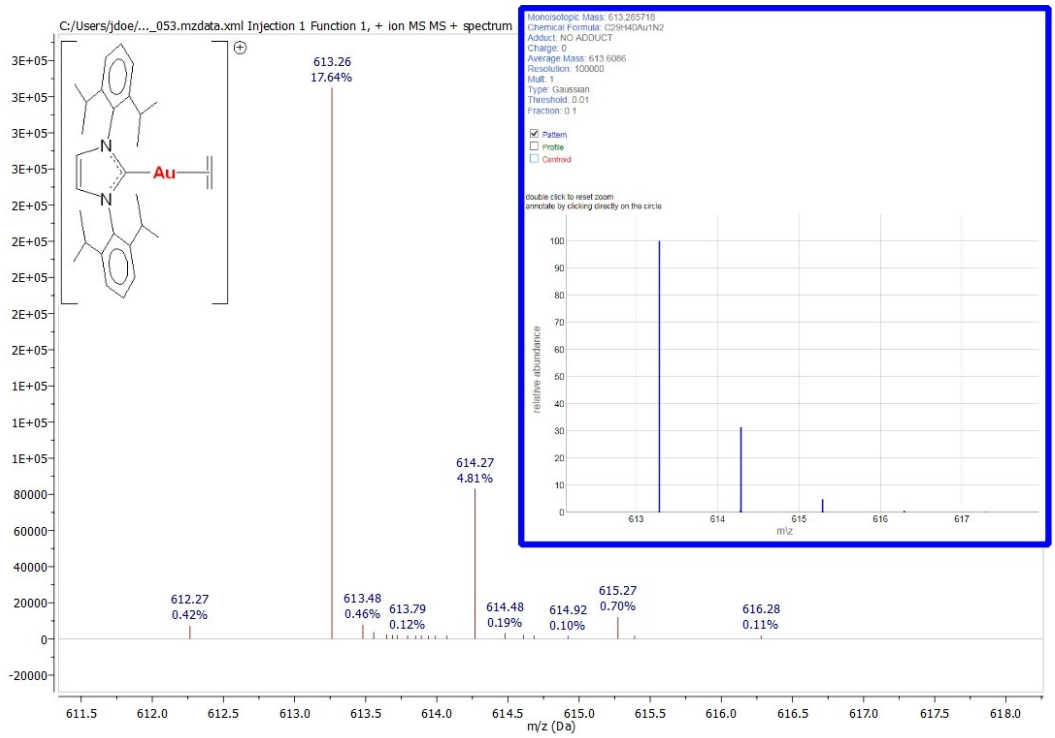

Figure S46. Magnification of peak at [m/z]: 613.26 $[Au(IPr)(CH_2{=}CH_2)]^+$ in MS ESI+ of compound **6** in CH_3CN/H_2O (95:5) solution. Insert: theoretical isotopic distribution.

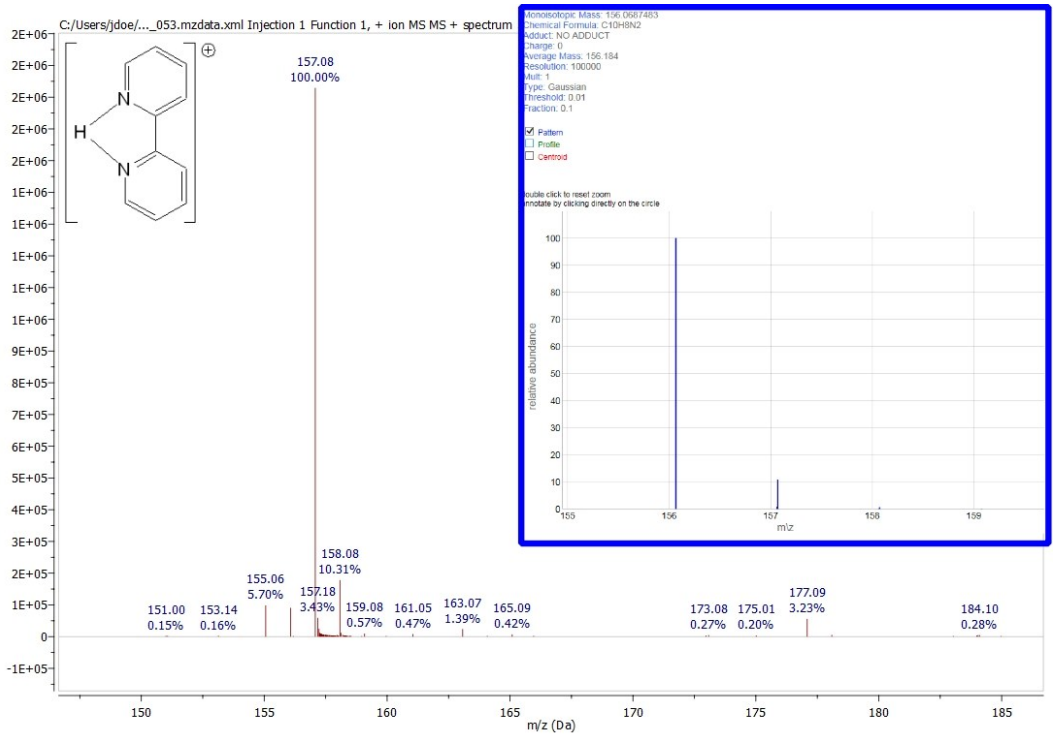

Figure S47. Magnification of peak at [m/z]: 157.08 $[bipy\text{-}H]^+$ in MS ESI+ of compound **6** in CH_3CN/H_2O (95:5) solution. Insert: theoretical isotopic distribution.

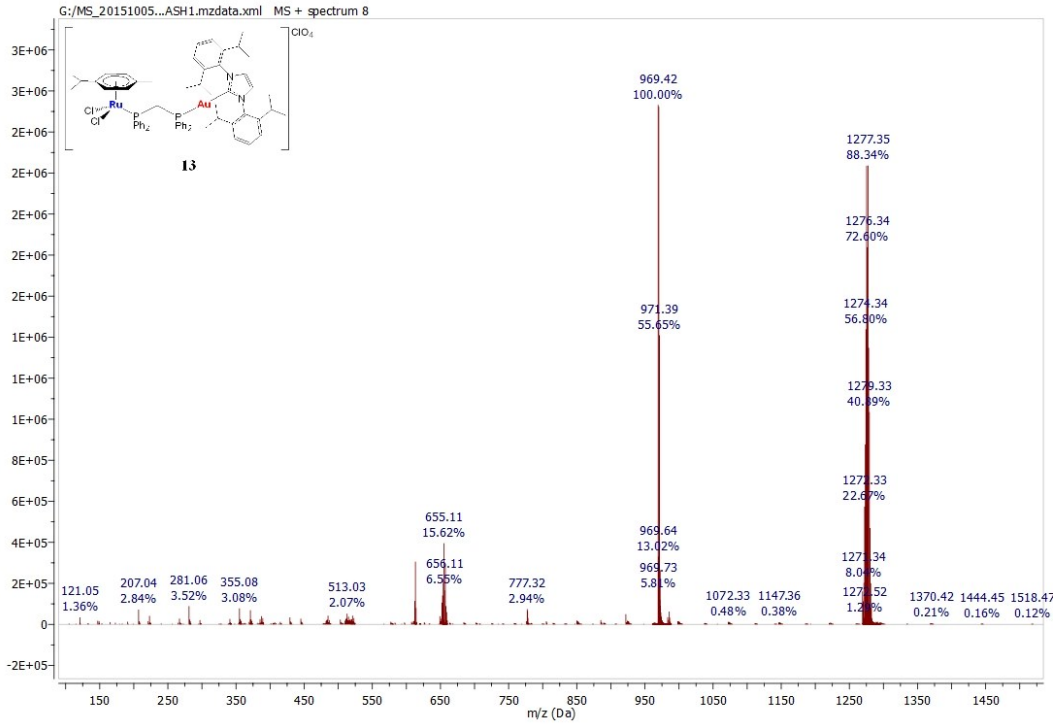

Figure S48. Overall MS ESI+ spectrum of compound **13** in CH_3CN/H_2O (95:5) solution.

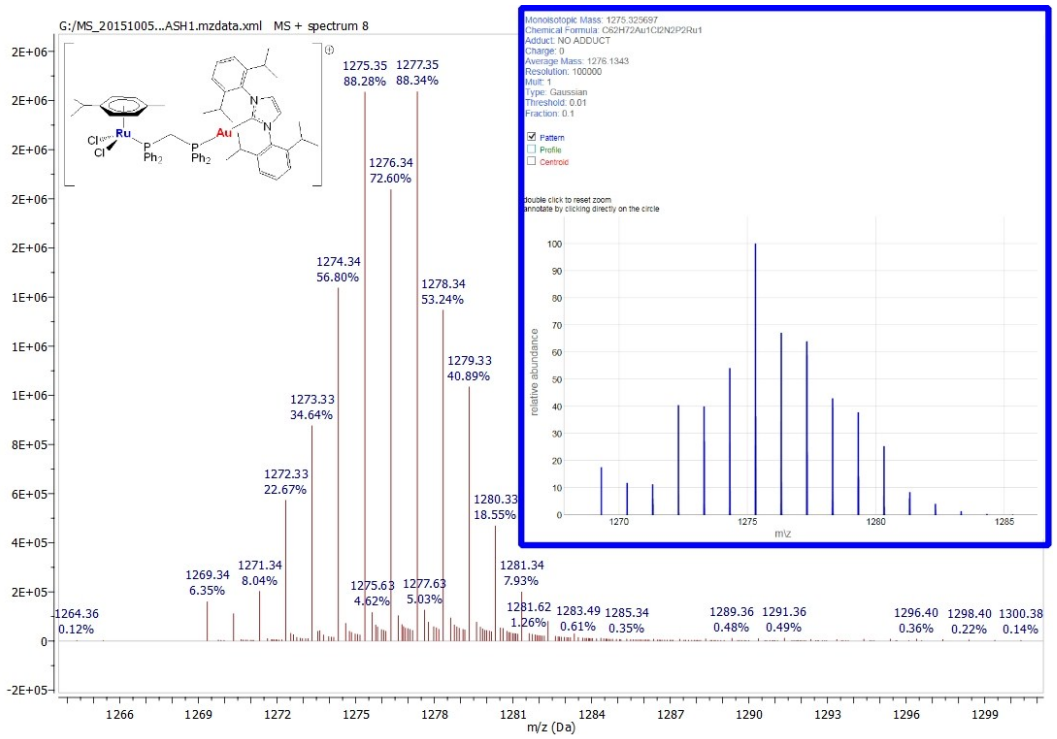

Figure S49. Magnification of peak at [m/z]: 1275.35 [Ru(*p*-cymene)Cl_2(μ-dppm)Au(IPr)]$^+$ in MS ESI+ of compound **13** in CH_3CN/H_2O (95:5) solution. Insert: theoretical isotopic distribution.

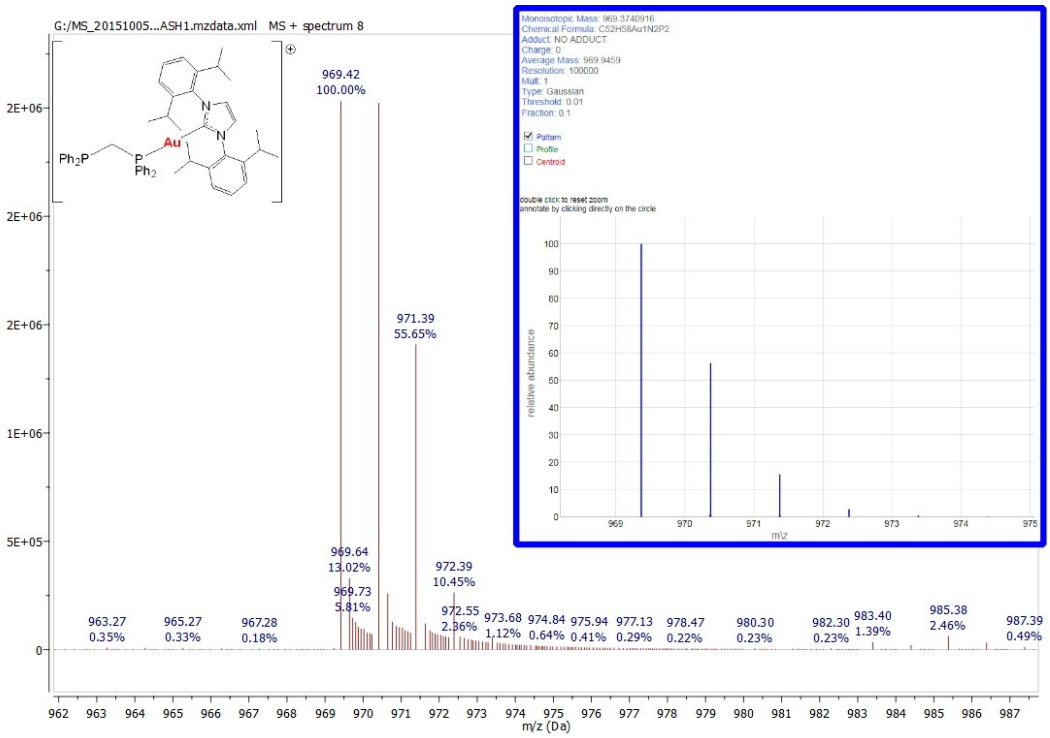

Figure S50. Magnification of peak at [m/z]: 969.42 [Au(IPr)(η^1-dppm)]$^+$ in MS ESI+ of compound **13** in CH_3CN/H_2O (95:5) solution. Insert: theoretical isotopic distribution.

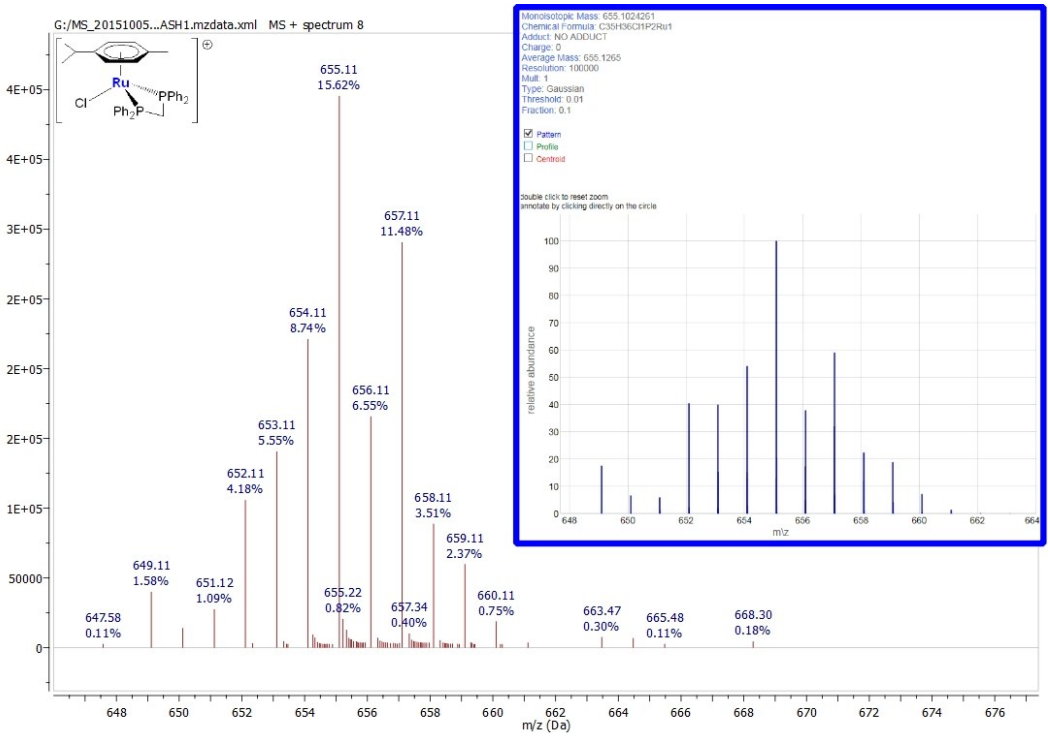

Figure S51. Magnification of peak at [m/z]: 655.11 [Ru(p-cymene)(η^2-dppm)Cl]$^+$ in MS ESI+ of compound **13** in CH_3CN/H_2O (95:5) solution. Insert: theoretical isotopic distribution.

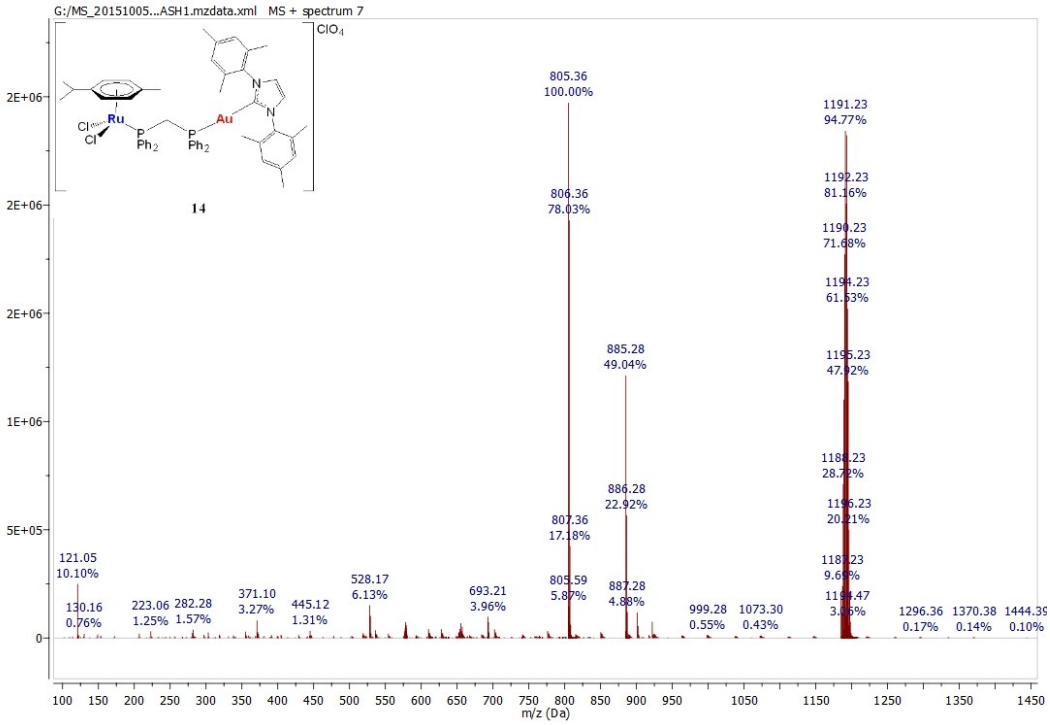

Figure S52. Overall MS ESI+ spectrum of compound **14** in CH_3CN/H_2O (95:5) solution.

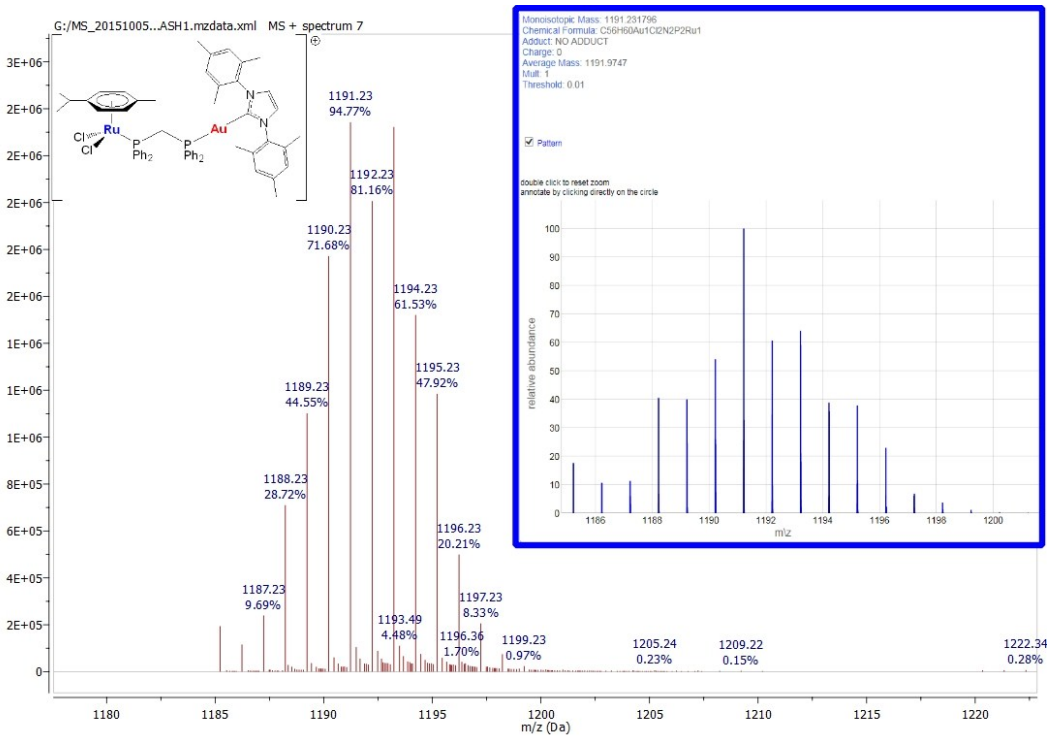

Figure S53. Magnification of peak at [m/z]: 1191.23 [Ru(*p*-cymene)Cl_2(μ-dppm)Au(IMes)]$^+$ in MS ESI+ of compound **14** in CH_3CN/H_2O (95:5) solution. Insert: theoretical isotopic distribution.

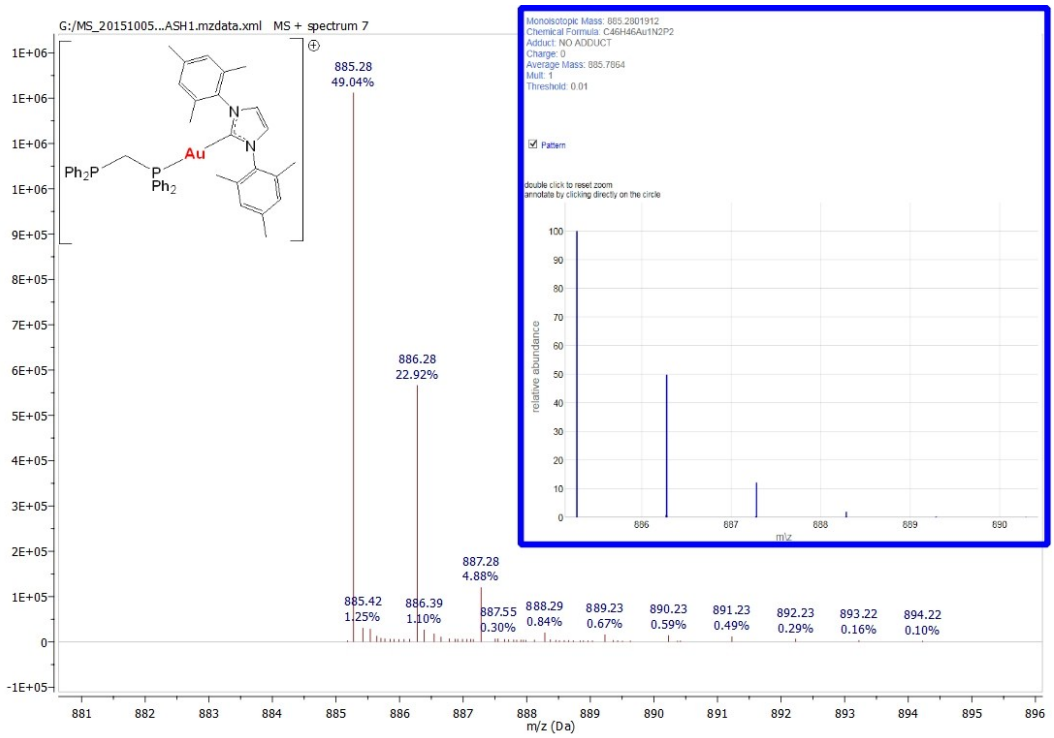

Figure S54. Magnification of peak at [m/z]: 885.28 [Au(IMes)(η^1-dppm)]$^+$ in MS ESI+ of compound **14** in CH_3CN/H_2O (95:5) solution. Insert: theoretical isotopic distribution.

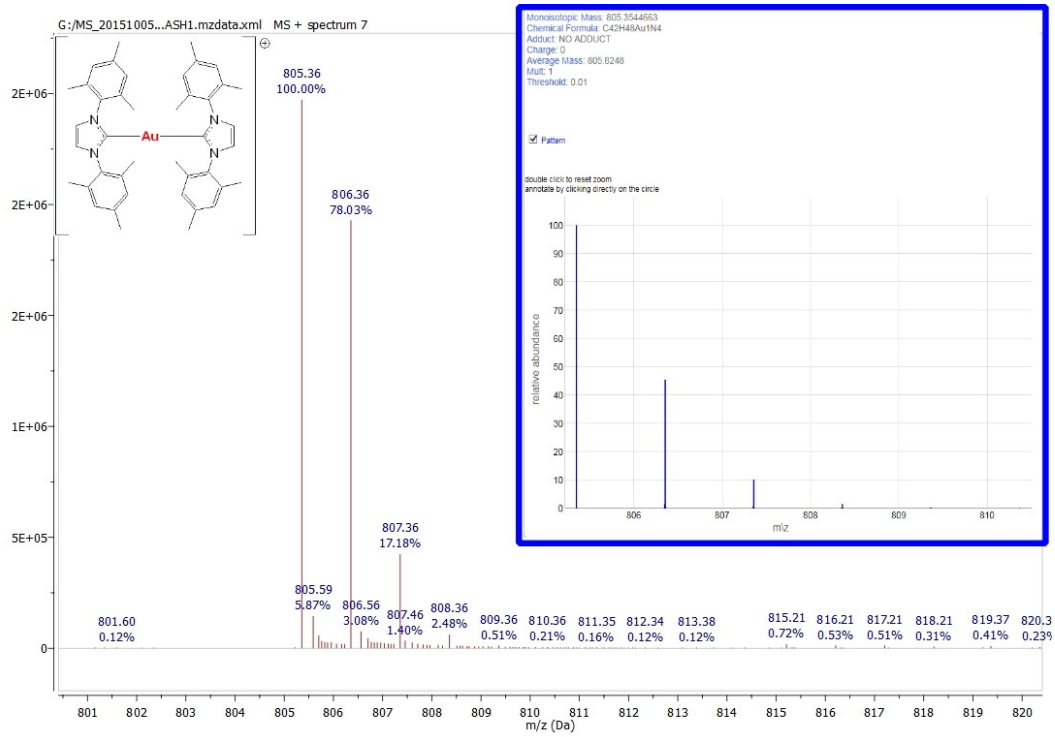

Figure S55. Magnification of peak at [m/z]: 805.36 [Au(IMes)$_2$]$^+$ in MS ESI+ of compound **14** in CH_3CN/H_2O (95:5) solution. Insert: theoretical isotopic distribution.

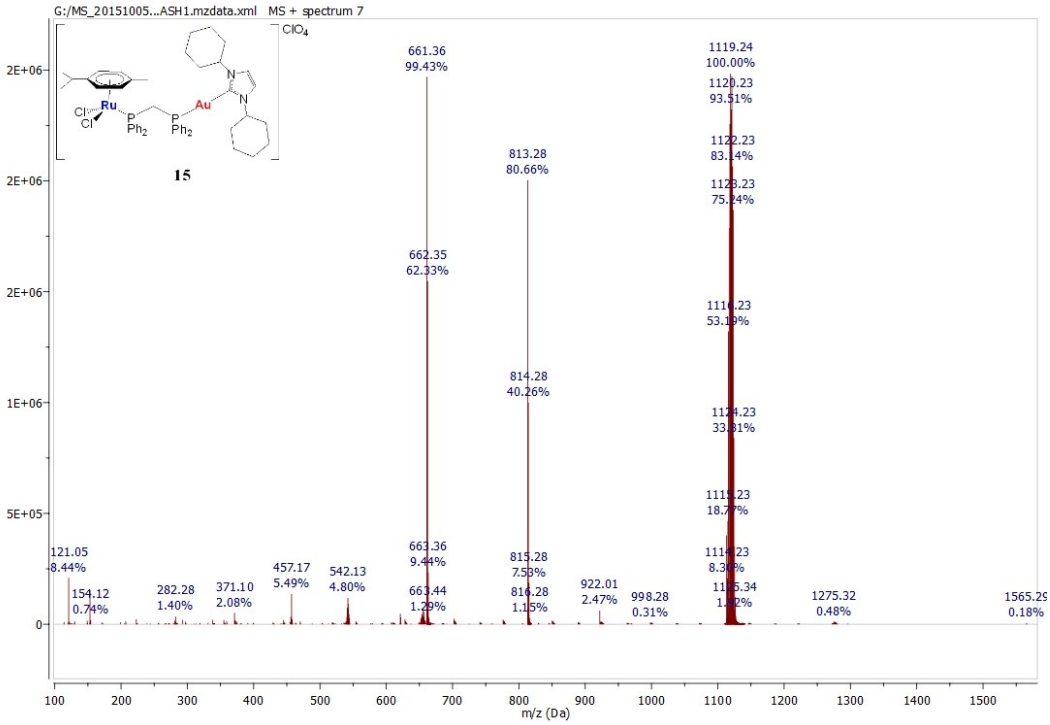

Figure S56. Overall MS ESI+ spectrum of compound **15** in CH_3CN/H_2O (95:5) solution.

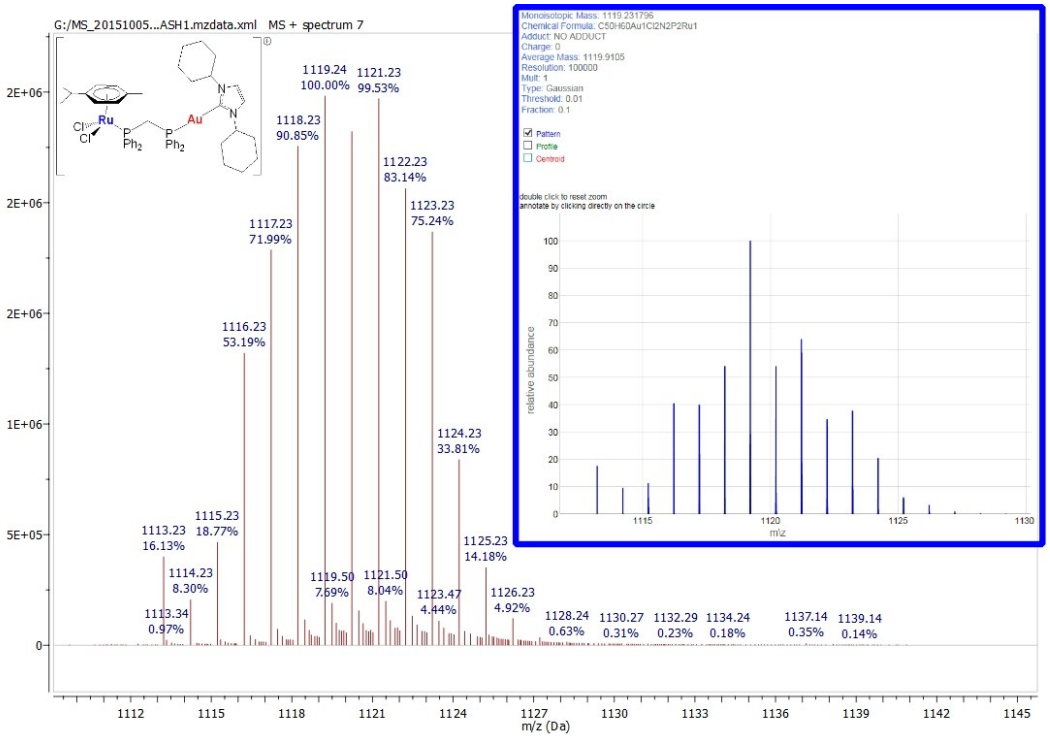

Figure S57. Magnification of peak at [m/z]: 1119.24 [Ru(*p*-cymene)Cl_2(μ-dppm)Au(ICy)]$^+$ in MS ESI+ of compound **15** in CH_3CN/H_2O (95:5) solution. Insert: theoretical isotopic distribution.

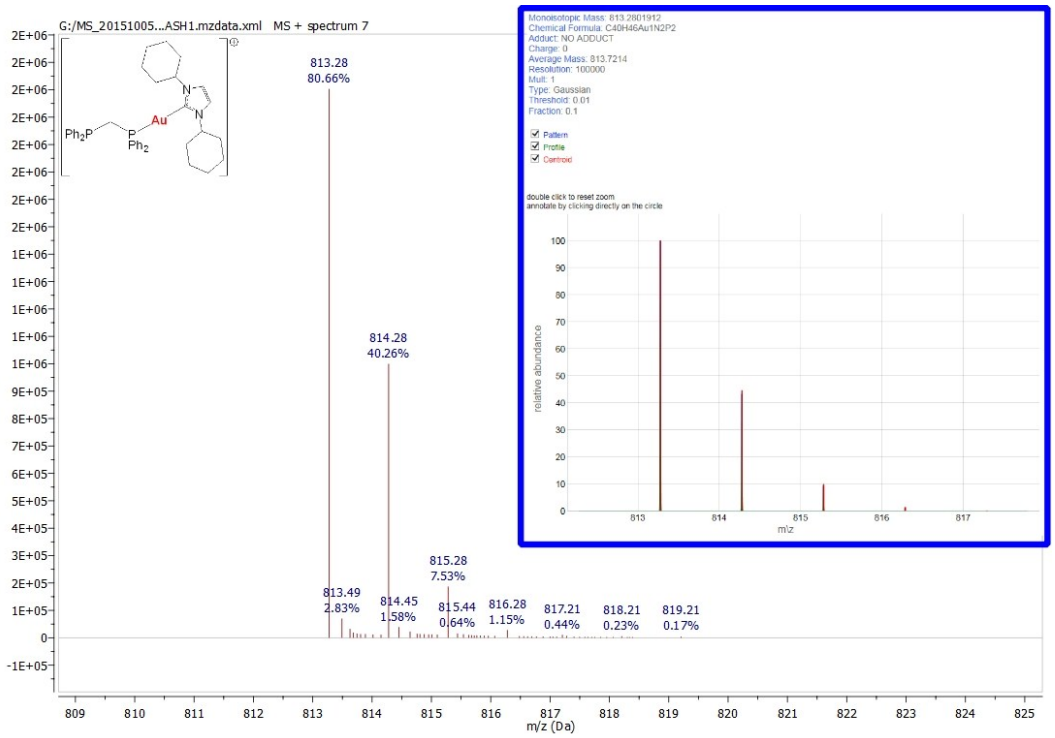

Figure S58. Magnification of peak at [m/z]: 813.28 $[Au(ICy)(\eta^1\text{-dppm})]^+$ in MS ESI+ of compound **15** in CH_3CN/H_2O (95:5) solution. Insert: theoretical isotopic distribution.

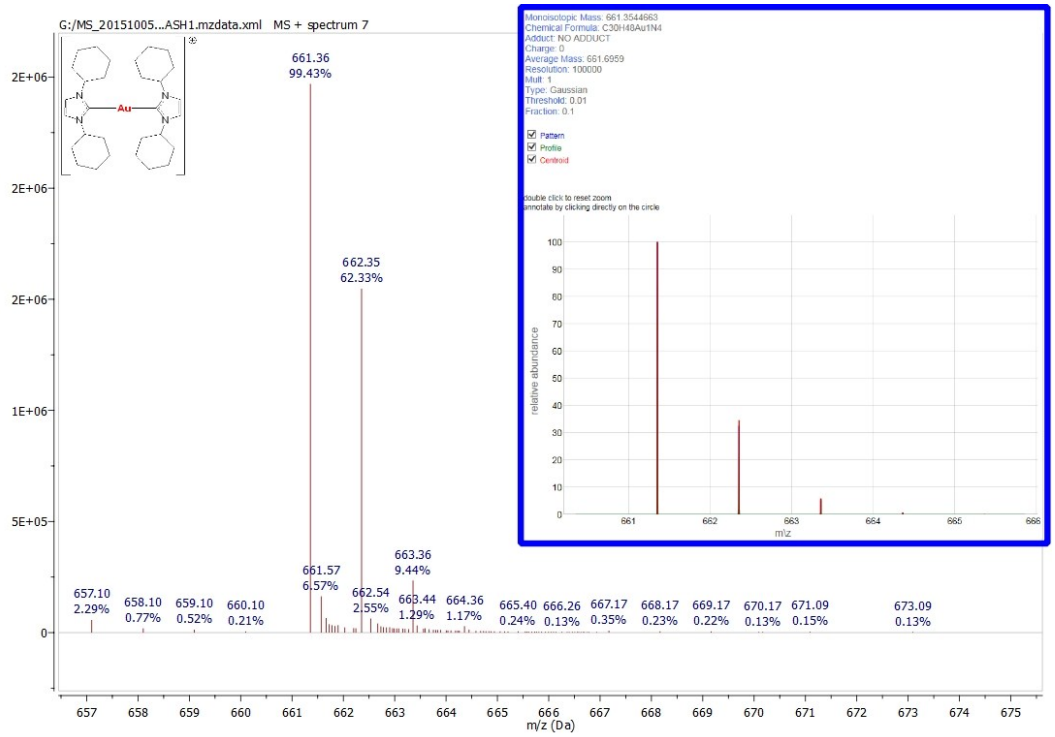

Figure S59. Magnification of peak at [m/z]: 661.36 $[Au(ICy)_2]^+$ in MS ESI+ of compound **15** in CH_3CN/H_2O (95:5) solution. Insert: theoretical isotopic distribution.

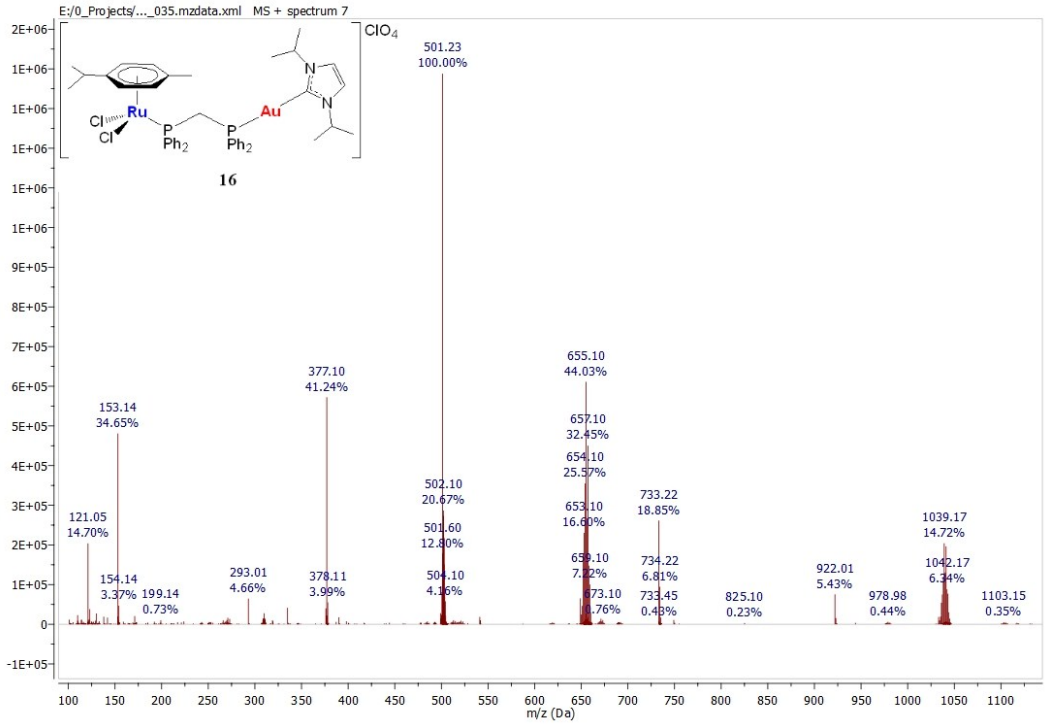

Figure S60. Overall MS ESI+ spectrum of compound **16** in CH_3CN/H_2O (95:5) solution.

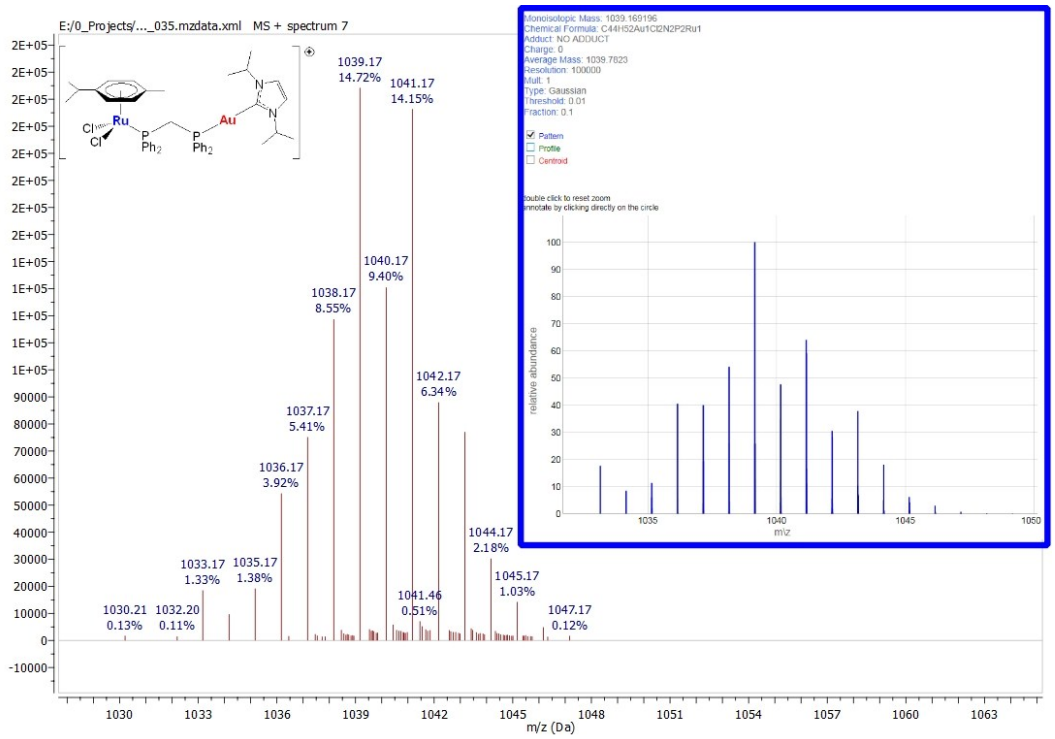

Figure S61. Magnification of peak at [m/z]: 1039.17 [Ru(*p*-cymene)Cl_2(μ-dppm)Au(IPr)]$^+$ in MS ESI+ of compound **16** in CH_3CN/H_2O (95:5) solution. Insert: theoretical isotopic distribution.

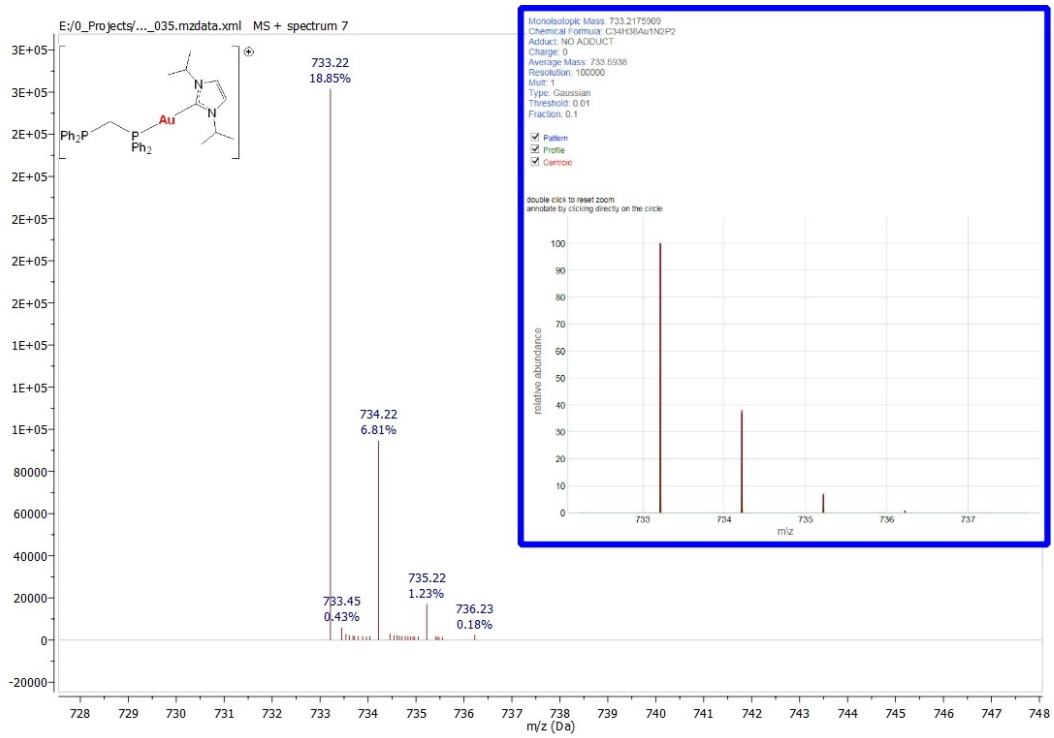

Figure S62. Magnification of peak at [m/z]: 733.22 [Au(Goofy)(η^1-dppm)]$^+$ in MS ESI+ of compound **16** in CH_3CN/H_2O (95:5) solution. Insert: theoretical isotopic distribution.

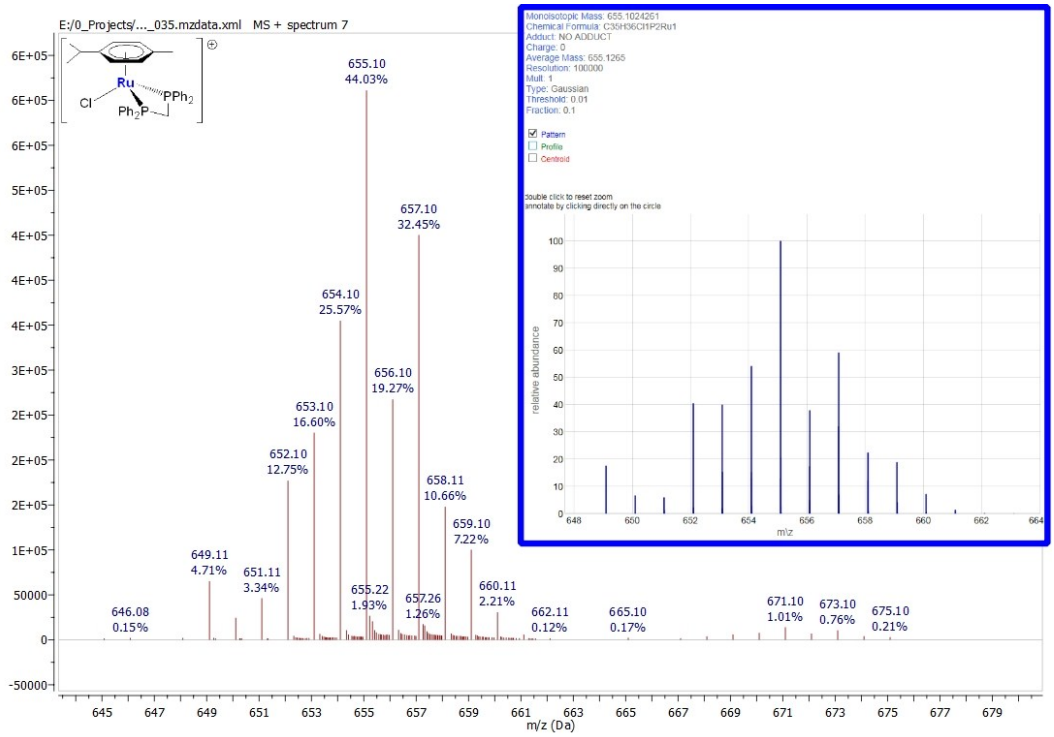

Figure S63. Magnification of peak at [m/z]: 655.11 [Ru(p-cymene)(η^2-dppm)Cl]$^+$ in MS ESI+ of compound **16** in CH_3CN/H_2O (95:5) solution. Insert: theoretical isotopic distribution.

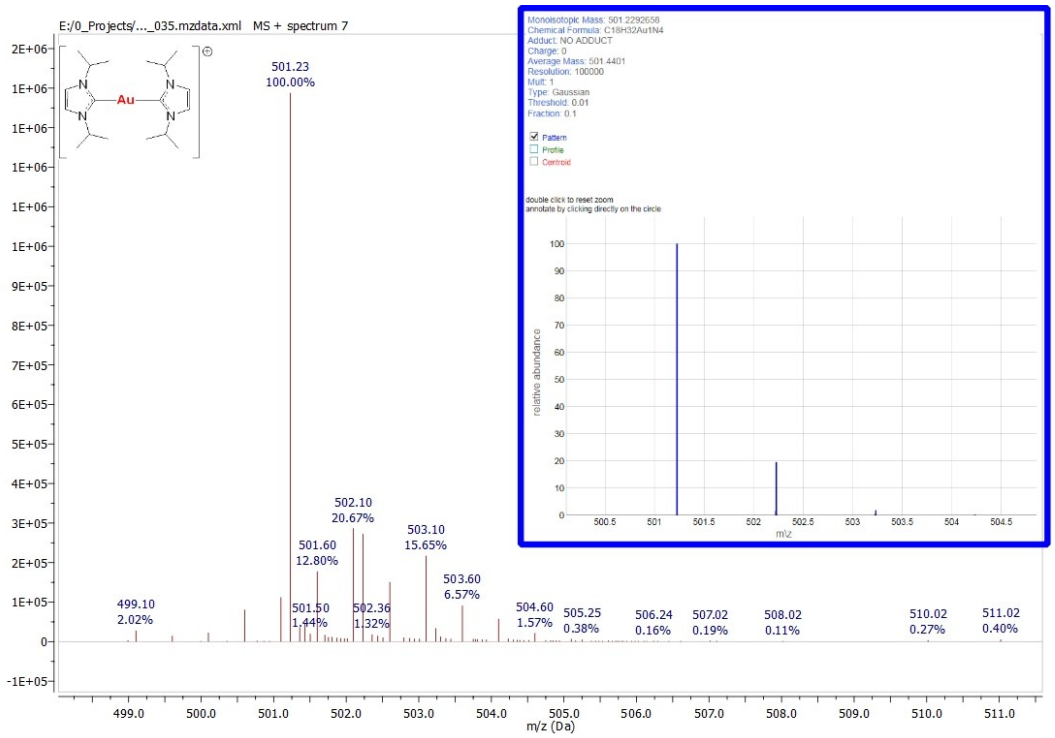

Figure S64. Magnification of peak at [m/z]: 501.23 $[Au(Goofy)_2]^+$, in MS ESI+ of compound **16** in CH_3CN/H_2O (95:5) solution. Insert: theoretical isotopic distribution.

5. Solid state IR spectra of all compounds

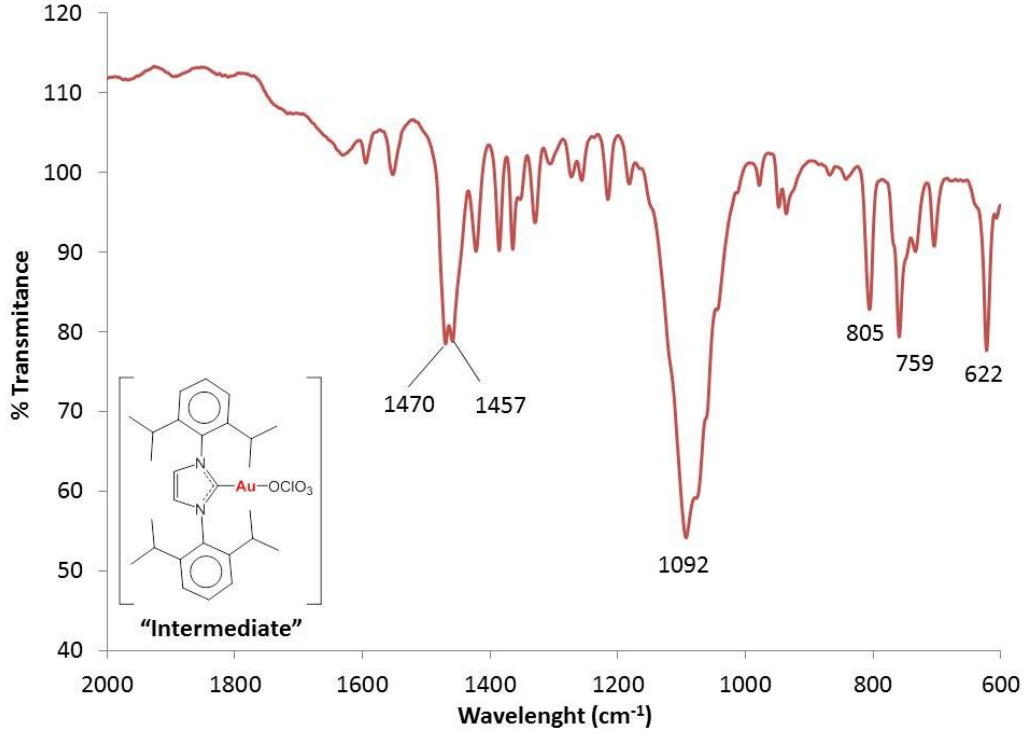

Figure S65. IR spectrum of [Au(IPr)($OClO_3$)] in solid state at RT.

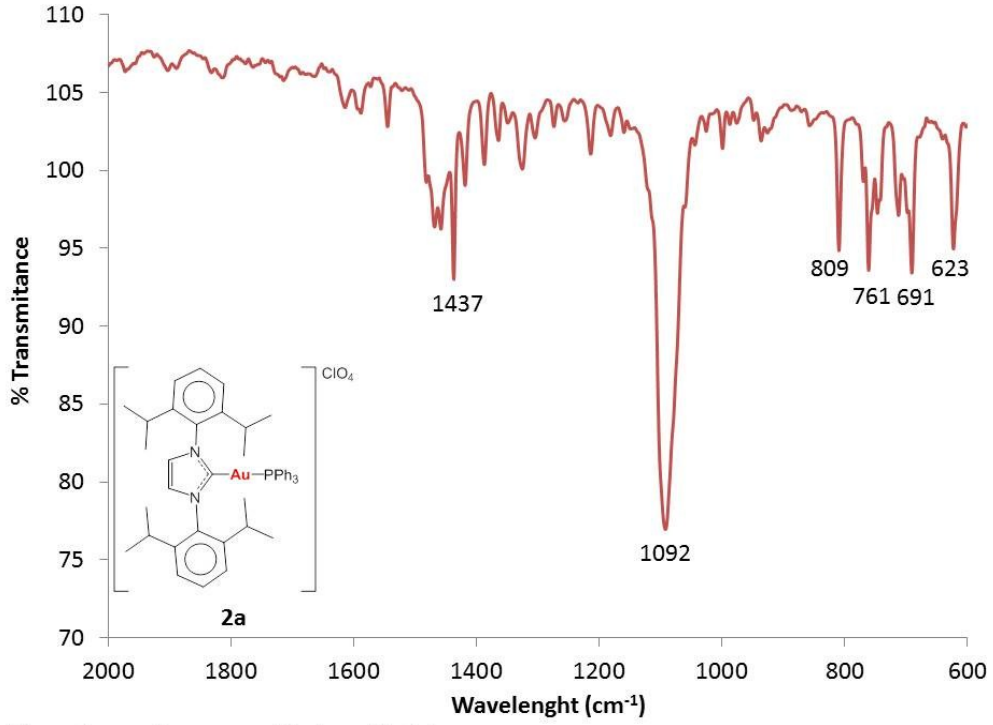

Figure S66. IR spectrum of compound **2a** in solid state at RT.

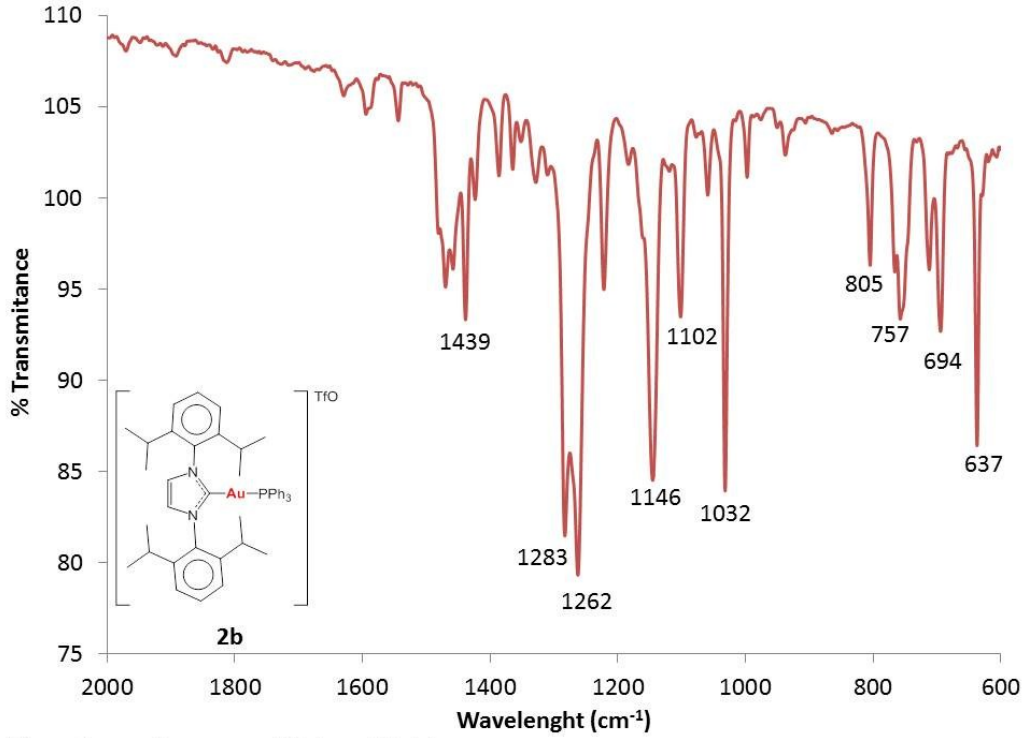

Figure S67. IR spectrum of compound **2b** in solid state at RT.

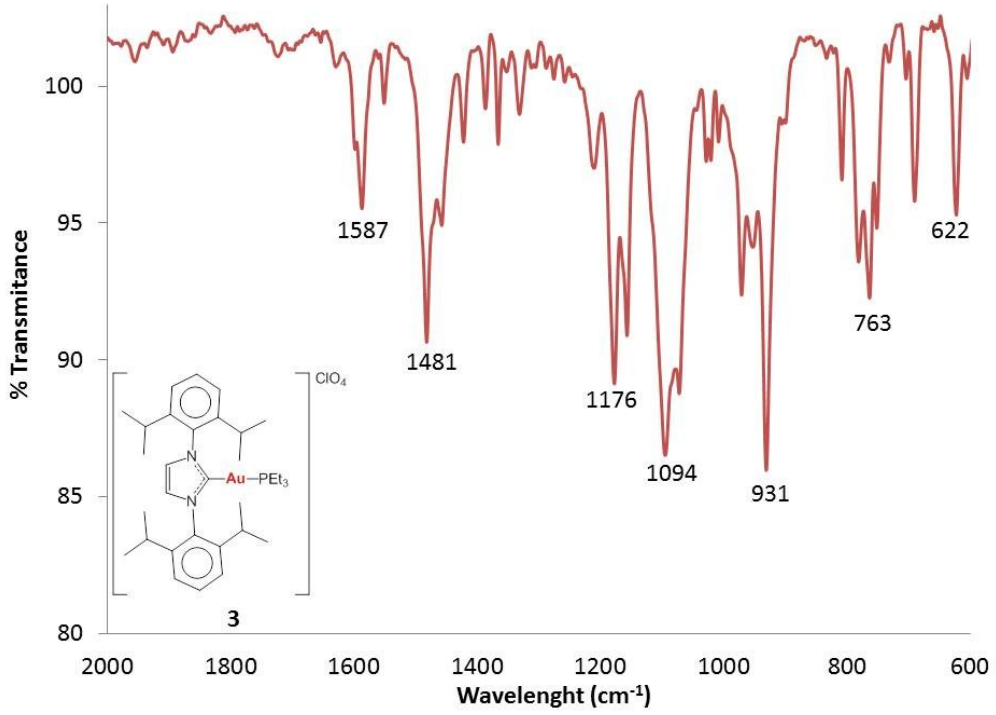

Figure S68. IR spectrum of compound **3** in solid state at RT.

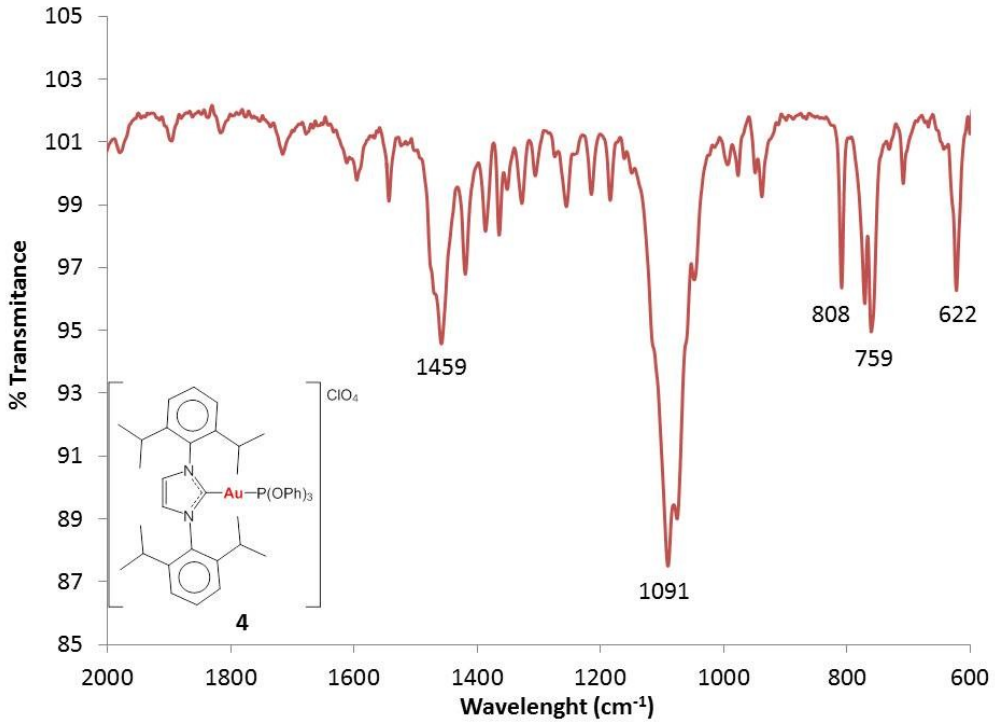

Figure S69. IR spectrum of compound **4** in solid state at RT.

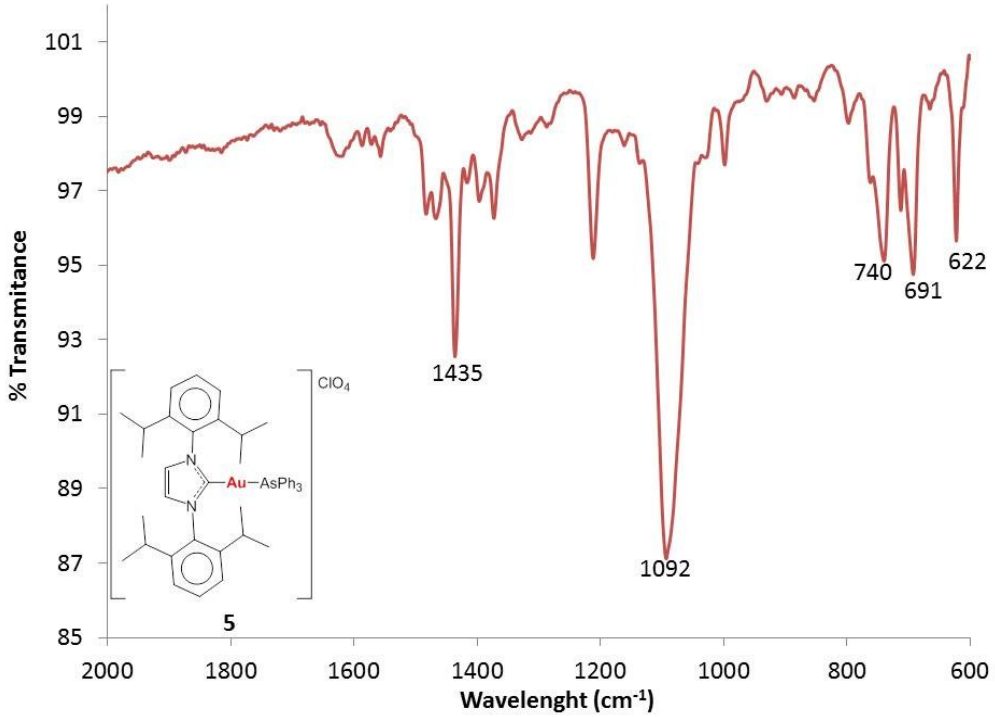

Figure S70. IR spectrum of compound **5** in solid state at RT.

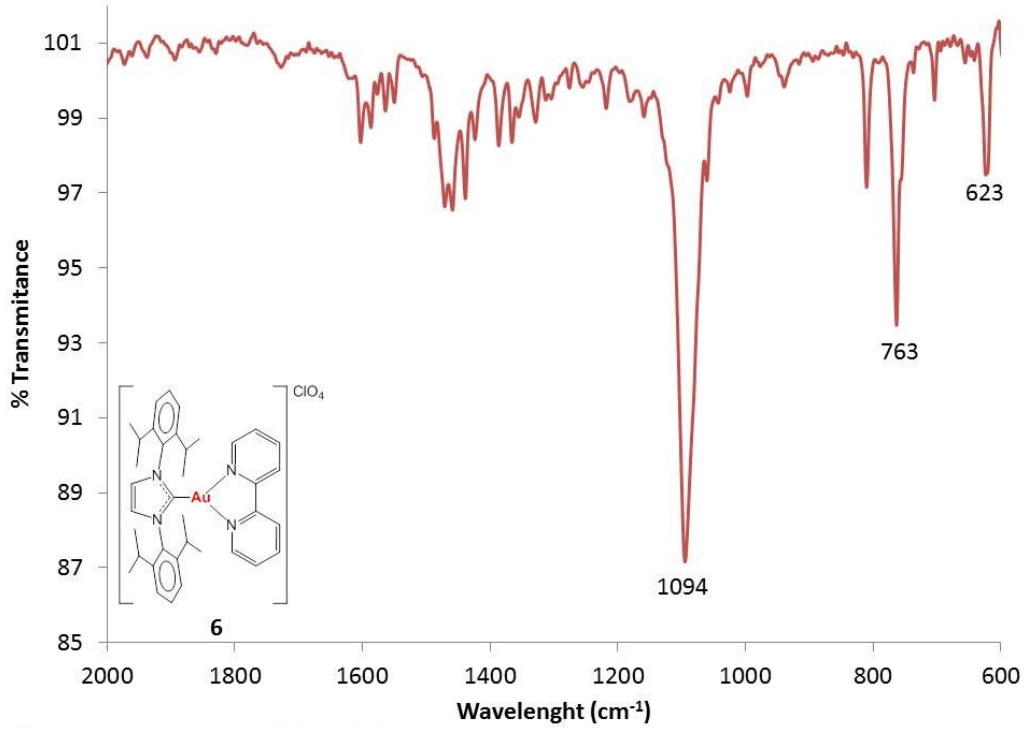

Figure S71. IR spectrum of compound **6** in solid state at RT.

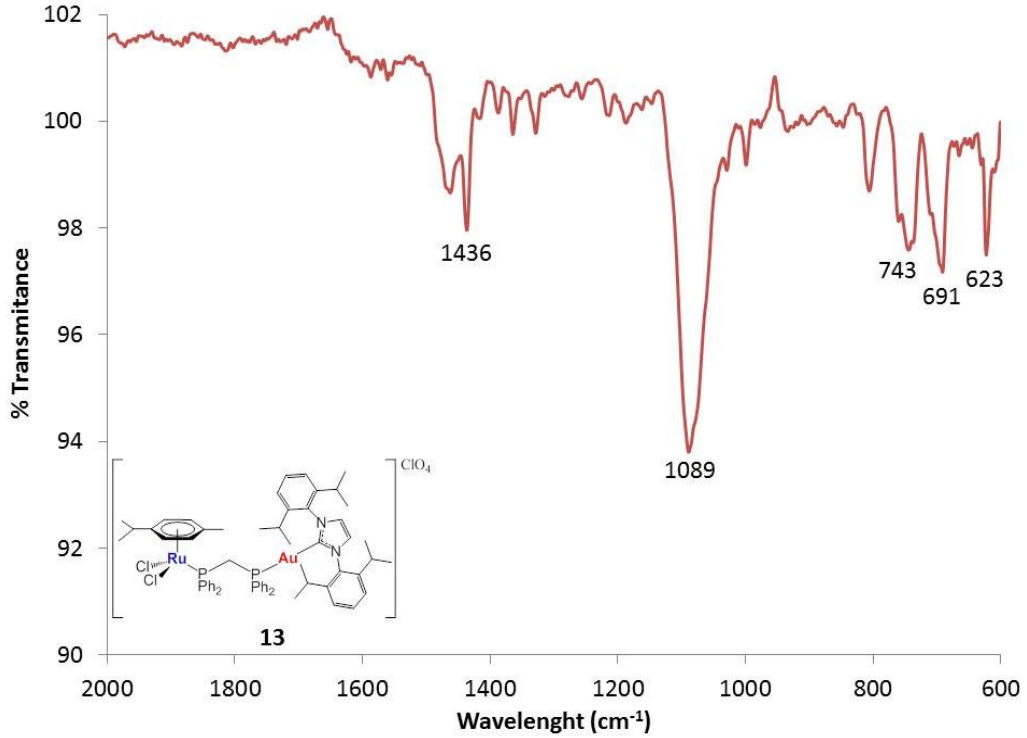

Figure S72. IR spectrum of compound **13** in solid state at RT.

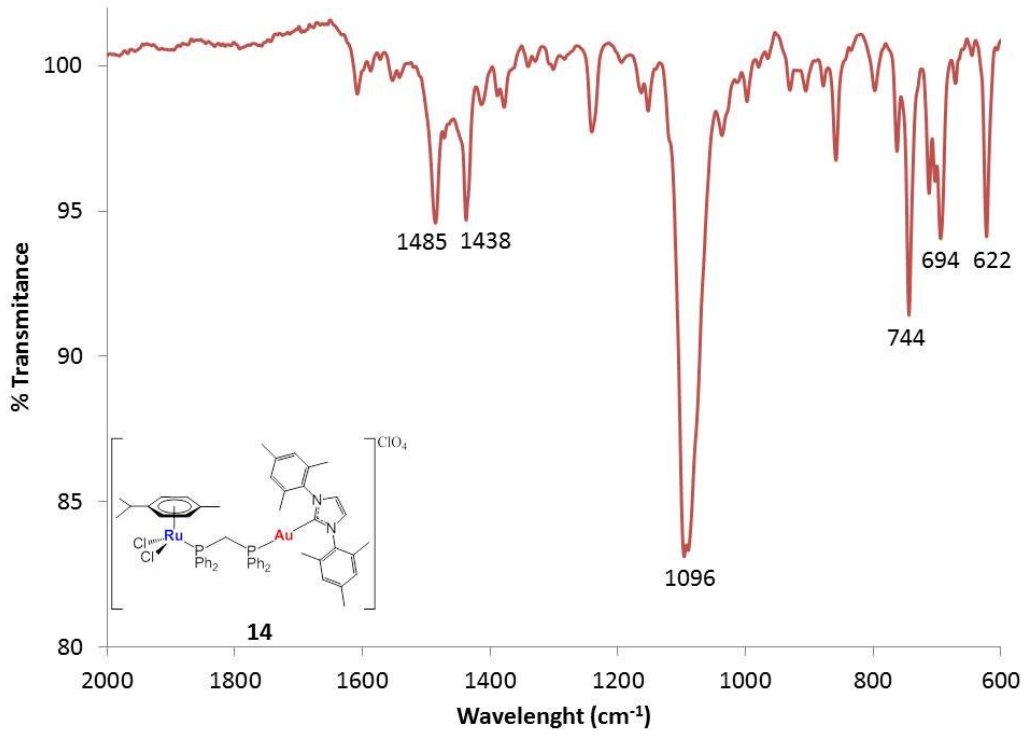

Figure S73. IR spectrum of compound **14** in solid state at RT.

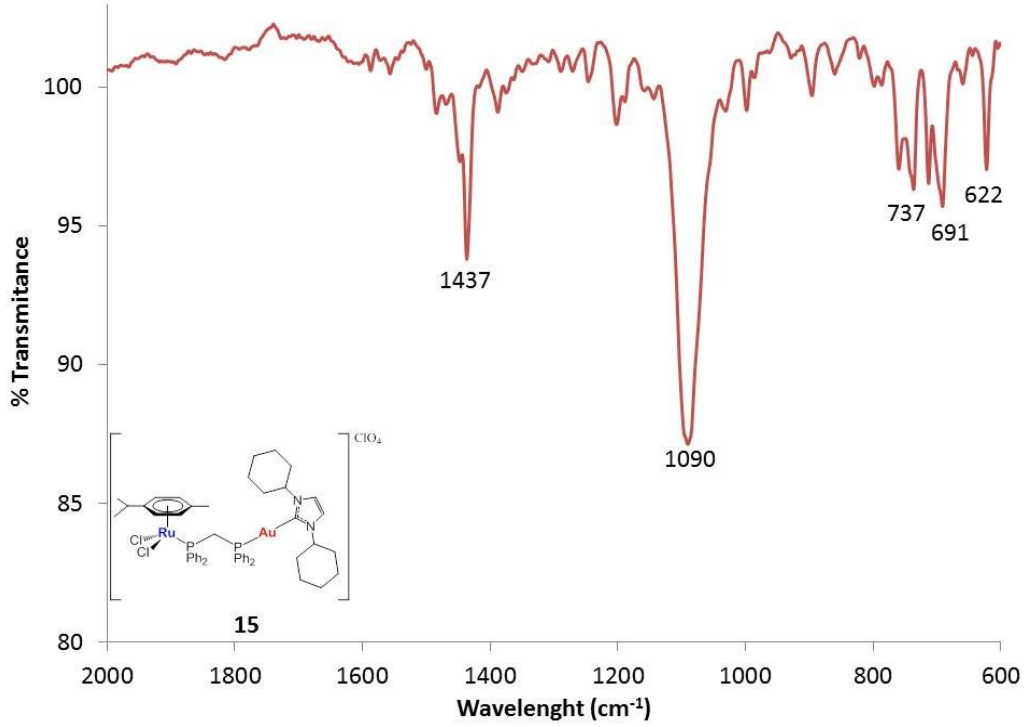

Figure S74. IR spectrum of compound **15** in solid state at RT.

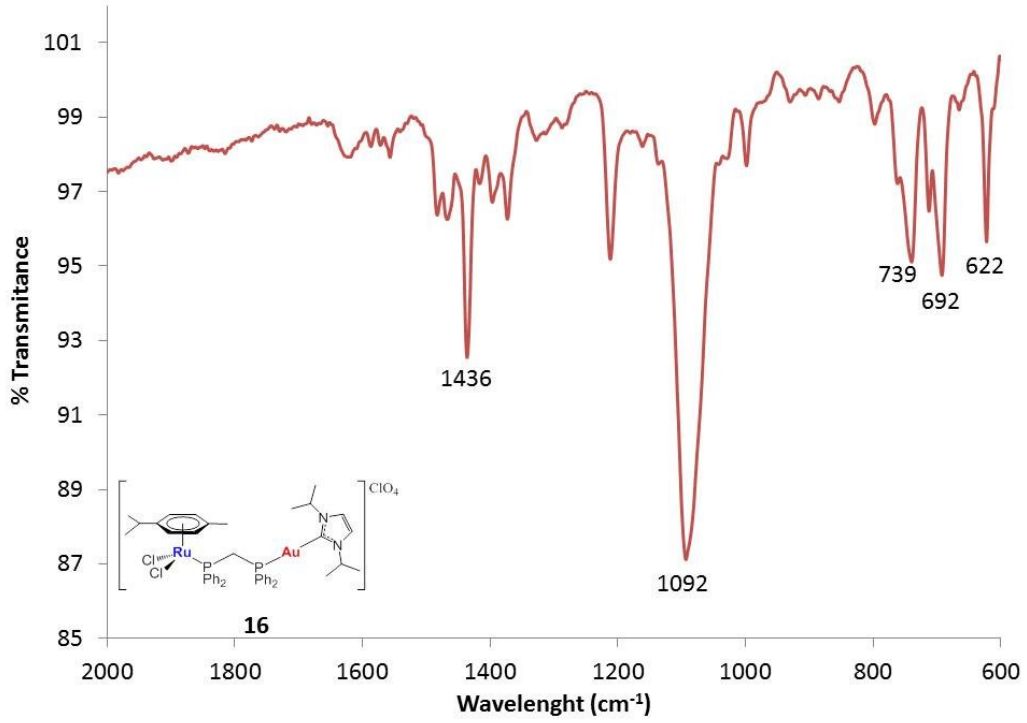

Figure S75. IR spectrum of compound **16** in solid state at RT.

6. UV-visible spectra of heterobimetallic compounds in dichloromethane and DMSO

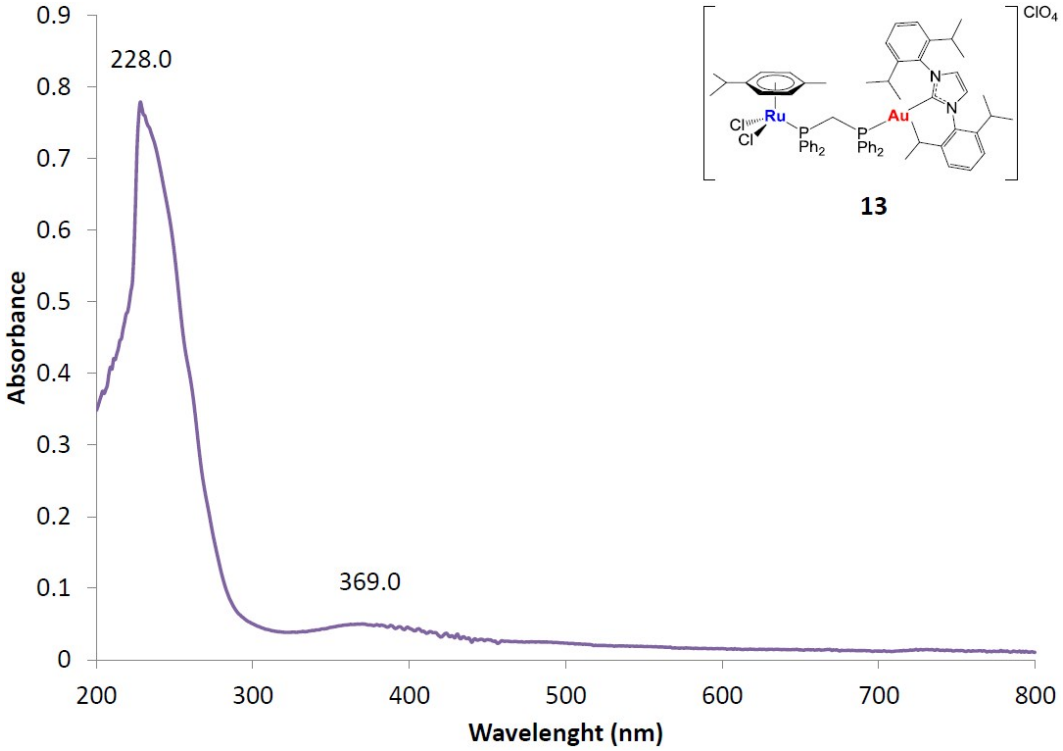

Figure S76. UV-visible spectrum of compound **13** ($2.5 \cdot 10^{-5}$ M) in dichloromethane.

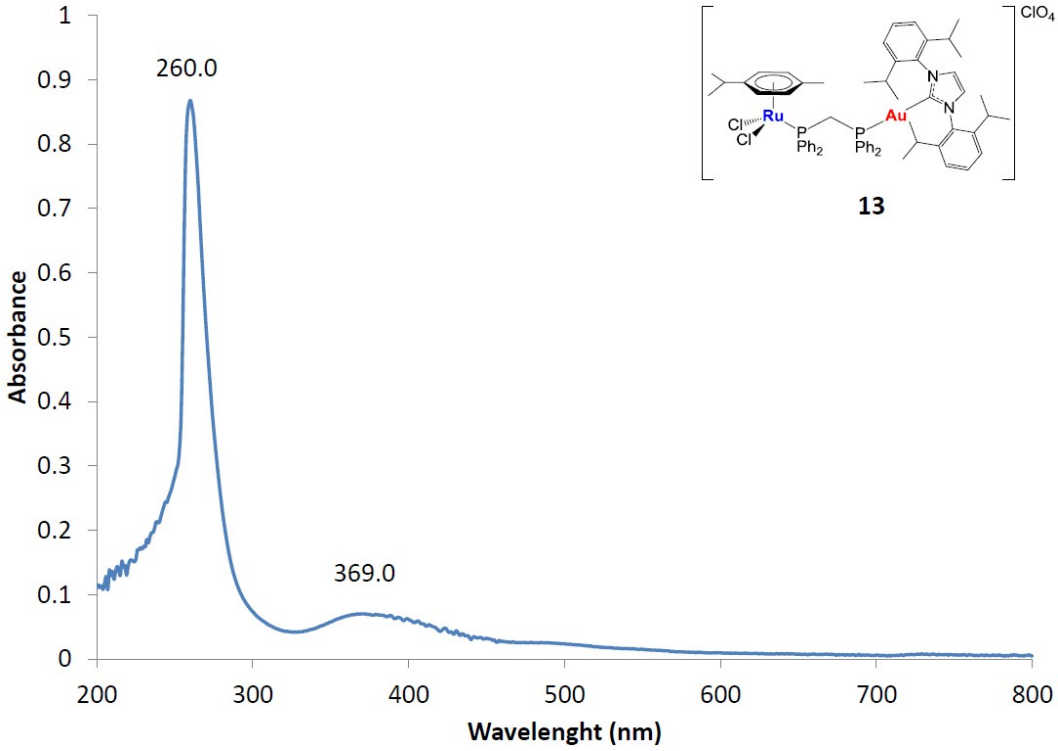

Figure S77. UV-visible spectrum of compound **13** ($1 \cdot 10^{-5}$ M) in DMSO.

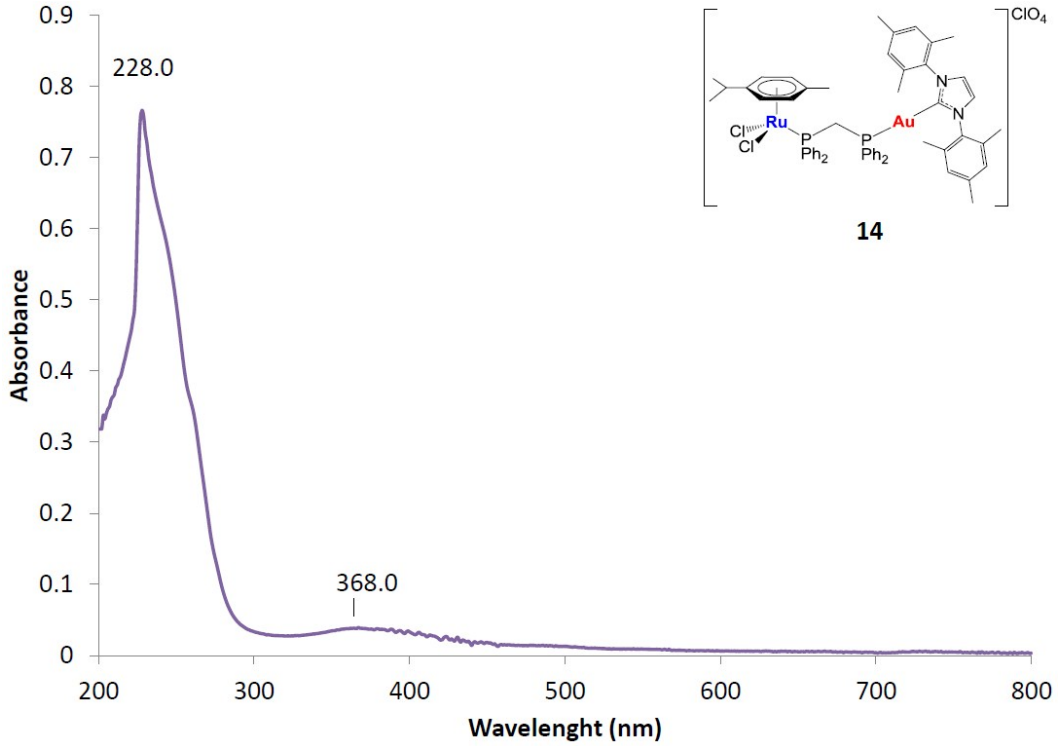

Figure S78. UV-visible spectrum of compound **14** ($2 \cdot 10^{-5}$ M) in dichloromethane.

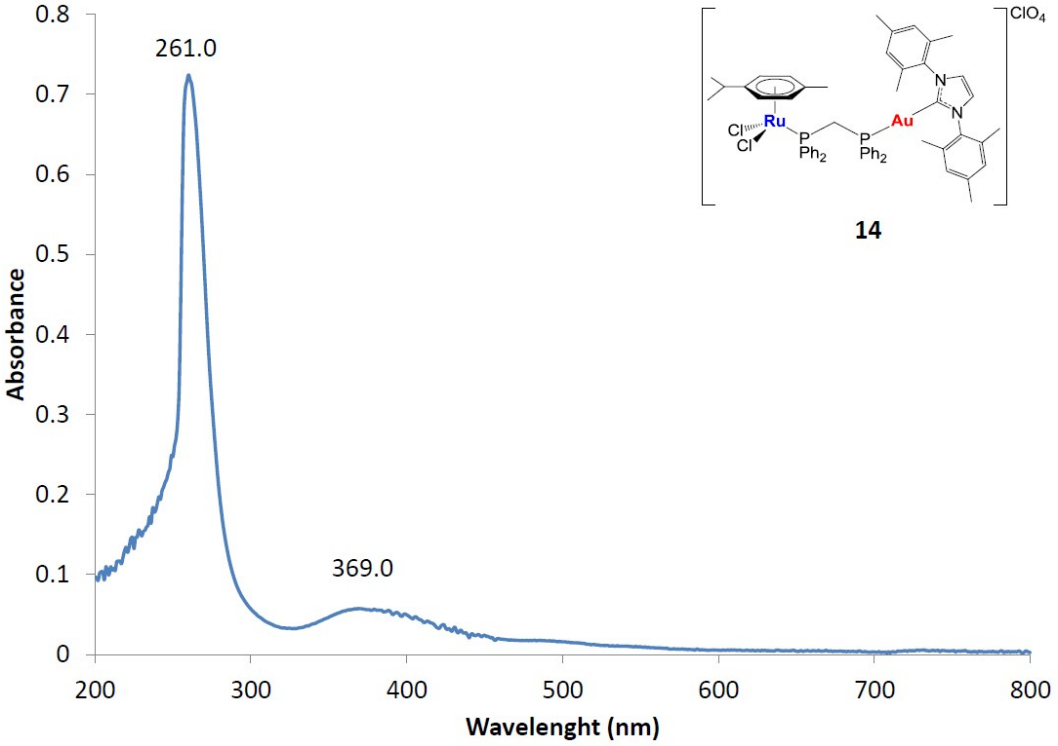

Figure S79. UV-visible spectrum of compound **14** ($1 \cdot 10^{-5}$ M) in DMSO.

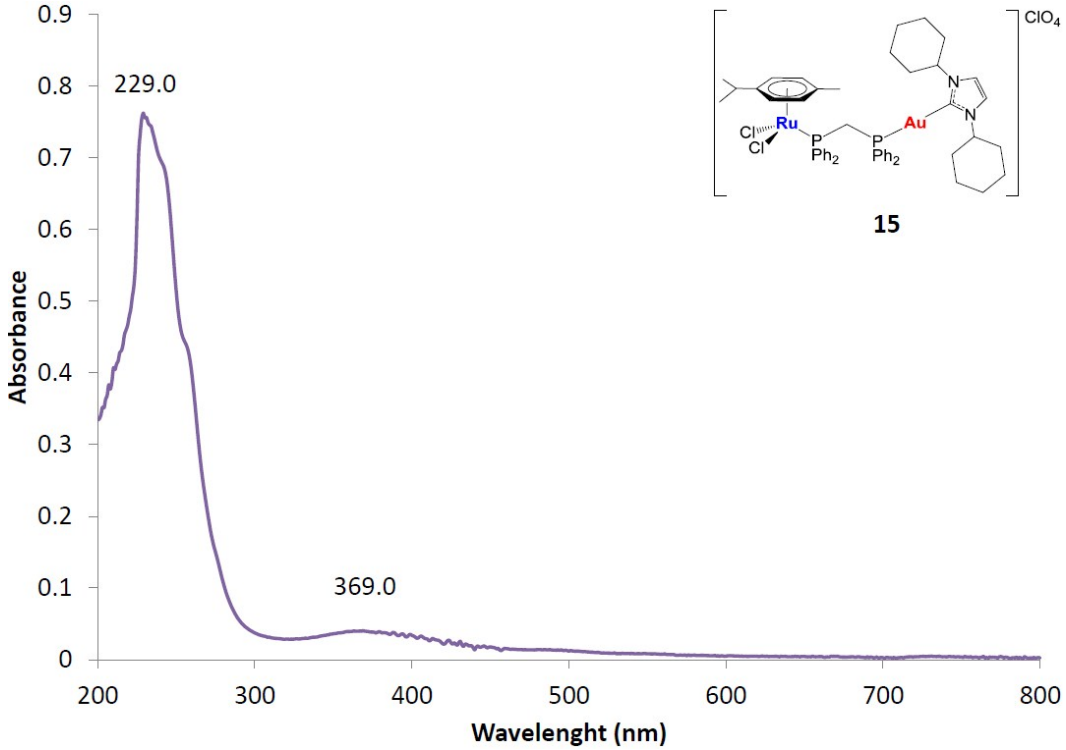

Figure S80. UV-visible spectrum of compound **15** ($1.5 \cdot 10^{-5}$ M) in dichloromethane.

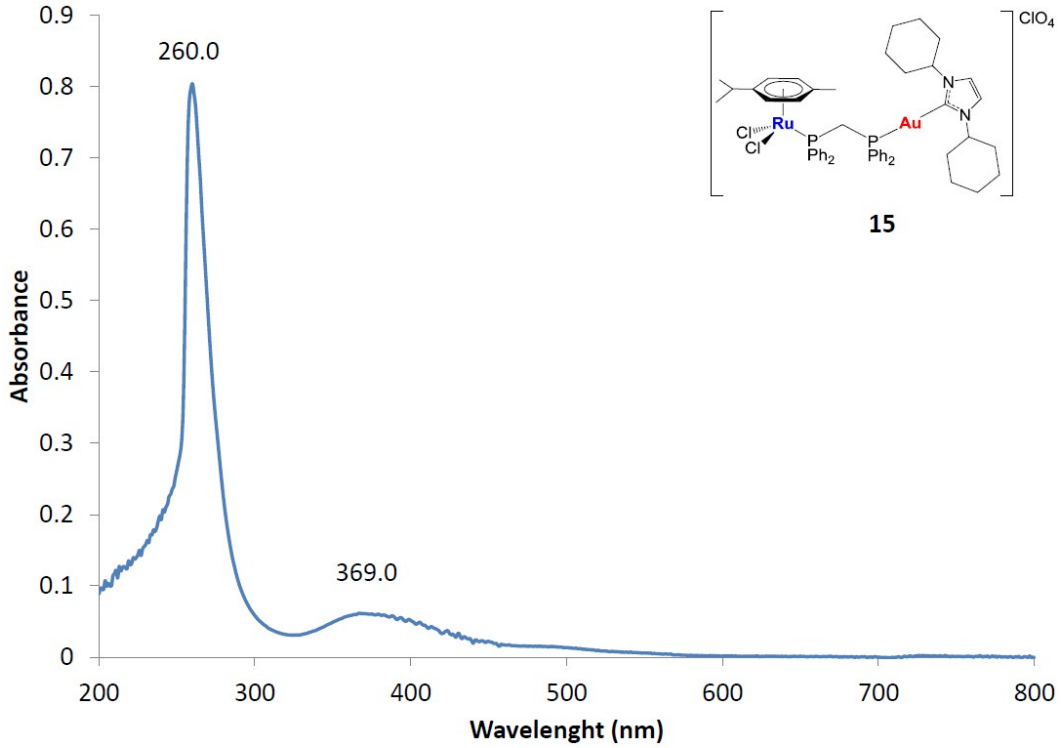

Figure S81. UV-visible spectrum of compound **15** ($2.5 \cdot 10^{-5}$ M) in DMSO.

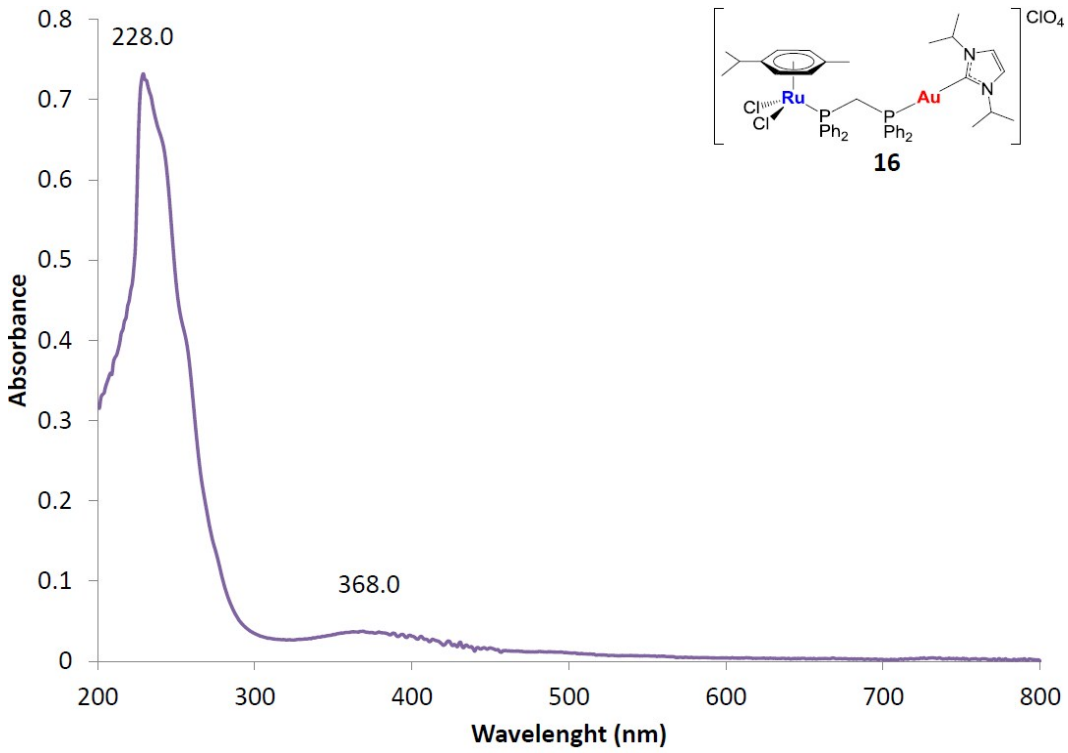

Figure S82. UV-visible spectrum of compound **16** ($3.5 \cdot 10^{-5}$ M) in dichloromethane.

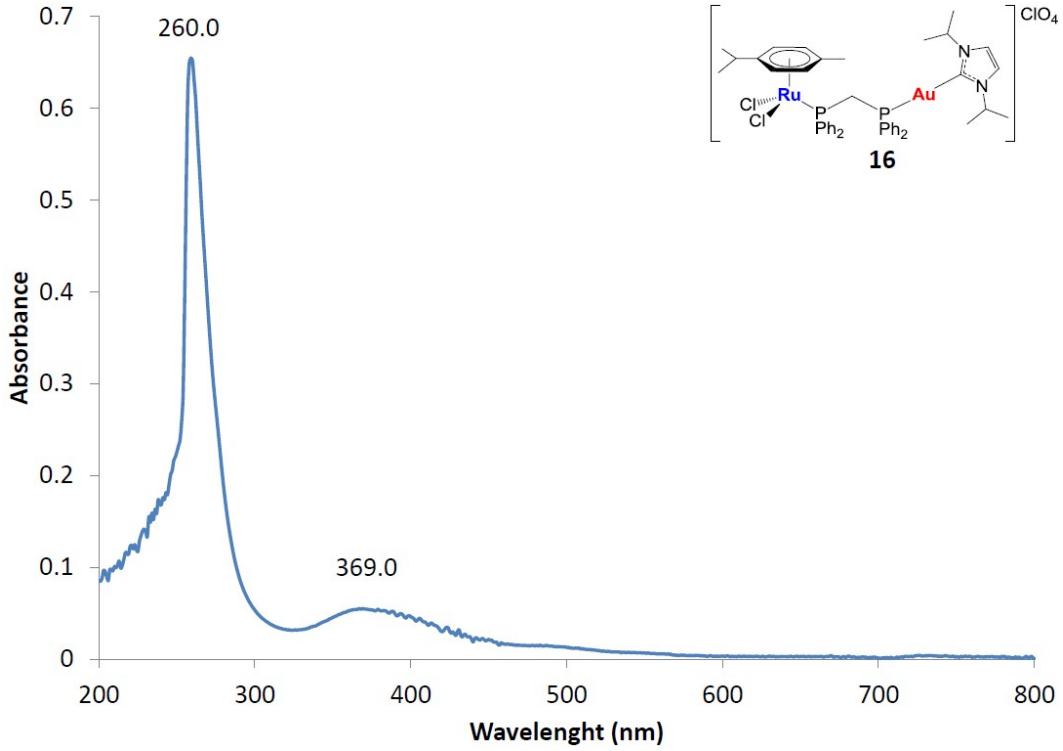

Figure S83. UV-visible spectrum of compound **16** ($3 \cdot 10^{-5}$ M) in DMSO.

7. Selected time-course UV-visible spectra of heterobimetallic compounds in DMSO/PBS-1X

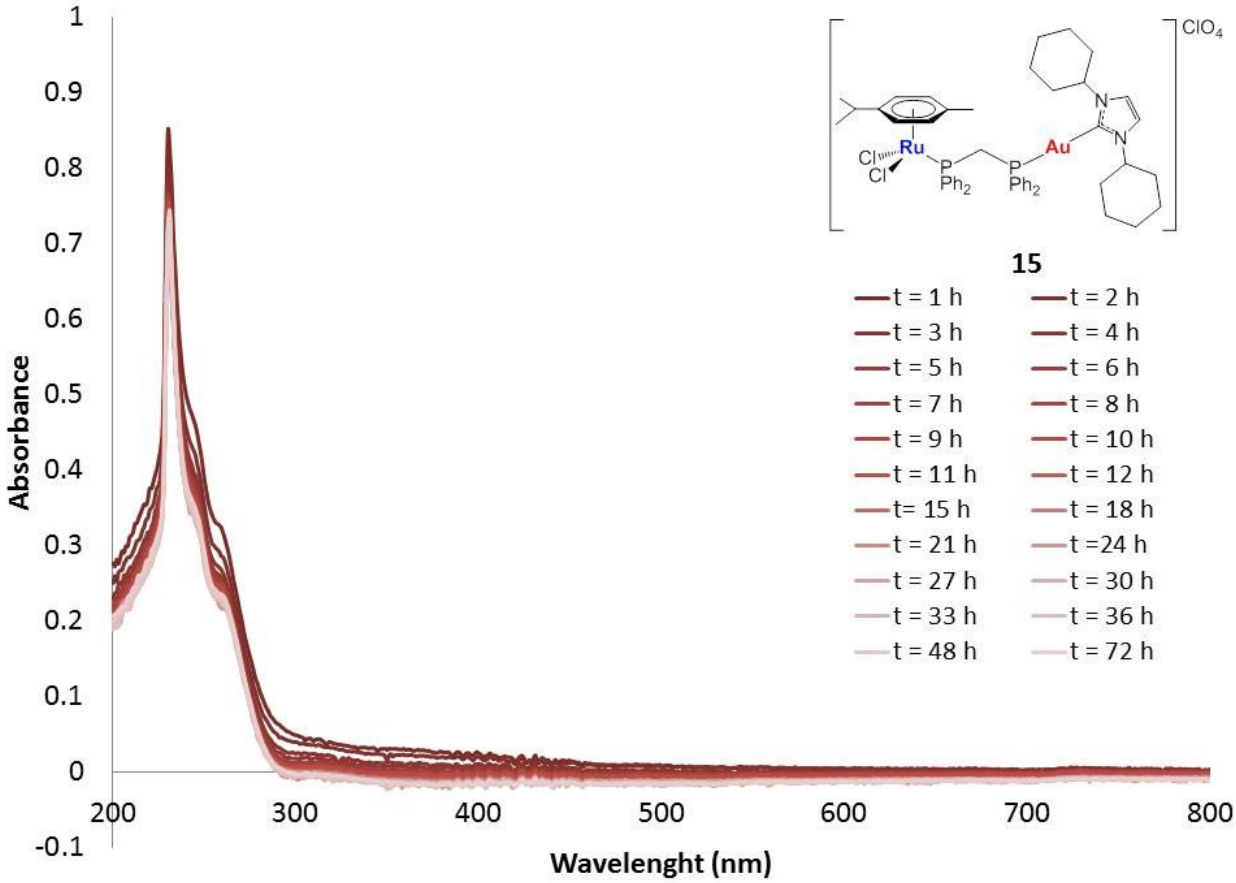

Figure S85. UV-visible spectrum of compound **15** ($2.0 \cdot 10^{-5}$ M) in 1:99 DMSO/PBS-1X (pH 7.4) recorded over 72h.

8. Crystallographic data

Suitable single crystals of the corresponding compounds (**13** and **14**) were obtained by layering pentane over dichloromethane solutions. The crystals were mounted on glass fibers, and the diffraction measurements were performed with a Nonius Kappa CCD area-detector diffractometer with Mo-*K*α radiation (λ = 0.71073 Å). The structures were solved by direct methods and refined by least-squares techniques on weighted F^2 values for all reflections (SHELXTL, 6.14).[8] All non-hydrogen atoms were assigned anisotropic displacement parameters and refined without positional constraints, except the atoms in the dicholometane molecule of crystallization, in compound **14**, that were refined isotropically. All hydrogen atoms, were calculated with a riding model. Complex neutral-atom scattering factors were used. The program SQEEZE, a part of the Platon[9] package of crystallographic software, was used to calculate the solvent disorder area and remove its contribution to the overall intensity data in the case of compound **13**. These data can be obtained free of charge from The Cambridge Crystallographic Data Center via www.ccdc.cam.ac.uk/data_request/cif. The assigned deposition number at the Cambridge Crystallographic Data Centre are 1436327 (**13**) and 1436326 (**14**).

Table S1. Crystal Data and Structure Refinement for compounds **13** and **14**.

	13	**14**
formula	$C_{62}H_{72}AuCl_3N_2O_4P_2Ru$	$C_{57}H_{62}AuCl_5N_2O_4P_2Ru$
fw	1375.54	1376.31
T [K]	293 (2)	293 (2)
λ ($Mo_{K\alpha}$)[Å]	0.71073	0.71073
crystal system	Monoclinic	Monoclinic
space group	P2(1)/c	P2(1)/n
a [Å]	21.200(4)	14.385(3)
b [Å]	14.090(3)	25.076(5)
c [Å]	22.972(5)	17.318(4)
α [°]	90	90
β [°]	93.02(3)	107.02(3)
γ [°]	90	90
V [Å]^3	6852(2)	5974(2)
Z	4	4
D_{calcd} (mg m^{-3})	1.333	1.530
μ (mm^{-1})	2.564	3.028
F(000)	2776	2752
Crystal size (mm)	0.26 x 0.23 x 0.20	0.25 x 0.23 x 0.20
Theta range for data collection	1.70 to 24.72 deg.	1.47 to 24.71 deg.
Limiting indices	-24<=h<=24,-16<=k<=16, -26<=l<=26	-16<=h<=16, -29<=k<=29, -20<=l<=20
Reflections collected / unique	42004 / 11692 [R(int) = 0.0670]	19833 / 10161 [R(int) = 0.0586]
Completeness to theta = 24.71	99.9 %	100.0 %
Refinement method	Full-matrix least-squares on F^2	Full-matrix least-squares on F^2
Data / restraints / parameters	11692 / 0 / 683	10161 / 0 / 643
GOF	0.889	1.026
Final R indices [I>2σ(I)]	R1 = 0.0657, wR2 = 0.1929	R1 = 0.0548, wR2 = 0.1491
R indices (all data)	R1 = 0.0845, wR2 = 0.2056	R1 = 0.1070, wR2 = 0.2066
Largest diff. peak and hole	3.800 and -0.909 e.A^-3	2.560 and -1.846 e.A^{-3}

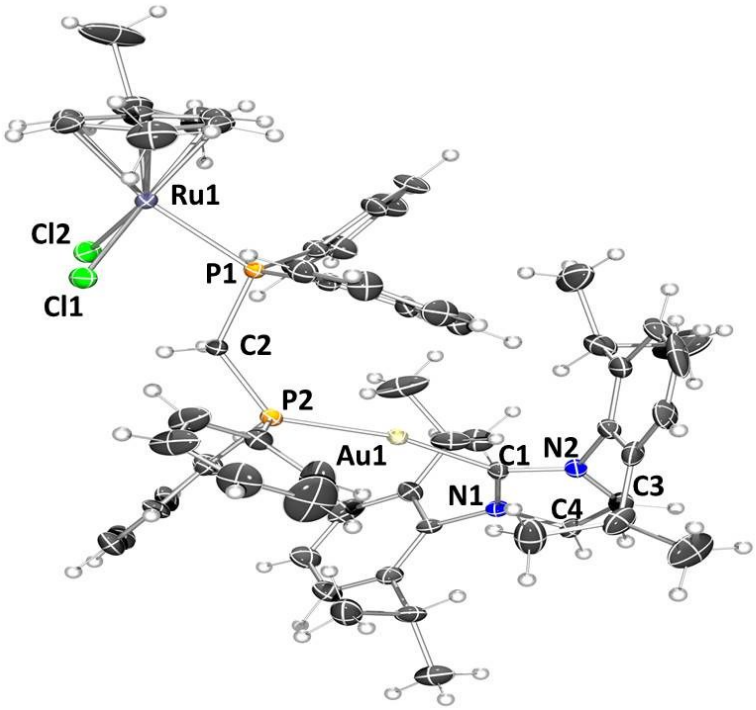

13

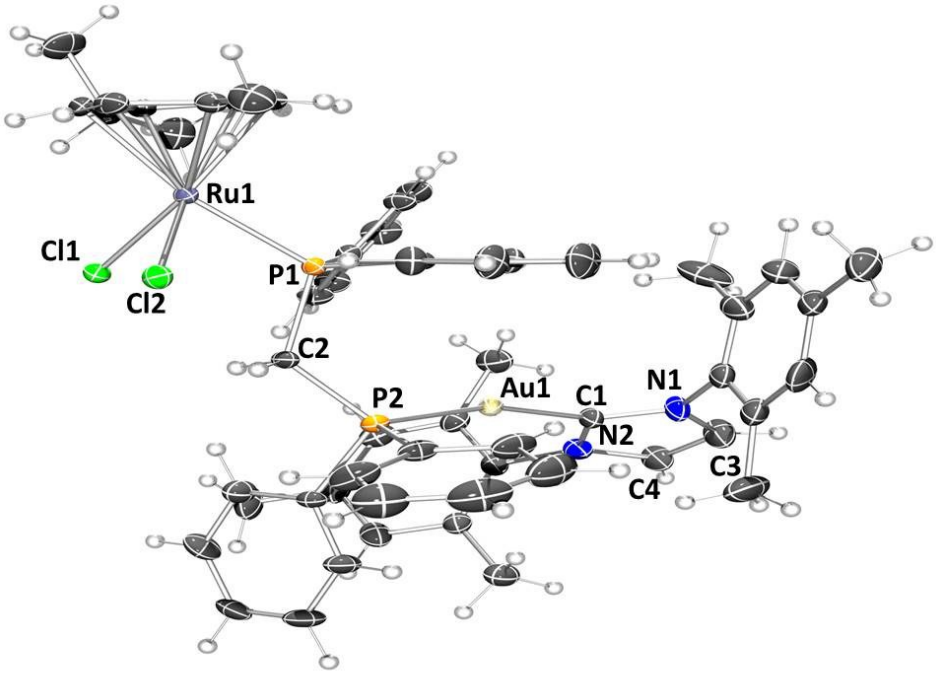

14

Figure S86. ORTEP view of the molecular structure of cations of compounds **13** and **14** showing the relevant labelling scheme.

Table S2. Selected Structural Parameters of compounds **13** and **14** obtained from X-ray single crystal diffraction studies. Bond lengths in Å and angles in °.

13		**14**	
Au(1)-C(1)	2.017(9)	Au(1)-C(1)	2.052(12)
Au(1)-P(2)	2.287(2)	Au(1)-P(2)	2.287(3)
P(2)-C(2)	1.824(9)	P(2)-C(2)	1.808(10)
P(1)-C(2)	1.842(9)	P(1)-C(2)	1.826(10)
P(1)-Ru(1)	2.350(2)	P(1)-Ru(1)	2.352(3)
Ru(1)-Cl(1)	2.415(3)	Ru(1)-Cl(1)	2.409(3)
Ru(1)-Cl(2)	2.409(3)	Ru(1)-Cl(2)	2.422(3)
Ru-Z*	1.719	Ru-Z*	1.718
N(1)-C(1)	1.361(11)	N(1)-C(1)	1.310(15)
C(1)-N(2)	1.377(11)	C(1)-N(2)	1.373(16)
N(1)-C(4)	1.369(12)	N(1)-C(3)	1.379(17)
N(2)-C(3)	1.377(13)	N(2)-C(4)	1.384(17)
C(3)-C(4)	1.358(15)	C(3)-C(4)	1.33(2)
N(1)-C(73)	1.455(12)	N(1)-C(61)	1.438(18)
N(2)-C(61)	1.472(13)	N(2)-C(71)	1.449(16)
P(1)-C(21)	1.818(10)	P(1)-C(21)	1.844(11)
P(1)-C(32)	1.833(10)	P(1)-C(31)	1.859(10)
P(2)-C(52)	1.823(10)	P(2)-C(51)	1.846(11)
P(2)-C(41)	1.826(10)	P(2)-C(41)	1.818(12)
C(1)-Au(1)-P(2)	168.2(3)	C(1)-Au(1)-P(2)	165.3(4)
P(2)-C(2)-P(1)	125.1(5)	P(2)-C(2)-P(1)	120.0(6)
C(2)-P(1)-Ru(1)	111.6(3)	C(2)-P(1)-Ru(1)	111.7(3)
P(1)-Ru(1)-Cl(1)	84.49(10)	P(1)-Ru(1)-Cl(1)	85.39(10)
P(1)-Ru(1)-Cl(2)	86.33(10)	P(1)-Ru(1)-Cl(2)	86.80(10)
P(1)-Ru(1)-Z*	132.32	P(1)-Ru(1)-Z*	126.53
Cl(1)-Ru(1)-Z*	126.25	Cl(1)-Ru(1)-Z*	125.97
Cl(2)-Ru(1)-Z*	124.67	Cl(2)-Ru(1)-Z*	130.36
C(21)-P(1)-Ru(1)	117.6(3)	C(21)-P(1)-Ru(1)	115.4(3)
C(32)-P(1)-Ru(1)	112.5(3)	C(31)-P(1)-Ru(1)	114.2(4)
C(2)-P(1)-Ru(1)	111.6(3)	C(2)-P(1)-Ru(1)	111.7(3)
C(52)-P(2)-Au(1)	113.3(4)	C(51)-P(2)-Au(1)	105.0(4)
C(2)-P(2)-Au(1)	124.9(3)	C(2)-P(2)-Au(1)	124.1(4)
C(41)-P(2)-Au(1)	104.9(3)	C(41)-P(2)-Au(1)	111.7(5)
N(1)-C(1)-N(2)	102.8(7)	N(1)-C(1)-N(2)	105.2(10)
N(1)-C(1)-Au(1)	124.6(7)	N(1)-C(1)-Au(1)	132.3(10)
N(2)-C(1)-Au(1)	132.0(6)	N(2)-C(1)-Au(1)	121.7(8)
C(1)-N(1)-C(4)	111.8(8)	C(1)-N(1)-C(4)	108.8(11)
C(1)-N(2)-C(3)	112.4(8)	C(1)-N(2)-C(3)	112.4(12)

* Z = centroid of *p*-cymene ring.

9. Interactions of the new compounds with plasmid pBR322 (gel electrophoresis mobility shift assay)

10 µL aliquots of pBR322 plasmid DNA (20 µg/mL) in buffer (5 mM Tris/HCl, 50 mM $NaClO_4$, pH = 7.39) were incubated with different concentrations of the compounds (**13**-**16**, and titanocene dichloride) (in the range 0.25 and 4.0 metal complex:DNA bp) at 37°C for 20 h in the dark. Samples of free DNA and cisplatin-DNA were prepared as controls. After the incubation period, the samples were loaded onto the 1 % agarose gel. The samples were separated by electrophoresis for 1.5 h at 80 V in Tris-acetate/EDTA buffer (TAE). Afterwards, the gel was stained for 30 min with a solution of GelRed nucleic acid stain.

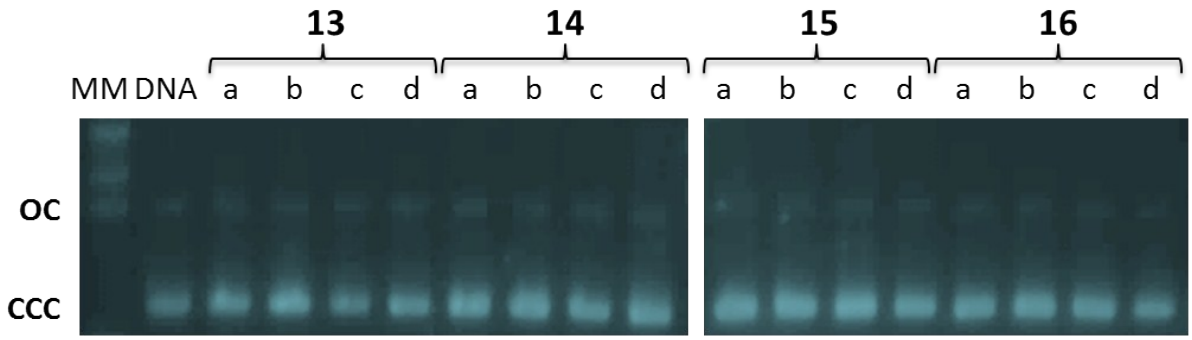

Figure S87. Electrophoresis mobility shift assays for heterometallic RuAu compounds **13**, **14**, **15** and **16**. DNA refers to untreated plasmid pBR322. a, b, c and d correspond to metal/DNAbp ratios of 0.25, 0.5, 1.0 and 2.0 respectively.

10. Cell culture and PrestoBlue™ cell viability assay for Caki-1, DLD-1, HCT-116 and HEK-293T cells.

Human renal clear-cell carcinoma Caki-1, human breast adenocarcinoma cells MDA-MB- 231, human colorectal adenocarcinoma cells DLD-1, as well as the human colorectal carcinoma HCT-116 in comparison with healthy human embryonic kidney cells HEK-293T were used to study compounds **1** and **9-16** cytotoxic activity. The cells were all obtained from the American Type Culture Collection (ATCC) (Manassas, Virginia, USA). All the cells were grown adherently.

The Caki-1 and DLD-1 cells were cultured in Roswell Park Memorial Institute (RPMI- 1640) (Mediatech Inc., Manassas, VA) medium while HEK-293T, MDA-MB-231 and HCT-116 cells were maintained in Dulbecco's modified Eagle's medium (DMEM) (Mediatech Inc., Manassas, VA), all media was supplemented with 10% fetal bovine serum (FBS, Life Technologies, Grand Island, NY), 1% Minimum Essential Media (MEM) nonessential amino acids (NEAA, Mediatech) and 1% penicillin–streptomycin (Pen Strep, Mediatech). All cells were cultured at 37 ^{o}C and 5% CO_2 and 95% air in a humidified incubator. For evaluation of cell viability, cells were seeded at a concentration of 5×10^3 cells/well in 90 µl of DMEM or RPMI without phenol red and without antibiotics, supplemented with 10% FBS and 2 mM L-glutamine into tissue culture grade 96-well flat bottom microplates (BioLite Microwell Plate, Fisher Scientific, Waltham, MA) and grown for 24h at 37 ^{o}C under 5% CO_2 and 95% air in a humidified incubator. All compounds were dissolved in DMSO and diluted to 1% in media before addition to cell culture medium. The intermediate dilutions of the compounds were added to the wells (10 μL) to obtain concentrations of 1 μM, 10 μM and 100 μM, 0.1% DMSO was used as control, and the cells were incubated for 72 h. PrestoBlue™ was used to quantitatively measure variations in cell viability of treated cells. Following 72 h drug exposure, 11 μL of per well of 10X PrestoBlue™ (Life Technologies, California, USA) labeling mixture was added to the cells at a final concentration of 1X and incubated for 1.5 h at 37°C under 5% CO_2 and 95% air in a humidified incubator. The optical absorbance of each well in a 96-well plate was quantified using BioTek ELx 808 absorbance microplate reader (BioTek Winooski, VT) set at 570 nm excitation and 600 nm emission wavelength. The percentage of surviving cells was calculated from the ratio of absorbance of treated to untreated cells. The IC_{50} value was calculated as the concentration reducing the proliferation of the cells by 50% and is presented as a mean (± S.E.M) of at least two independent experiments each with triplicate measurements.

Table S3. IC_{50} values (μM) in human cell lines were determined with monometallic [(NHC)AuCl] (**1**, **10-12**) monometallic [Ru(p-cymene)Cl_2(η^1-dppm)] (**9**), new heterometallic Ru-Au compounds (**13-16**) and mixtures of monometallic gold (**1**, **10-12**) and ruthenium (**9**) derivatives (1:1 equivalents). These mixtures were freshly prepared in DMSO stock solutions and diluted before incubation.

Compound or Mixture			HCT-116	Caki-1	DLD-1	HEK-293T
Monometallic	**Au**	**1**	39.7 ± 4.9	21.2 ± 1.6	55.3 ± 6.3	>100
	Au	**10**	31.2 ±3.2	27.1 ±2.0	31.9 ± 4.2	61.5± 5.1
	Au	**11**	59.1 ± 5.8	58.8 ± 3.9	61.6 ± 4.8	>100
	Au	**12**	27.7 ± 4.9	17.5 ± 2.2	40.6 ± 1.2	>100
	Ru	**9**	18.2 ± 2.2	36.75 ± 4.0	49.6 ± 3.1	81.3± 6.0
Bimetallic Au-Ru		**13**	8.1 ± 1.8	14.1 ± 1.9	61.2 ± 3.6	>100
		14	5.22 ± 0.7	5.2 ± 0.9	29.7 ± 3.1	73.2± 3.5
		15	6.4 ± 1.0	3.8 ± 0.6	71.1 ± 4.8	>100
		16	9.6± 3.1	12.7 ± 2.7	53.2 ± 2.9	78.8± 7.7
Mixtures		**9 + 1**		21.5 ± 3.8		
		9 + 10		30.9 ±5.2		
		9 + 11		42.8 ± 5.0		
		9 + 12		32.5 ± 3.3		

11. Inhibition of thioredoxin reductase with compounds **1**, **9** and **13**

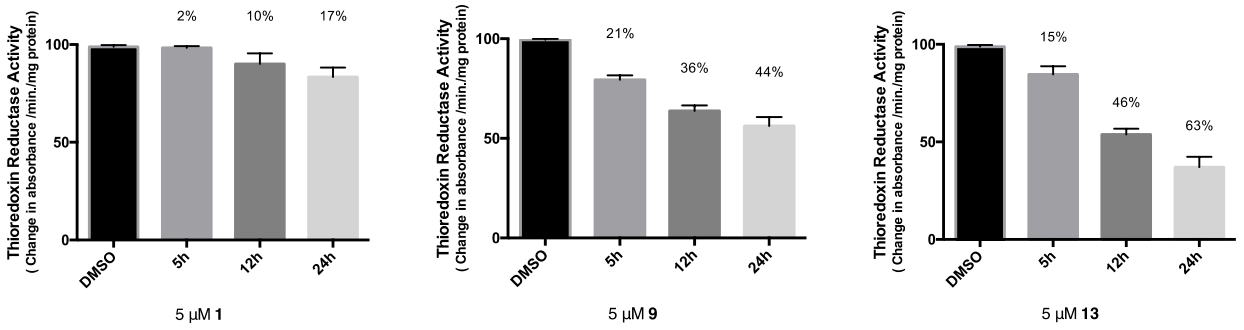

A **B** **C**

Figure S88. Thioredoxin reductase activity in **1**, **9** or **13** treated Caki-1 cells. Activity of endogenous Caki-1 thioredoxin reductase from soluble whole cell lysates following incubation with 5 µM of monometallic gold compound **1** (Graph A), monometallic ruthenium compound **9** (Graph B), heterobimetallic gold-ruthenium compound **13** (Graph C), or 0.1% DMSO for 5, 12 and 24 hours.

Method:

For the thioredoxin reductase activity assay, whole cell lysates were obtained from Caki-1 cells treated *in vitro* with 5 µM of **1**, **9** or **13** or 0.1% DMSO. After 5, 12 or 24 hours of treatment, incubation cells were washed three times in PBS, and lysed by douncing using scrappers and sheer force though syringe with a 34 gauge needle in assay buffer (Abcam Thioredoxin Reductase Assay kit, ab83463) added to 1 mM Protease Inhibitor Cocktail (Abcam, ab65621). The lysates were centrifuged at 10,000 rcf for 15 minutes at 4°C to isolate insoluble material. The total protein concentrations of soluble lysates were measured using the BCA Protein Assay (Pierce™ BCA Protein Assay Kit, Life Technologies, 23225). The soluble lysates were incubated for 20 minutes in assay buffer with a proprietary thioredoxin reductase specific inhibitor before adding a specific substrate, DTNB (5, 5′-dithiobis (2-nitrobenzoic) acid), and measuring activity at 1 minute intervals for 30 minutes using the BioTek Fluorescence Microplate Reader (BioTek U.S., Winooski, VT) at λ = 412 nm. Lysates were tested in duplicate. Thioredoxin reductase activity was calculated based on the linear amount of TNB produced per minute per mg of total protein and adjusted for background activity from enzymes other than thioredoxin reductase in the lysates.

Details on the kit are as follows: The Thioredoxin Reductase Assay Kit (ab83463) is a specific assay for detecting Thioredoxin Reductase (TrxR) activity in various sample types, including cell lysates. The kit can measure both activation or inhibition of TrxR relative to an untreated, vehicle-treated or baseline control. TrxR catalyzes the reduction of DTNB (5, 5'-dithiobis (2-nitrobenzoic) acid) to TNB^{2-} (5-thio-2-nitrobenzoic acid) in presence of NADPH, which generates a strong yellow color (ODmax = 412 nm). Since other enzymes present in crude biological samples such as glutathione reductase and glutathione peroxidase can also reduce DTNB. In order to measure TrxR-only activity, a TrxR specific inhibitor is used in a separate reaction to determine TrxR specific activity. The difference between total DTNB reduction in the sample and DTNB reduction in the sample in presence of TrxR inhibitor is the value of specific TrxR activity in the sample. Additional information: TrxR Assay Buffer is a phosphate buffer containing BSA and mild detergent. TrxR Positive Control is a thioredoxin reductase isolated from rat liver. TrxR Negative Control is a metallocomplex inhibitor of TrxR enzyme.

12. References

1 Loos, M., Gerber, C., Corona, F., Hollender, J., Singer, H. (2015). Accelerated isotope fine structure calculation using pruned transition trees, Analytical Chemistry 87(11), 5738-5744. LINK http://pubs.acs.org/doi/abs/10.1021/acs.analchem.5b00941

2 R. Uson, A. Laguna and M. Laguna, *Inorg. Synth.*, **1989**, 26, 85.

3 R. Visbal, A. Laguna and M.C. Gimeno, *Chem. Commun.*, **2013**, *49*, 5642.

4 P. Fremont, N. M. Scott, E. D. Stevens and S. P. Nolan, *Organometallics* **2005,** *24,* 2411.

5 J. Tönnemann, J. Risse, Z. Grote, R. Scopelliti and K. Severin, *Eur. J. Inorg. Chem.*, **2013**, 4558.

6 M.N. Gowda, S.B. Waikarand G.K.N. Reddy. *Adv. Inorg. Chem. Radiochem*. **1984**, *28*, 255.

7 L. Massai, J. Fernández-Gallardo, A. Guerri, A. Arcangeli, S. Pillozzi, M. Contel and L. Messori, Dalton Trans., **2015**, 44, 11067.

8 SHELXTL (Version 6.14); Brucker, **2000**.

9 Spek, A. L. *Acta Cryst.*, **2009**, D65, 148–155.